Thermocouple Temperature Measurements for Twin Jet Thermal Mixing

A Thesis Presented for the Master of Science in Nuclear Engineering Degree
The University of Tennessee, Knoxville

Spero Michael Peters

December 2011

Acknowledgments

There are various individuals whom I would like to thank for their roles in my education and this thesis. First and foremost, I would like to thank my advisor, Dr. Arthur Ruggles for his support and advice throughout this thesis project and my graduate studies and my committee, Dr. Lawrence Heilbronn and Dr. Belle Upadhyaya for reviewing my thesis. Special thanks are also in order to a few of my fellow students who provided assistance during experimental tests: Christopher Baxter, Lane Carasik, and Lee Tschaepe.

I would also like to take this opportunity to acknowledge a few individuals from my alma mater, The University of Mississippi, who helped me to become a better engineer. Thank you, Dr. Nathan Murray, Dr. James Chambers, and Mrs. Marni Kendricks, for a positive experience during my undergraduate career at the University of Mississippi.

Thanks again to everyone listed above and to my family and friends for supporting me throughout my education.

Abstract

Thermocouples are commonly used devices for temperature measurement. This study concerns the implementation of thermocouples to collect thermal mixing data in an environment in which two parallel water jets are mixing. The measurements are taken with the purpose of modeling the jet mixing region so that Computational Fluid Dynamics (CFD) models can be validated against the test data. This thesis covers the design, construction, implementation and evaluation of a thermocouple system for immersion in a water environment to measure the thermal mixing of twin jets.

The measurement system being used is a thermocouple rake whose design and fabrication is covered. Thermocouple single effects tests, providing conclusions on time response, calibration, and signal filtering are included as well. The implantation of the thermocouple rake in a water test environment is discussed in detail such that the experimental process can be repeated. The rake is used to provide thermal data taken along the jet centerline, which is post processed, and presented. Conclusions are drawn based upon average temperature profiles and time based temperature data.

Table of Contents

Chapter 1. Introduction 1

Chapter 2. Scope of Work 3

Chapter 3. Thermocouple Background and Theory 5

3.1 The Seebeck Effect 5

3.2 The Peltier Effect 7

3.3 The Thomson Effect 8

3.4 Correlation between Seebeck, Thomson, and Peltier Effects 10

3.5 Typical Thermocouple System Setup 12

3.6 Thermocouple Time Response 13

3.6.1 Forced Convection 15

3.6.2 Natural Convection 17

3.6.3 Transient Conduction 17

Chapter 4. Water Thermocouple Rake 19

4.1 Design Criteria 20

4.1.1 Rake Size 20

4.1.2 Materials 21

4.1.3 Geometry and Shape 21

4.1.4 Thermocouple Choice 22

4.2 Rake Final Design 23

4.3 Rake Build 25

4.4 Summary of Construction 33

Chapter 5. Thermocouple Tests 34

5.1 Thermocouple Plunge Test 34

5.1.1 Initial Objectives 34

5.1.2 Setup 34

5.1.3 Procedure 36

5.1.4 Results 37

5.1.5 Conclusions 40
5.2 Additional Plunge Test Work 41
5.2.1 Objectives, Setup and Procedure 41
5.2.2 Results 41
5.2.3 Conclusions 44
5.3 First Flow Test 45
5.3.1 Objectives 45
5.3.2 Setup 45
5.3.3 Procedure 47
5.3.4 Results 48
5.3.5 Conclusions 52
5.4 Calibration 54
5.4.1 Objectives 54
5.4.2 Setup 54
5.4.3 Procedure 54
5.4.4 Results 55
5.4.5 Conclusions 58
5.5 Interference and Signal Filtering 59
5.5.1 Examples of Electromagnetic Interference 59
5.5.2 Causes of Electromagnetic Interference in the Lab 61
5.5.3 Filtering 61
5.6 In-Tank Tests 65
5.6.1 Objectives 65
5.6.2 Procedure and Setup 65
5.6.3 Results 66
5.6.4 Conclusions 69
Chapter 6. Experimental Implementation of Thermocouple Rake 70
6.1 Mounting and Positioning 70
6.2 Data Acquisition 73

6.3 Post Processing 74
Chapter 7. Twin Jet Thermal Mixing Experimental Data and Discussion 77
7.1 Centerline Data Acquisition Information 77
7.2 Centerline Data Presentation and Discussion 80
7.3 Data Acquisition Conclusions 87
Chapter 8. Conclusions and Future Work 88
List of References 89
Vitae 91

List of Figures

Figure 1 Test Tank 3
Figure 2 Twin Jets 4
Figure 3 Seebeck Effect [3] 6
Figure 4 Thermocouple Circuit 6
Figure 5 Peltier Effect [3] 7
Figure 6 Thomson Effect [3] 9
Figure 7 Twisted Pair (left) and Welded TC (right) 12
Figure 8 Transient Response of a Thermocouple [6] 15
Figure 9 Rake Concept 20
Figure 10 Final Design: Full View 23
Figure 11 Final Design: Rake Head Detail 24
Figure 12 Rake Head on Milling Machine 25
Figure 13 Rake Head with Spoke Holes 26
Figure 14 Welding Diagram 26
Figure 15 Full View of Finished Steel Work 27
Figure 16 Close up of Rake Head 27
Figure 17 Rake in Dye Run 28
Figure 18 Thermocouple Welding 29
Figure 19 Thermocouple Wires through Mast 30
Figure 20 Clove Hitch 31
Figure 21 Sheer Lashing Step 3 (bottom wire) and Step 4 (top wire) 31
Figure 22 Finished Thermocouple Rake 32
Figure 23 Rake Mounted in Test Tank 33
Figure 24 Test Setup 35
Figure 25 Room Temperature 36
Figure 26 LabVIEW Front Panel 36
Figure 27 NI 6211 Cooling Curve 37
Figure 28 NI 6212 Cooling Curve 38
Figure 29 Cooling Curve 1 43
Figure 30 Cooling Curve 2 43
Figure 31 View of Inlet with Ice Chamber and Thermocouples in View 46
Figure 32 View from the End of the Flow Channel 47
Figure 33 Full Data from Run 1 49
Figure 34 Data of Interest from Run 1 50
Figure 35 Full Data from Run 2 51

Figure 36 Data of Interest from Run 2 51
Figure 37 Single TC Calibration Curve 56
Figure 38 Close Up of Single TC Calibration Curve 57
Figure 39 EMI Example 1 59
Figure 40 EMI Example 2 60
Figure 41 EMI Example 3 60
Figure 42 EMI caused by Laptop Charging Circuit 61
Figure 43 Low Pass Filter 63
Figure 44 Filtered (blue) vs Unfiltered Data (red) 64
Figure 45 General Rake Positioning, with Thermocouples and Jets Labeled 65
Figure 46 Run 1 66
Figure 47 Run 2 67
Figure 48 Run 3 68
Figure 49 Run 4 69
Figure 50 Rake Mounting and Positioning Annotated 70
Figure 51 Coordinate System Close Up 71
Figure 52 Vertical 'Z' Direction Positioning 72
Figure 53 'X' Direction Positioning 73
Figure 54 LabVIEW Operator View 74
Figure 55 Filter used for Final Data Collection 75
Figure 56 Filtered vs. Unfiltered Data 76
Figure 57 Centerline Measurement Positioning Diagram 77
Figure 58 Approximate Thermocouple Locations for Centerline Data Acquisition 78
Figure 59 Distances between Thermocouples 79
Figure 60 Centerline Data at 5 cm 81
Figure 61 Centerline Data at 10 cm 82
Figure 62 Centerline Data at 15 cm 83
Figure 63 Centerline Data at 25 cm 84
Figure 64 Centerline Data at 35 cm 85
Figure 65 Centerline Data at 45 cm 85
Figure 66 Centerline Data at 55 cm 86
Figure 67 Centerline Data at 65 86

List of Tables

Table 1 316L Composition by Weight [9] 21
Table 2 Thermocouple Sizes and Types 22
Table 3 Plunge Test: 5τ Response Times 38
Table 4 Transient Conduction vs. Natural Convection Time Constant Calculation 39
Table 5 Natural Convection Time Constant Calculation 42
Table 6 Time Constant Data Comparison 43
Table 7 Times of Interest from Run 1 50
Table 8 Times of Interest from Run 2 51
Table 9 Forced Convection Time Constant Calculation 52
Table 10 Calibration Values for a Single Type K Thermocouple 55
Table 11 Rake Calibration Values 58
Table 12 Statistical Data for Rake Calibration 58

List of Attachments

File 1 Major Directory (zip)…… NEUP_TwinJet_Thermal_Data.zip
File 2 Rake Location Notes……...……intanktests 10-10-2011\location notes 10-10-2011.txt
File 3 Data File (EXCEL)……intanktests 10-10-2011\5cm.xls
File 4 Data File (EXCEL)……..……intanktests 10-10-2011\10cm.xls
File 5 Data File (EXCEL)……..……intanktests 10-10-2011\15cm.xls
File 6 Data File (EXCEL)……..……intanktests 10-10-2011\25cm.xls
File 7 Data File (EXCEL)……..……intanktests 10-10-2011\35cm.xls
File 8 Data File (EXCEL)……..……intanktests 10-10-2011\45cm.xls
File 9 Data File (EXCEL)……..……intanktests 10-10-2011\55cm.xls
File 10 Data File (EXCEL)……intanktests 10-10-2011\65cm.xls
File 11 Rake Location Notes……..…...……intanktests 10-18-2011\location notes 10-18-2011.txt
File 12 Comma Separated Values (.csv)……..……intanktests 10-18-2011\5cm.xls
File 13 Comma Separated Values (.csv)……intanktests 10-18-2011\10cm.xls
File 14 Comma Separated Values (.csv)……intanktests 10-18-2011\15cm.xls
File 15 Comma Separated Values (.csv)……intanktests 10-18-2011\25cm.xls
File 16 Comma Separated Values (.csv)……intanktests 10-18-2011\35cm.xls
File 17 Comma Separated Values (.csv)……intanktests 10-18-2011\45cm.xls
File 18 Comma Separated Values (.csv)……intanktests 10-18-2011\55cm.xls
File 19 Comma Separated Values (.csv)……intanktests 10-18-2011\65cm.xls
File 20 Rake Location Notes……..…...……intanktests 10-25-2011\location notes 10-25-2011.txt
File 21 Comma Separated Values (.csv)……intanktests 10-25-2011\5cm.xls
File 22 Comma Separated Values (.csv)……intanktests 10-25-2011\10cm.xls
File 23 Comma Separated Values (.csv)……intanktests 10-25-2011\15cm.xls
File 24 Comma Separated Values (.csv)……intanktests 10-25-2011\25cm.xls
File 25 Comma Separated Values (.csv)……intanktests 10-25-2011\35cm.xls
File 26 Comma Separated Values (.csv)……intanktests 10-25-2011\45cm.xls
File 27 Comma Separated Values (.csv)……intanktests 10-25-2011\55cm.xls
File 28 Comma Separated Values (.csv)……intanktests 10-25-2011\65cm.xls

Chapter 1. Introduction

Fluid mechanics is an engineering discipline focused on the study of gases and liquids. There are a variety of opportunities in engineering that require the extensive study of moving fluids. A few commonly studied scenarios include flow around objects and inside pipes or ducts. Newtonian fluid flow behavior is often described using the Navier-Stokes equations. These equations were derived independently by G.G. Stokes and M. Navier in the latter half of the 1800s [1]. The full equations are a set of coupled differential equations that relate the velocity, pressure, temperature, and density of a fluid in motion.

The equations are generally too difficult to be solved analytically. In the past, engineers and researchers have made simplified approximations that are applicable in individual cases. However modern computing power allows for solving the Navier-Stokes equations. This has given rise to the field of Computational Fluid Dynamics or CFD. Today, powerful commercial software packages use CFD codes to provide detailed, engineering models of fluid systems. During the use of any CFD code for the design of critical components, there is a need to provide an assessment of the accuracy of the code. This is known as 'Verification and Validation' or V & V. V&V is a process undertaken to fully document the usefulness and accuracy of a CFD code. Various professional organizations have published standards and guidelines for tasks to be done when performing a V&V for CFD codes. In many of these standards, the CFD model results are often compared with exact analytical solutions and established test results. Test results can typically include any type of scale test done in a lab where reasonably accurate measurements were performed on a fluid flow of interest.

One scenario that provides a complication for CFD codes is the turbulent region created by the mixing of multiple jets. Current research at the University of Tennessee Knoxville (UTK) in conjunction with The University of Idaho, Idaho Falls, and Argonne National Laboratory (ANL) aims to make accurate fluid measurements within the turbulence created by two jets mixing (referred to hereafter as the twin jet project). The final goal of this research is to use the

measurements to validate CFD models for the scenario briefly described above and will utilize data taken in both liquid water and mercury environments.

Laboratory testing during this research will require both velocity and temperature measurements. If the two jets are at different temperatures; heat energy will be transferred only with the physical mixing of water. This makes the temperature distribution in the mixing region of the two jets a quantity that can readily be compared to CFD models. To that end, a temperature measurement system is constructed and evaluated thoroughly for use in the twin jet project. The system makes temperature measurements via thermocouples. This thesis covers the design, construction, implementation and evaluation of a thermocouple system for immersion in a water environment to measure the thermal mixing of twin jets.

Chapter 2. Scope of Work

As mentioned in the introduction, this project is part of a larger research objective. The purpose of the work being done is to provide new methods for the comparison of experimental data to computational fluid dynamic (CFD) simulation tools. The research calls for test sections to be created for separate effects tests. The data from the tests could then be compared to simulations of the experiment in a V&V effort to determine the accuracy and effectiveness of the code. The environment for the thermocouple rake in this project is twin jet mixing. The test area involved will have two turbulent water jets that are injected parallel to each other at two different temperatures. This creates a turbulent mixing region. The test tank is shown in Figure 1 and a close up of the jets is shown in Figure 2. In Figure 2, colored dye was added to the feed water for each jet allowing it to be visualized.

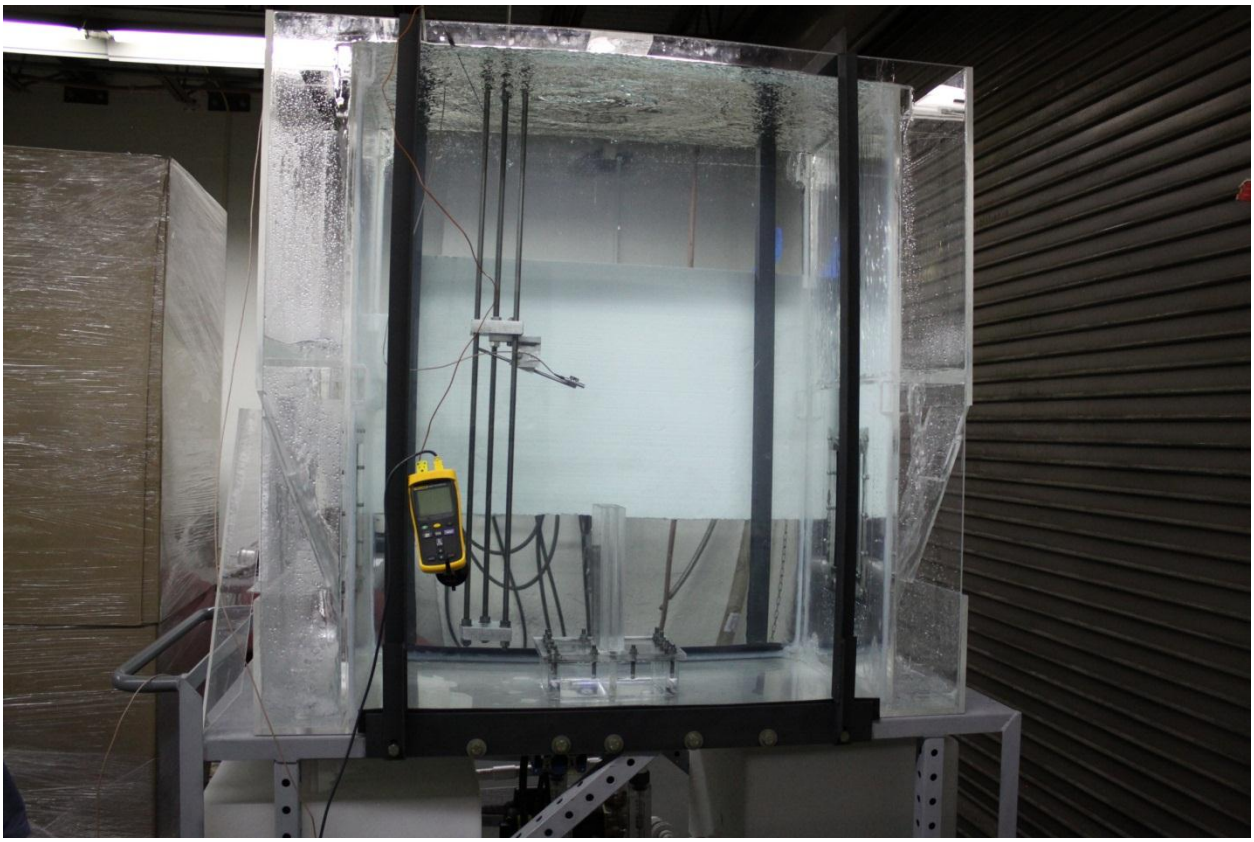


Figure 1 Test Tank

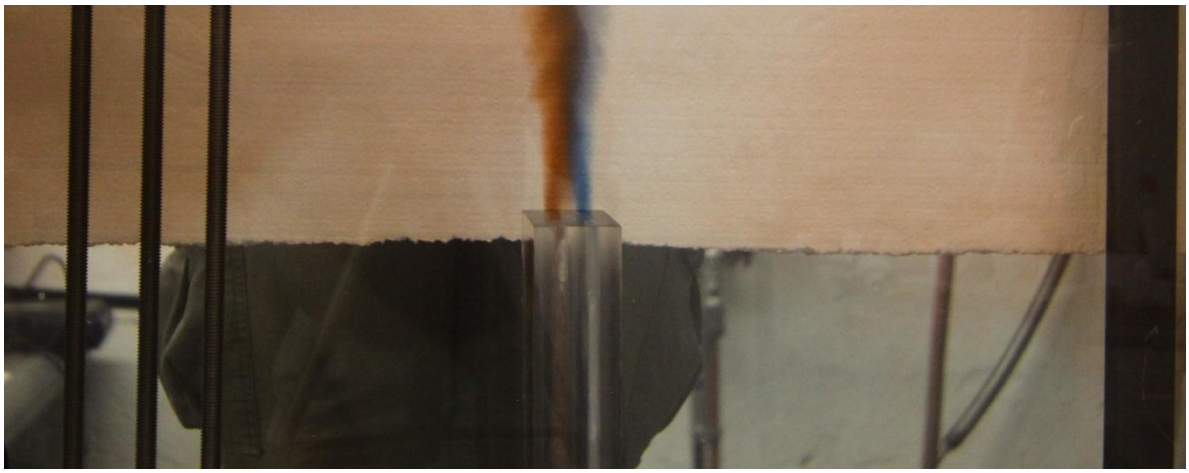


Figure 2 Twin Jets

The system was designed so that each jet has its own pump and inlet reservoir tank. This makes running with each jet at a different temperature possible. When one jet is hotter than the other, thermal energy is mainly transmitted via turbulent mixing particles, because of this the temperature profiles during thermal mixing can be measured, and compared with CFD simulation outcomes. This test section was designed to take three types of measurement: a thermocouple rake for thermal mixing data, an ultrasound probe for velocity measurements, and optical measurements of velocity and fluid mixing using various approaches through the clear walls.

This research is of interest in nuclear engineering through the concentration of thermal hydraulics in the study of liquid metal reactors. Liquid metal reactors have large temperature distributions in the core flow and as such, utilize jet mixing within the plenum in order to avoid large temperature gradients in pipes which lead to thermal stresses. It is thus of interest to provide accurate validation data to ensure that CFD models properly predict the thermal mixing of parallel jets.

Chapter 3. Thermocouple Background and Theory

Transducers take energy of some type (i.e. mechanical or thermal) and convert it to another type, typically electrical. Thermocouples (TCs or TC) act as a transducer converting thermal energies into electrical; and are commonly used devices for making temperature measurements. A simple description of a thermocouple is two wires made of dissimilar metals connected at one end that transfer thermal energy as a voltage measured across the two 'cold junction' ends. Thermocouples are flexible, inexpensive, and provide fairly accurate temperature measurements. Thermocouples have a wide array of applications; ranging from power plants to monitoring the pilot light on home appliances and research applications. Thermocouples can provide measurements while immersed in a fluid and also, if treated as disposable, corrosive environments. There are three phenomena, known as thermoelectric effects that explain the behavior of thermocouples. These phenomena are: the Seebeck, Peltier, and Thomson effects [2]. These effects were all discovered in the 19th century by the scientists they are named for. These effects are reversible and are not independent of each other.

3.1 The Seebeck Effect

Discovered in 1826, the Seebeck effect is named after German physicist Thomas Johann Seebeck. This effect is what allows the measurement of temperature with thermocouples [2]. Seebeck found that when two dissimilar metals are connected in a series circuit, an electric current is observed, given that the two junctions of the materials are at different temperatures. Seebeck arranged a list of materials into a thermoelectric series, an excerpt of which is shown below with bismuth (Bi) at the top of the list:

{Bi, Ni, Co, Pt, Cu, Mn, Hg, Pb, Sn, Cr, Au, Ag, Zn, Cd, Fe, Sb}

Circuits created from any two metals in this series with different junction temperatures, experience an electromotive force (emf). An emf is a force that transforms some any type of energy, such as thermal energy in the context of this paper, into electrical energy. The emf is stronger the further apart the two materials are in the list (Sb-Bi will produce a higher emf than Fe-Cu). Seebeck also found that current will flow from the hot junction toward the material that

is lowest on the list. Figure 3 below from Duckworth highlights the Seebeck effect [3]. Two metals, copper and iron, are connected at two junctions kept at different temperatures. Since iron is lower on the thermoelectric series than copper, current flows from the hot junction through the iron and is measureable by the galvanometer. The effect is reversible in that switching the cold and hot junctions will reverse the current direction.

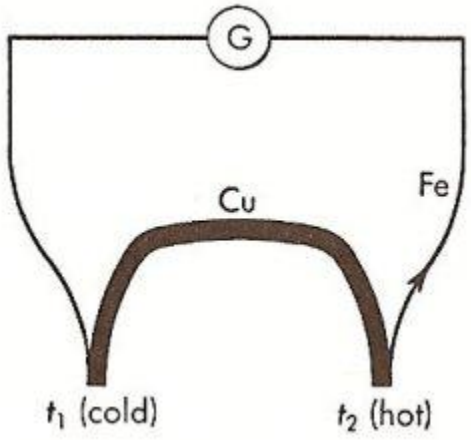


Figure 3 Seebeck Effect [3]

The Seebeck coefficient (S_A) of a material A is defined as the potential difference created by the application of a unit temperature and typically has units of volts/°C [2]. The voltage in a thermoelectric circuit can then be represented as a product of the differences of the Seebeck coefficients and temperatures at each junction. Take a typical thermocouple system shown below in Figure 4.

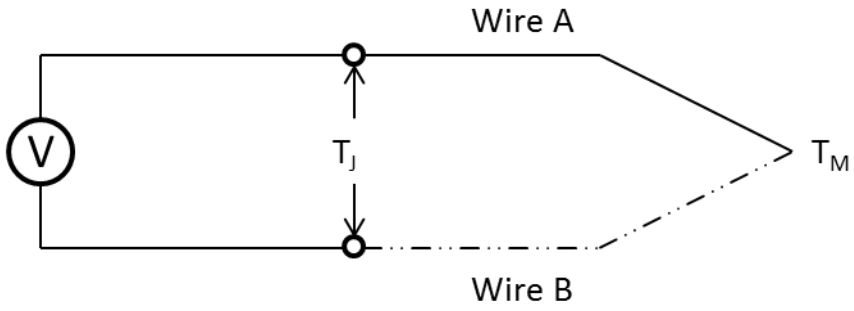


Figure 4 Thermocouple Circuit

The voltage V created by the Seebeck effect can be found by:

$$V = (S_A - S_B)(T_M - T_J) \quad (1)$$

Where

V	=	Measured voltage
T_J	=	Temperature at the junction between the voltmeter and each wire
T_M	=	Temperature being measured
S_A , S_B	=	Seebeck coefficient of wires A and B respectively

3.2 The Peltier Effect

The Peltier effect was discovered in 1834 by the French physicist Jean Charles Athanase Peltier. The Peltier effect describes the heating or cooling at the junctions of dissimilar metals that have a current passed through them [3]. Figure 5 from Duckworth shows a diagram of a circuit experiencing the Peltier effect. The Peltier effect is essentially part of the Seebeck effect. In the Seebeck effect temperature gradients between two junctions cause an emf induced current in the circuit. While in the Peltier effect, cooling and heating of the junctions occurs because of an applied current in the circuit. Like the Seebeck effect, the effect is reversible and changing the direction of the current will change which junction is heated and cooled.

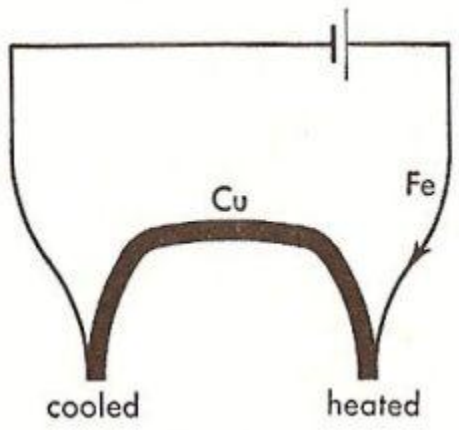


Figure 5 Peltier Effect [3]

The Peltier effect can take place whenever a current is present in a circuit of dissimilar metals. It does not matter whether the current is supplied by an external source or is weakly induced by the Seebeck emf of the circuit [4]. Peltier found that the heat produced by this effect is proportional to the current this is presented by Eq. (2).

$$\frac{dQ_P}{dt} = \pi I \tag{2}$$

Where

dQ_P = Heat generated or absorbed by the Peltier effect

π = Peltier coefficient

I = Current

dt = Change in time

The Peltier coefficient is also known as the Peltier voltage. It is a representation of the emf present in the junctions causing the heat to either be absorbed or emitted. As mentioned previously, the Peltier effect was discovered based on the simultaneous heating and cooling of junctions. However, if one junction is kept at a constant temperature, a net current force driven by emfs is observed; which is very similar to the Seebeck effect.

3.3 The Thomson Effect

The Thomson effect was discovered in 1851 by William Thomson (also known as Lord Kelvin). The Thomson effect is defined as "the change in the heat content of a single conductor of unit cross section when a unity quantity of electricity flows along it through a temperature gradient of 1 K (Kelvin)" [4]. The Thomson effect is essentially, the change of the temperature gradient of a single material when an electric current is passed through it.

Thomson's experiment, described by Duckworth and shown in Figure 6, involved running current through a U-shaped iron rod that is heated at the bottom. Two resistance coils R_1 and R_2 are wound around the iron rod and connected to a Wheatstone bridge circuit. A Wheatstone bridge is a circuit used to measure an unknown resistance. Since the coils are identical, at the beginning of the experiment the Wheatstone bridge is balance, signaling that the resistances of

each coil are, in fact, identical. The result of the heating and current in the rod creates two temperature gradients: positive between A-C and negative between C-B. The Wheatstone bridge becomes unbalanced signaling that the resistance of R_1 has increased and is higher than the resistance of R_2. The changing of the resistances shows that R_1 is heating up and R_2 cooled through thermoelectric effects. Between A to C the thermal emf is going in the direction of the current, while the B to C region the opposite is occurring. In iron, this shows that an emf will flow from hot to cold regions; this behavior is referred to as the 'positive Thomson effect' [3]. Conversely for other metals such as nickel or copper, the emf flows from cold to hot and is referred to as the 'negative Thomson effect'.

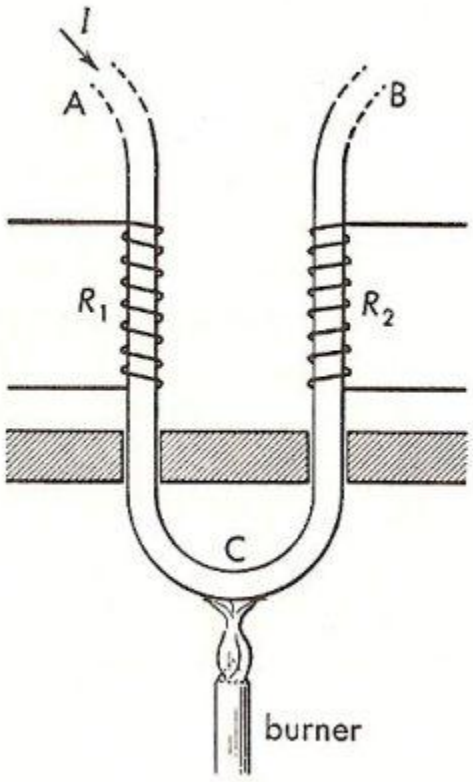


Figure 6 Thomson Effect [3]

The Thomson emf present in a material is defined in terms of the Thomson coefficient σ which has dimensions of emf/degree. This coefficient can be negative or positive based upon the behavior of the material with regards to the Thomson effect. The heat absorbed per second by the Thomson effect is given by Eq. (3)

$$\frac{dQ_{Th}}{dt} = I\int_{T_1}^{T_2}\sigma dT - I^2R \tag{3}$$

The emf produced by the Thomson effect is given by Eq. (4) which has units of volts.

$$\varepsilon_{TH} = \int_{T_1}^{T_2}\sigma dT \tag{4}$$

For a single conductor experiencing heating at a single point, there will be a single hot region surrounded by two cold regions on either side. Thus, the Thomson emfs present in the conductor will oppose each other producing heat transfer effects, but no measureable current [4]. This can be shown mathematically. Take a single material such as iron (Fe), then for the scenario pictured in Figure 6, where T_1 and T_2 represent the temperatures at the end of the rod and at the point where the burner is applied. One can then express the emfs in two regions that follow the current that is being applied, one region from T_1 to T_2 and another from the reverse (T_2 to T_1). Each integral in Eq. (5) is the emf in each leg of the U shaped iron bar, while their values are non-zero, the integrals have opposite limits of integrations and thus the sum of the emfs in the bar is zero.

$$\int_{T_1}^{T_2}\sigma_{Fe}dT + \int_{T_2}^{T_1}\sigma_{Fe}dT = \int_{T_1}^{T_2}(\sigma_{Fe} - \sigma_{Fe})dT = 0 \tag{5}$$

In a thermocouple circuit, with two different metals there would be differing Thomson coefficients leading to a non-zero result. The opposing nature of Thomson emfs in a single conductor is one of the physical reasons why a thermocouple circuit cannot be made from a single conductor and must use dissimilar metals [5].

3.4 Correlation between Seebeck, Thomson, and Peltier Effects

As mentioned previously, the three thermoelectric effects that describe thermocouple behavior are not independent of each other. Seebeck's emf is, in fact, a combination of the emfs observed by Thompson and Peltier [3]. Electromotive forces are typically represented by the Greek letter

epsilon ε; Seebeck's emf will be denoted by ε_{SB}. The total Seebeck emf in a thermocouple circuit with two junctions is equal to the sum of Peltier and Thomson emfs present. For a circuit made up of for example, antimony (Sb) and bismuth (BI) with two junction temperatures T_1 and T_2 the total Seebeck emf is represented by Eq. (6).

$$\varepsilon_{SB} = \pi_{Sb,Bi}|_{T_1}^{T_2} + \int_{T_1}^{T_2} (\sigma_{Sb} - \sigma_{Bi}) dT \qquad (6)$$

The Peltier emf is represented by the difference of the Peltier coefficients evaluated at the junction temperatures T_1 and T_2. The Thomson effect is represented by the integral which is a combination of the integral of each leg (Sb and Bi) of the circuit. This was done just as in Eq. (5), however unlike the single conductor example; the difference of the Thomson coefficients is not only nonzero but positive. This is because antimony experiences a positive Thomson effect (positive coefficient) and bismuth has a negative Thomson effect (negative coefficient) [3]. Thus it has been shown how the three thermoelectric effects that describe thermocouple behavior are related and the physical necessity for making thermocouples from two dissimilar metals or alloys.

3.5 Typical Thermocouple System Setup

A simple thermocouple system, as shown previously in Figure 4 Thermocouple Circuit, is comprised of two wires and a voltmeter. Thermocouple wire, as sold commercially, contains two wires made of dissimilar metals that are sheathed into a single wire strand. The wires are sheathed internally with sheathing of different colors. This prevents any contact along the wire and allows identification of the positive/negative leads of the wire. Figure 7 below shows two type K thermocouples, one with a welded tip and the other with a mechanically twisted tip. The outer sheathing is brown; the interior sheaths for each individual wire are yellow and red. Thermocouple 'type' refers to the materials that comprise each wire in the thermocouple. A type K thermocouple is comprised of Chromel (a nickel chromium alloy, yellow sheathing) and Alumel (nickel aluminum alloy, red sheathing). The yellow lead is positive, and the red lead is negative.

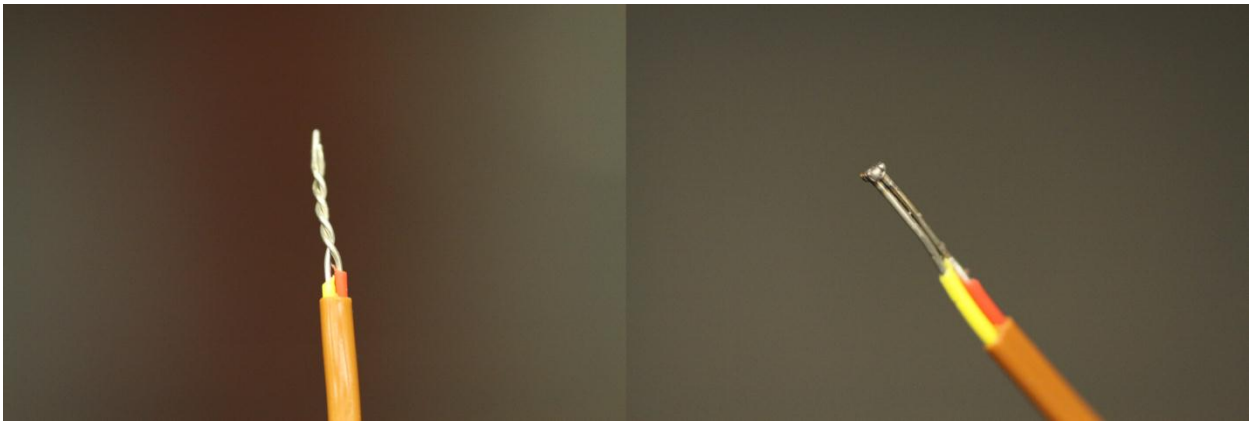


Figure 7 Twisted Pair (left) and Welded TC (right)

The other two ends of the thermocouple are interfaced into a data acquisition (DAQ) system or a voltmeter in order to measure temperature. The temperature measurement is done using Eq. (1), where the cold junction temperature, Seebeck coefficients of the materials, and voltage created by the emf are used to find the temperature at the end of the thermocouple.

3.6 Thermocouple Time Response

When taking measurements with thermocouples, the time response of the thermocouple must be considered. When a thermocouple is exposed to a transient change in temperature, there is a finite amount of time for the thermocouple's emf to correspond the full amount of change. The transient response time of a thermocouple can be defined from a first order, linear differential equation that results from the heat balance between the thermocouple and the surrounding fluid [4]. Figure 8 shows a thermocouple with a temperature (T). This thermocouple is surrounded by fluid with temperature (T_e) at time zero.

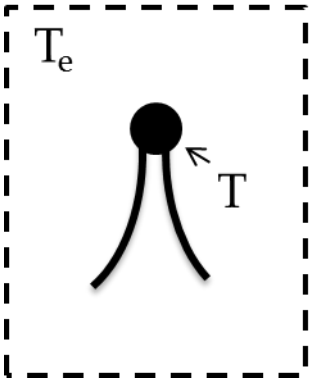


Figure 8 Thermocouple (T) and Environment (T_e) temperature balance

The energy balance for the thermocouple, neglecting thermal radiation transport, balances the convective loss from the thermocouple with the time rate of change in the thermocouple stored energy:

$$hA(T_e - T) = mc\frac{dT}{dt} \tag{7}$$

Where

m = Thermocouple mass

c = Specific heat capacity of the thermocouple material

h = Heat transfer coefficient

A = Thermocouple heat transfer surface area

Eq. (11) is rewritten in the form of a first-order ordinary differential equation [6]:

$$\tau \frac{dT}{dt} + T = T_e \tag{8}$$

Where the time constant, τ, for thermocouple is defined as [6]:

$$\tau = \frac{mc}{hA} \tag{9}$$

For the sudden change in fluid temperature at time zero, the thermocouple temperature can be solved as a function of time,

$$T = Ce^{-t/\tau} + \frac{1}{\tau}\int_0^t T_e\, e^{-t/\tau} dt \tag{10}$$

Where

T = Thermocouple temperature

C = Integration constant

τ = Time constant

t = Time

T_e = Environment temperature

Temperature may be normalized to form the non-dimensional outcome:

$$\frac{T_e - T}{dT} = e^{-t/\tau} \tag{11}$$

Where dT is the temperature change in the fluid at time equal zero.

The heat balance between the thermocouple and its environment as presented by ASTM [4] defines time constant, τ, as the time it takes for a thermocouple to reach 63.2% of its final value. This corresponds to the time when the temperature difference between the thermocouple and the environment has been reduced by e^{-1} (36.8%) of the initial difference [4]. When this value is subtracted from one ($1-e^{-1}$) the result is 63.2%. Figure 9 from the University of Colorado shows the transient response of a thermocouple. The response curve is based on an exponential of the actual time over the time constant. While 63.2% of the final, or new, temperature is reached after one time constant, it takes 5τ for the value to reach 99.3% of the new temperature value.

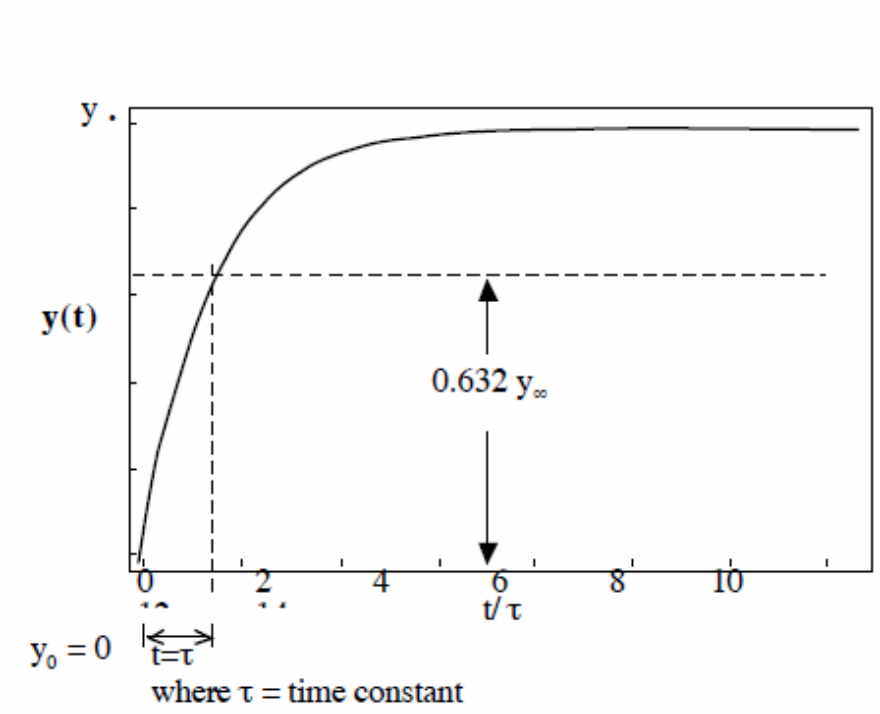


Figure 9 Transient Response of a Thermocouple [6]

Thus, the time constant is directly related by both thermocouple and flow properties. Thermocouple properties include *m*, *c*, and *A*. The heat transfer coefficient, *h*, is based on the type of heat transfer. For twin jet mixing, forced convection is of primary interest and is presented here in detail. The mixing may also produce eddies whose heat transfer to the thermocouples may act as transient conduction. Natural convection and transient conduction are also of interest in tests presented later, and are presented briefly in this section.

3.6.1 Forced Convection

Flow properties influence the time constant through the convection heat transfer coefficient, which is a function of not only flow velocity but material properties such as viscosity and thermal conductivity.

In order to find the heat transfer coefficient, we must find the Reynolds and Nusselt numbers for the flow in question.

In terms of geometry, the thermocouple will be modeled as a cylinder.

Reynolds number (Re) is a non-dimensional number that corresponds to the ratio of inertial and viscous forces in a flow. For a cylinder in a flow the Reynolds number is equal to:

$$Re = \frac{\rho V D}{\mu} \tag{7}$$

Where

Re = Reynolds number

ρ = Density of flow medium

V = Flow velocity

D = Diameter of the thermocouple

μ = Dynamic viscosity

The Nusselt number (Nu) is a non-dimensional number that corresponds to the ratio of temperature gradient at the wall of a surface to the overall temperature difference in the flow. There a various correlations for the Nusselt number corresponding to various flow scenarios and Reynolds numbers. For water, an equation that holds well for all ranges of Reynolds number is the Churchill–Bernstein Equation shown in Eq. (8).

$$Nu = 0.3 + \frac{0.62 Re^{1/2} Pr^{1/3}}{[1 + (0.4/\mathrm{Pr})^{2/3}]^{1/4}} \left[1 + \left(\frac{Re}{282000}\right)^{5/8}\right]^{4/5} \tag{8}$$

Where

Nu = Nusselt number

Pr = Prandtl number

For liquid metals, such as mercury, a different correlation for the Nusselt number is used.

$$Nu = 5 + 0.025(RePr)^{0.8} \tag{9}$$

Equation (9), as presented in Todreas and Kazimi, is applicable for liquid metal flows around a circular tube with a uniform axial wall temperature. [7]

Finally the heat transfer coefficient can be calculated as:

$$h = \frac{Nu * k}{D} \tag{10}$$

Where

k = Thermal conductivity of the medium

D = Thermocouple diameter

This can then be used to solve Eq. (9) for the time constant for a thermocouple experiencing a transient temperature change in a flow.

3.6.2 Natural Convection

As with forced convection, the heat transfer coefficient for natural convection is based on finding the Nusselt number. The Nusselt number is dependent on the Raleigh number (*Ra)* which is a ratio of convection terms multiplied by the Prandtl number.

$$Ra = \frac{g\beta(T_s - T_\infty)L_c^3}{\upsilon^2} Pr \tag{11}$$

Where

g = Acceleration due to gravity

β = Thermal expansion coefficient (1/Temp for an ideal gas)

L_c^3 = Characteristic length

υ^2 = Kinematic viscosity

A correlation for Nusselt number is chosen based on the flow scenario and Raleigh number; typically of the form of a constant '*C*' multiplying '*Ra'* raised to an exponent 'n' as in Eq. (12).

$$Nu = CRa^n \tag{12}$$

3.6.3 Transient Conduction

Transient Conduction is used to describe thermocouple response during a plunge test in which they are plunged into water. Transient conduction for a thermocouple can be approximated using lump system analysis. For small bodies such as a thermocouple, the temperature is assumed to be only a function of time (the interior temperature of the body is uniform) [8]. The Biot number (Bi) is the ratio of surface conductance over internal conduction of a solid [7]. For

lumped system analysis, it is assumed that the internal conduction of the solid is much greater than the surface conduction. Essentially, any heat transferred at the surface is quickly transmitted throughout the body. This results in Biot numbers for thermocouples being small less than 0.001.

$$Bi = \frac{hL_c}{k} \tag{13}$$

Where 'Bi' is Biot number, 'h' is the heat transfer coefficient, and 'k' is the thermal conductivity.

The time response can be calculated as shown in (14) from Cengel [8].

$$\%\ of\ Final\ Temp = \frac{T(t) - T_\infty}{T_i - T_\infty} = e^{-\frac{h}{\rho c_p L_c}t} \tag{14}$$

As shown in (14), the ratio of the heat transfer coefficient to the density and specific heat of the material drive the time response of a thermocouple in transient conduction. The time response can be found by solving for 't' which is in the exponential on the right hand side of the equation.

In the jet mixing region area, the thermocouples may be exposed to an eddy in which the heat transfer turns into a mix of forced convection and transient conduction. Due to the scenario just mentioned, transient conduction as it relates to the time response will be examined in a later test.

Chapter 4. Water Thermocouple Rake

It has been established that thermocouples are simple, reliable temperature sensors that have a variety of applications. For each application a system has to be designed to allow the thermocouple to be moved into the position of interest or remain there. The system being monitored dictates the manner in which the thermocouples are applied. A single thermocouple can be placed inside a thermocouple well to measure bulk temperature in a pipe flow. Multiple thermocouples can be used to find the temperature gradient of an object, such as an aircraft wing which requires thermocouples be attached and spaced along it. The twin jet project requires multiple thermocouples immersed in a flow to measure temperature along a specified length. A simple rake design meets the criteria to provide the necessary measurements. An AutoCAD drawing of a simple rake concept was done by an undergraduate research assistant and is shown below in Figure 10. The simple concept includes a long mast that is attached to a rake head, which has thermocouples protruding from it. This simple concept was used as a basis for the design.

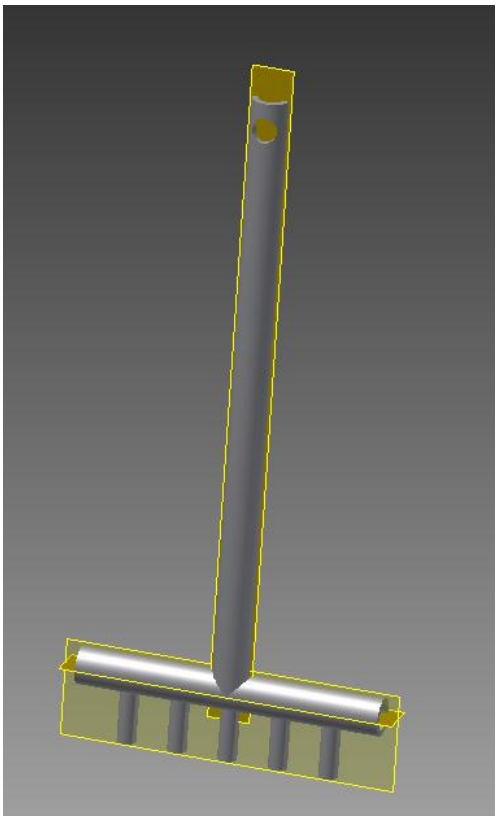


Figure 10 Rake Concept

4.1 Design Criteria

The fact that the water rake was to be built first was advantageous from the standpoint of design constraints. Working in mercury adds extra constraints to the rake design, as will be discussed later. While some mercury specific constraints were ignored; others were incorporated into the water design in order to provide insight for the mercury design. Rake size and geometry, materials, and thermocouple choice play into the design decisions made about the thermocouple rake. Budget was also a factor. Whenever possible, parts that were readily available on the shelf were used. This not only saved money, but it eliminated having to wait for shipped parts.

4.1.1 Rake Size

The thermocouple rake is to make measurements in a large water tank that has two mixing jets in the middle of it. The estimated jet length to be measured was estimated as being 10″ inches.

This was used as the length of the rake head. The thermocouples protruding from the rake head would need to be delivered to a depth of roughly 3' feet inside the tank.

4.1.2 Materials

Any material that would not have corrosion issues could be used for the water run. These include PVC piping, aluminum, and stainless steel. However, the selection for materials was made with the mercury rake design in mind. Stainless steel is corrosion resistant and non-reactive with mercury (unlike aluminum which is reactive). Additionally, there was stainless steel stock tubing suitable for the rake mast and head in house. The final material selected for use in the thermocouple rake was 316L stainless steel. 316L Stainless steel is a steel alloy made up of chromium (Cr), nickel (Ni), and molybdenum (Mo), with 'L' denoting a low carbon steel that is a no more than 0.03% carbon by weight. The percent by weight fractions of each element in 316L is shown in Table 1.

Table 1 316L Composition by Weight [9]

Element	% by Weight
Fe	62-72%
Cr	16-18%
Ni	10-14%
Mo	2-3%
C	0.03%

4.1.3 Geometry and Shape

The simple geometry is essentially set by the concept of a rake. However, two choices were made in regards to this category. The first was that the thermocouple rake did not have to be sealed. While this will be necessary for a mercury rake, it was unnecessary for the design of the water rake. The benefit of not sealing the rake is that various gaps could be added to the design to decrease the difficulty of running the thermocouples through the rake mast and into the head. The second choice was to attach smaller stainless steel tubing to the rake head to act as

spokes for the thermocouples. Putting a cylinder such as the rake head into a flow causes an interaction with the flow, changing what is being measured. Minimizing this flow interaction was viewed as a design goal. Attaching the smaller tubing to the head and running the thermocouples through it allows the thermocouple wire to be extended further away from the head. Without the spokes the thermocouples, being flexible, could be buffeted by the flow. This could cause inaccurate data, as the position of the thermocouple would be in question.

4.1.4 Thermocouple Choice

The choice of thermal couple was made largely by what was on the shelf. Thermally, the thermocouple should experience a temperature range of temperatures ranging from 68°F (20 °C) up to 165°F (74 °C). Another factor influencing thermocouple choice was the space requirements of fitting ten thermocouple wires through a 0.625" in mast. There are a variety of inexpensive thermocouples that are suitable for the given temperature range. Three spools of thermocouple wire were on hand in the lab. They are shown below in Table 2 where AWG stands for "American Wire Gauge". The decision on which thermocouples to use was a size consideration. The 20 gauge thermocouple wire seemed to small and flimsy; there were concerns with its sheathing durability to being dragged through the thermocouple rake and the increased difficulty in constraining a smaller thermocouple wire at the end of the rake . The AWG 30 wire was too fat and would require larger tubing than what was available to fit ten wires through.

Table 2 Thermocouple Sizes and Types

Type	AWG	Diameter (in)
K	20	0.0320
K	24	0.0201
T	30	0.0100

In terms of accuracy, Type T thermocouples over a range of -59 to 93 °C have an accuracy of +/-1 °C, where as a Type K thermocouples from 0 to 277 °C have an accuracy of +/- 2.2 °C [2]. While an ideal choice would be a lower gauge Type T thermocouple, a choice had to be made between thermocouples available on the shelf and as mentioned above, there was design concerns based

on the thermocouple wire size. Based on all of the observations made above; 24 gauge Type K thermocouples were settled on for the thermocouple rake.

4.2 Rake Final Design

The final design for the water rake is shown below in Figures Figure 11 and Figure 12.

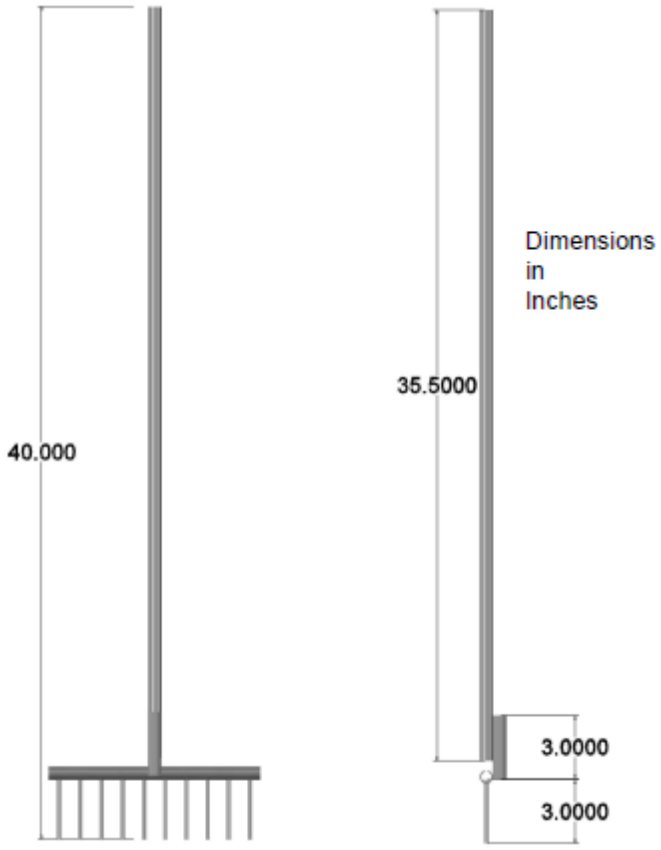


Figure 11 Final Design: Full View

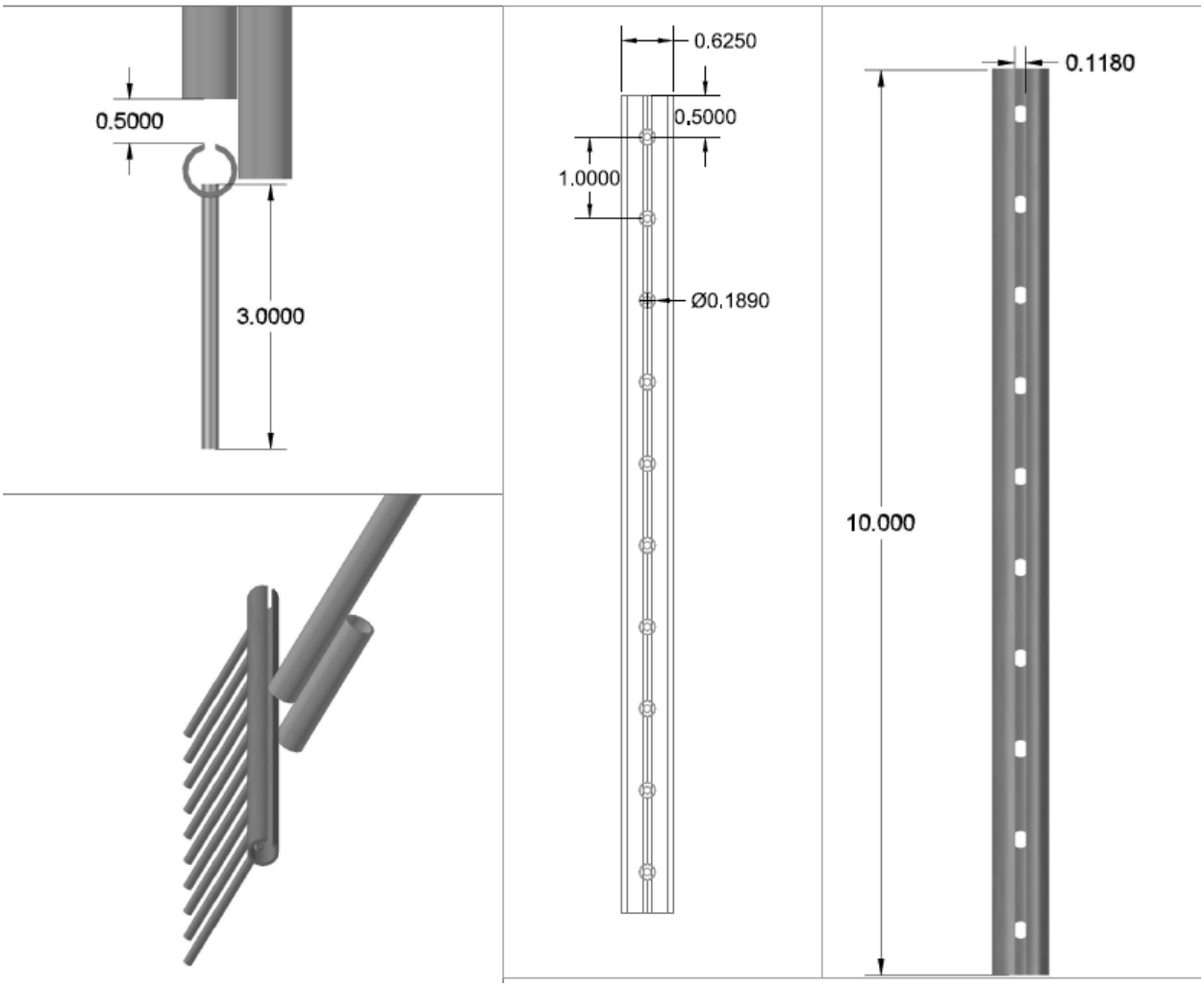


Figure 12 Final Design: Rake Head Detail, Dimensions in Inches

The final design used two sizes of stainless steel tubing. The larger tubing used in the mast and head has dimensions OD 0.625 inch/ID 0.490 inch (outside diameter/inside diameter). The smaller tubing used in the rake spokes measures OD 0.188 inch/ID 0.1 inch. The head has a 0.1180 inch wide notch cut out along the top and has holes for the spokes to be inserted into. The spoke holes begin ½ inch from the end of the head and are spaced 1 in apart. The mast head is comprised of two parts, a 3 inch support length that the longer mast attaches to. This is done in order to leave a ½ inch gap over the rake to decrease the difficulty involved with pulling wire through the rake mast and ultimately the spoke tubing. The rake is designed to be attached by welding, in total 12 parts require welding. The 10 rake spokes weld into the head,

which in turn is welded onto the 3 inch support length which, finally is welded onto the longer mast.

4.3 Rake Build

The initial step toward building the rake was to properly machine the head piece from the stock tubing. After using a band saw to cut a 10 inch length of tubing, the tubing was placed on a milling machine. The notch in the head was then made using the milling machine as shown in Figure 13.

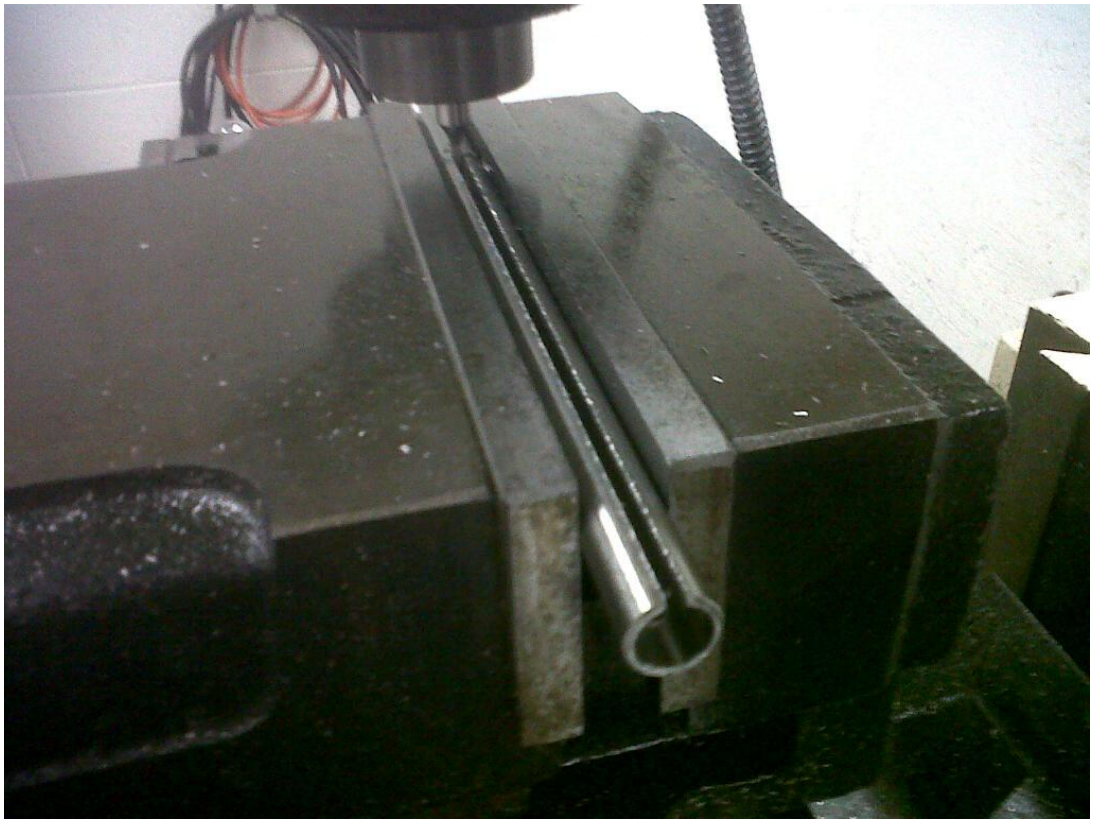


Figure 13 Rake Head on Milling Machine

Following the carving of the notch, the milling machine was used to accurately drill the 10 holes for the spokes into the rake head. The result of that operation is shown in Figure 14.



Figure 14 Rake Head with Spoke Holes

Finally, the rake had three major areas of welding: (1) between the mast and the 3 in support length, (2) attaching the support length to the head, and (3) to attach the 10 rake spokes to the head. The numbers previously shown correspond to labels shown in Figure 15 which highlight the locations of each weld. The welding was done by Larry Roberts who is a technical specialist in the Civil and Environmental Engineering machine shop at the University of Tennessee. Gas tungsten arc wielding (GTAW), which is also known as tungsten inert gas (TIG) welding, was used.

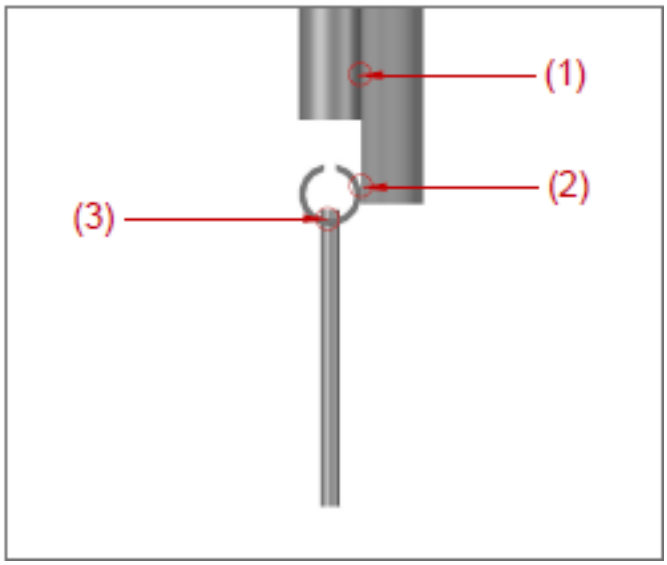


Figure 15 Welding Diagram

The finished steel product is shown in various pictures below.

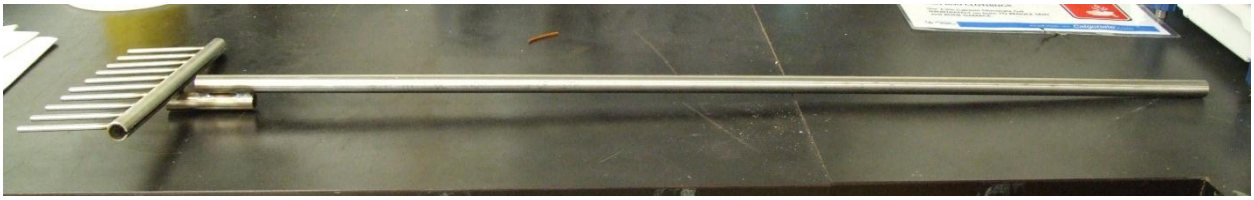


Figure 16 Full View of Finished Steel Work

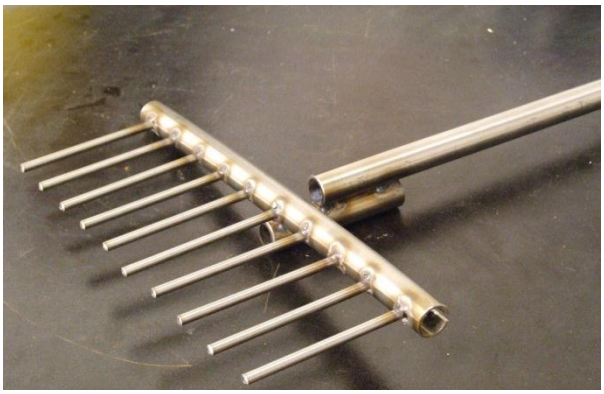


Figure 17 Close up of Rake Head

Once fabrication of the rake was complete, the next step was to run thermocouple wires down the mast and through the spokes. It was discovered, however, that the tubing used for the spokes had become obstructed during the welding process. The weld had undergone a phenomenon known as 'sugaring' to welders. Sugaring occurs when the backside (in this case the inside of the tubing) of a GTAW stainless steel weld is exposed to oxygen [10]. Chromium is leeched from the steel and produces an oxide with the oxygen; this chromium oxide is the obstruction mentioned above. After discussing the problem with the civil shop technician who performed weld, it was determined that the problem could be fixed in the future by using larger tubing and a purging gas. 'Purging' a weld is the process in which an inert gas is ran through the backside of the welding surface while part is being welded. This removes oxygen and will prevent or cut down on sugaring. It was initially intended to run the thermocouples through the spokes. However, the thermocouple wire could be directly exposed to water, making the obstruction problem surmountable using an alternative method that didn't involve running through the spokes.

With the spokes obstructed, an alternate method of running the thermocouples had to be used. The wires would still be run down the mast; however once they exited the mast the wires would be run on the outside of the rake and would be lashed to the spokes using fishing line. The benefit of this method was that the thermocouples could still be attached to the spokes. Thus extending them out from the head and minimizing the flow interaction without worrying about the wire moving in the flow, which was the intended design purpose of the spokes.

Before the thermocouples were run, the rake was put into the testing tank during a dye test. Figure 18 shows the rake sitting inside the flow created by two jets. The feed water for each jet had flow visualization dye added to it in order to visualize the flow field.

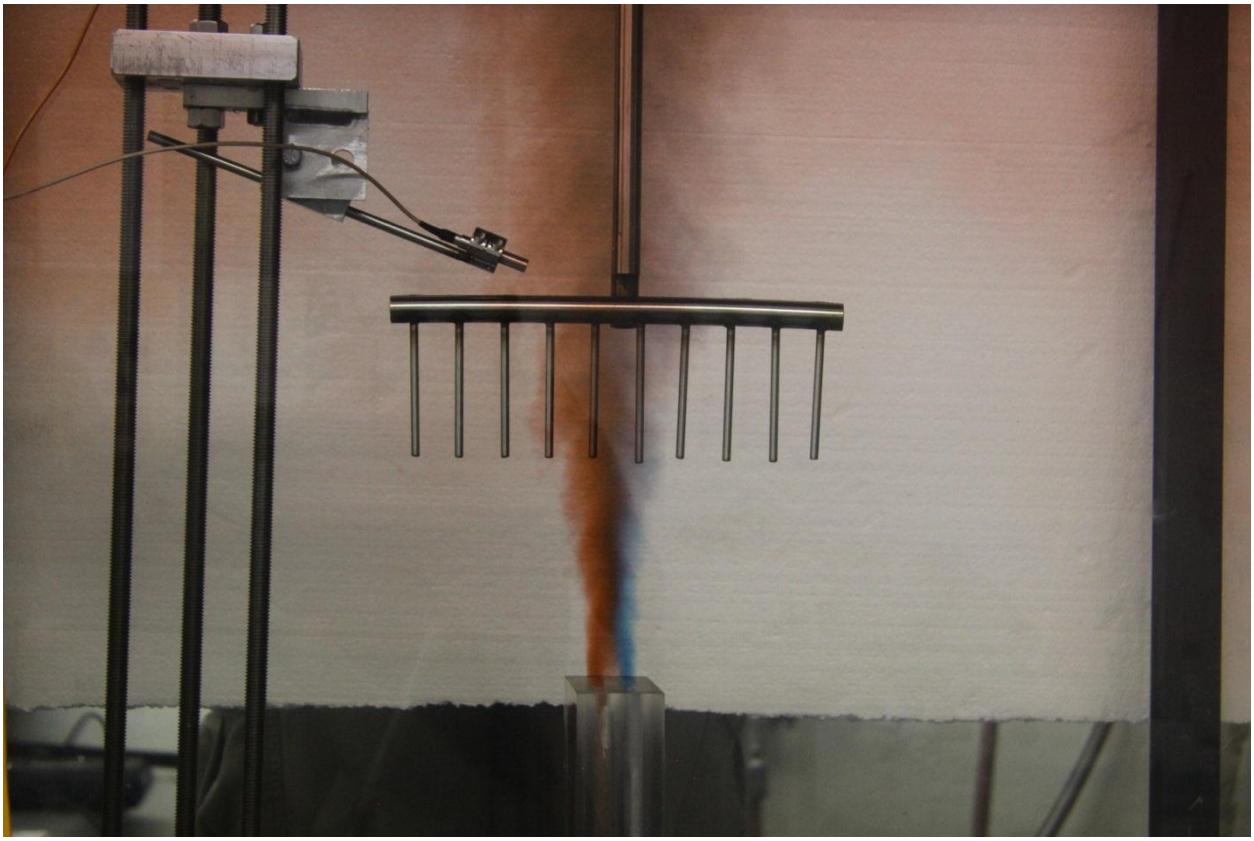


Figure 18 Rake in Dye Run

The rake was designed to provide measurements all the way to the top of the tank, where the width of the jet approaches 10 inches. However, more thermocouples were desired in the region where the jets first merged. It was decided that the inner two spokes in the middle of the

rake would each have two thermocouples lashed on either side of a spoke. This provides a higher resolution of measurement at the center of the rake.

Finally, the thermocouples could be prepared and attached to the rake. It was determined that the thermocouples needed to be cut into approximately 108 inch (approximately 274 cm) strands in order to provide enough wire when the rake was positioned at the top of the tank. Ten thermocouples were cut and had both ends stripped in order to expose the individual wires at both ends. One end of each thermocouple was then welded using a Hot Spot II TC Welder shown in Figure 19.

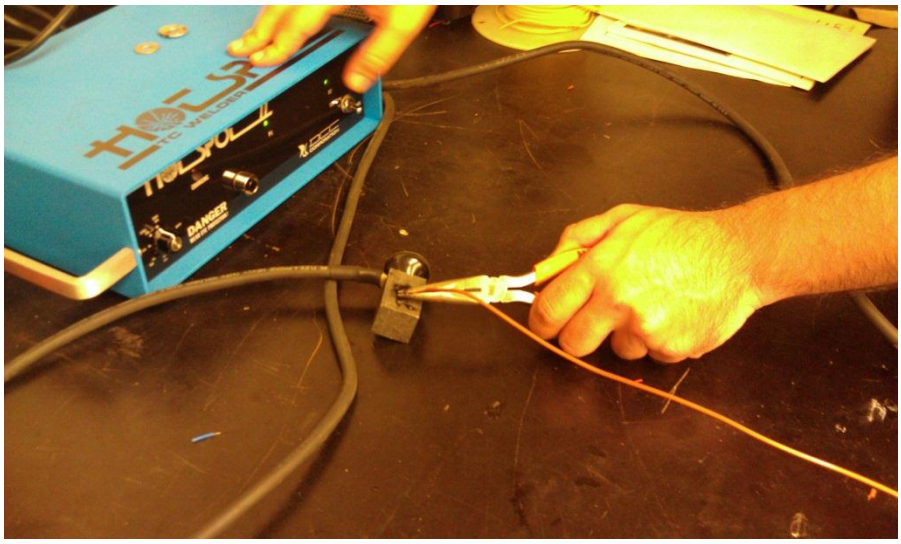


Figure 19 Thermocouple Welding

The wires were then tested for connectivity between the welded tip and each end using a multimeter before being run through the mast. This is shown in Figure 20.

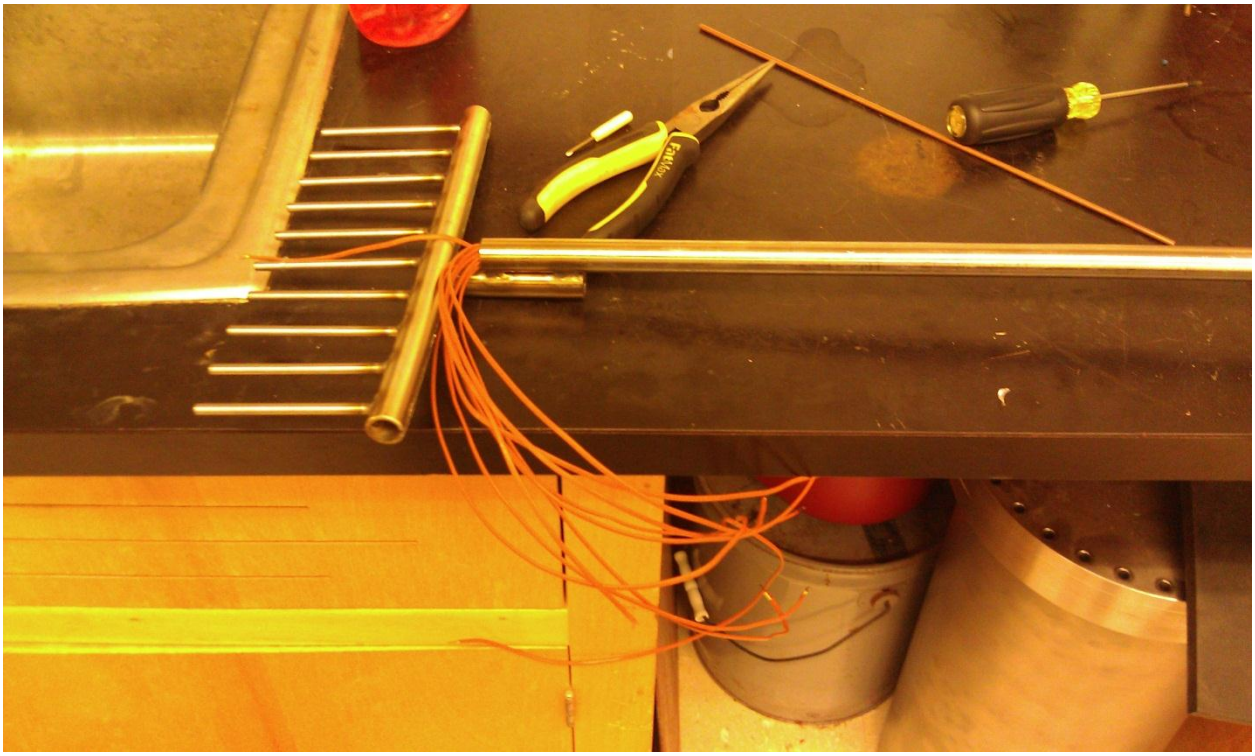


Figure 20 Thermocouple Wires through Mast

The next step was to attach the thermocouples to the spokes using a sheer lashing tied with fishing line. A shear lash requires three steps and two types of knots to construct:

1. Tie a 'clove hitch' around the spoke, Figure 21
2. Make three to four wraps around both the wire and the spoke
3. Tie another clove hitch, Figure 22 (bottom)
4. Tie the remaining ends from the clove hitches into a square knot and tighten, Figure 22 (top)

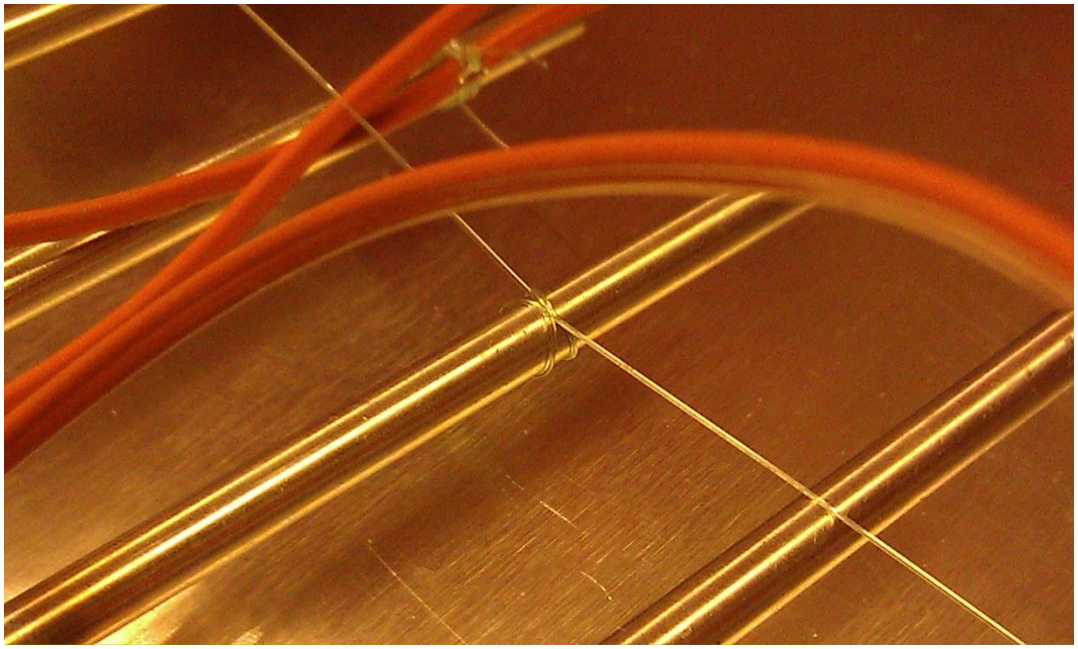


Figure 21 Clove Hitch

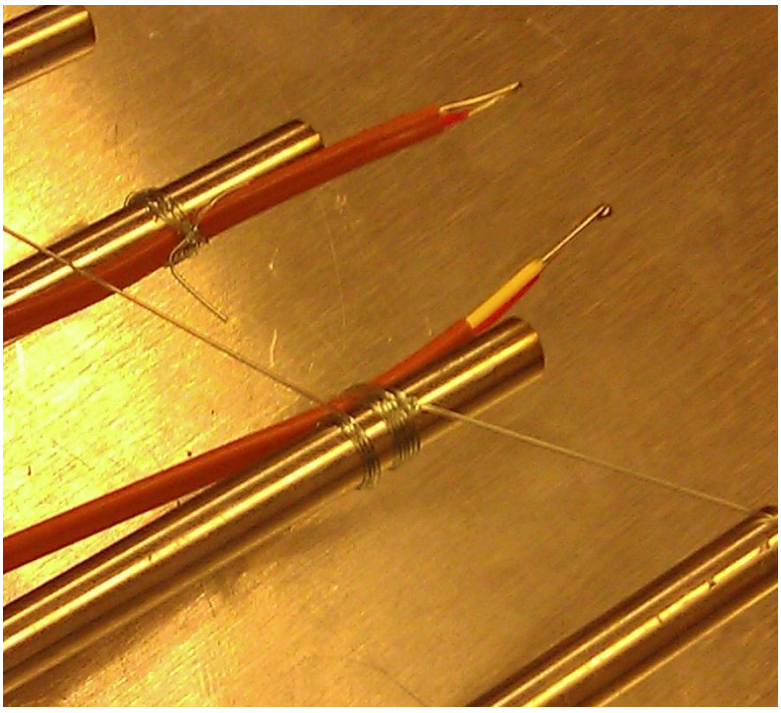


Figure 22 Sheer Lashing Step 3 (bottom wire) and Step 4 (top wire)

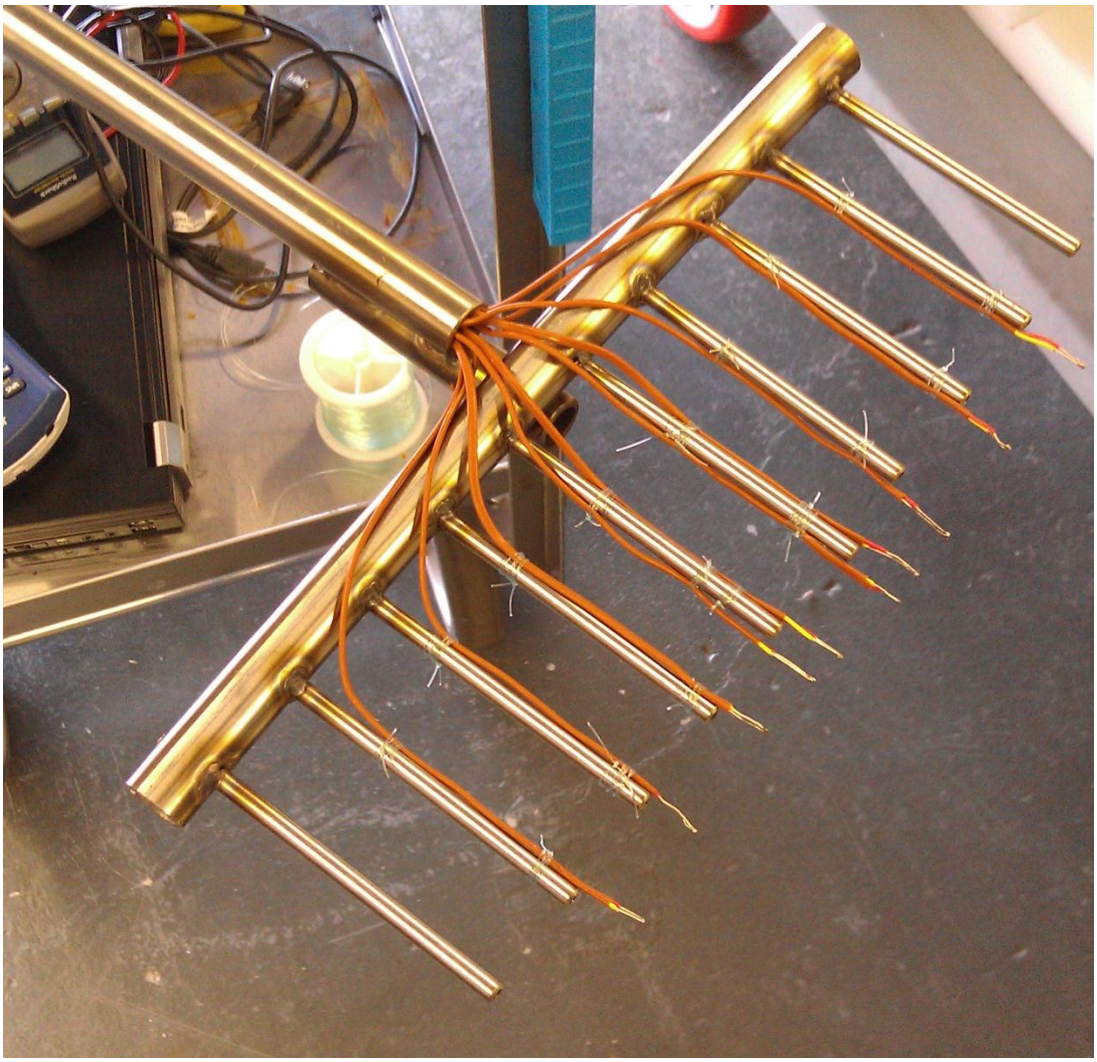


Figure 23 Finished Thermocouple Rake

Figure 23 shows the completed thermocouple rake. 10 Thermocouples were attached each requiring 2 shear lashes, the spokes with two thermocouples only needed 3 lashes for 2 thermocouples. This results in a total of 18 lashes for 10 Thermocouples.

At last, the thermocouple was connected to a National Instruments DAQ NI-6112 and mounted in the test section to log data.

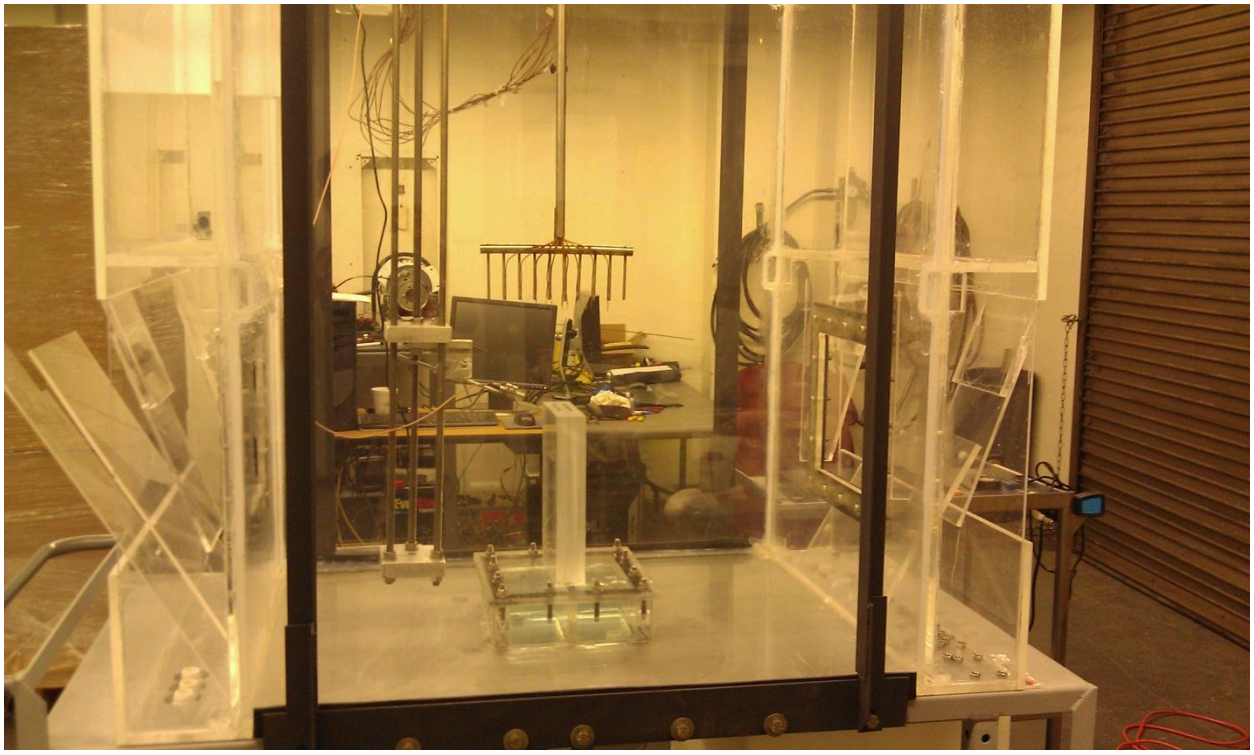


Figure 24 Rake Mounted in Test Tank

4.4 Summary of Construction

Despite encountering a few minor problems, the design and build of the thermocouple rake for use in water was largely a success. Being able to design and build the water rake before the mercury was very beneficial. As mentioned previously, water had less design constraints than mercury; and this allowed some flexibility in dealing with the encountered problems. Being able to encounter problems and have the flexibility to actually overcome them allowed this rake to be finished and provided crucial information for the design of the mercury rake. Essentially only two major problems were encountered: the obstruction of the rake spokes and the need for more thermocouples in the middle of the rake. The solution to lash the wires to the outside of the spokes not only solved the first problem, but provided an almost inherent solution to the second problem.

Chapter 5. Thermocouple Tests

This chapter lists various tests to characterize the time response and accuracy of the thermocouples. While the ultimate objective of this project was to take measurements in the twin jet test environment; various separate effects tests were done in order to move closer toward the final goal. These tests included, among others, gaining familiarity with the basic setup of a thermocouple system and characterizing thermocouple accuracy and time response.

5.1 Thermocouple Plunge Test

A basic 'plunge' test was undertaken as an initial step toward understanding thermocouple response time for the design of a thermocouple rake. The basic test involved plunging a thermocouple from room temperature into an ice water bath and recording the response. Being the first test undertaken, a variety of basic goals were set.

5.1.1 Initial Objectives

1. Gain familiarity with the setup of a thermocouple DAQ system
    - Thermocouple connection to DAQ
    - DAQ interface with the computer
2. Gain familiarity with taking measurements using National Instruments' LabVIEW software
3. Record time response data for Type K thermocouples
4. Do the previous steps using both DAQ systems available in the lab

5.1.2 Setup

The following materials were used in this test:

- 1x NI USB-6211 Multifunction DAQ
- 1x NI USB-6212 Multifunction DAQ
- 1x Omega HH11B Thermometer
- 2x Type K thermocouples 24 AWG made from Omega TT-K-24 spool
- 1x computer

- 1x ice bath

Figure 25 below shows the test setup, one thermocouple wired to each DAQ, which are in turn hooked into the computers USB slots, and an ice bath in proximity. It should be noted the ends of the thermocouples are twisted, as opposed to soldering or welding.



Figure 25 Test Setup

Since thermocouples require a cold junction correction 'CJC' for the temperature at the DAQ terminal, an omega thermometer was used to record the room temperature for the lab as shown in Figure 26. This value helps the DAQ make an accurate measurement of the temperature. An incorrect CJC would shift the temperature measurements up or down by a fixed amount based on the difference between room temp and the CJC specified in the system. This test was mainly designed to investigate time response issues, which are not necessarily dependent on the accuracy of the measurement. However, for the sake of learning proper usage of a thermocouple DAQ system, an accurate CJC temperature was used.



Figure 26 Room Temperature

Once a proper CJC was found, a LabVIEW file had to be setup to present the data. In the software's DAQ assistant, the system was setup to take 150 samples at 20 Hz using the CJC measurement of 20.6 C. The 'front panel' display is shown in Figure 27. This allowed the data for both DAQ systems to be presented in a neat, consistent, manner.

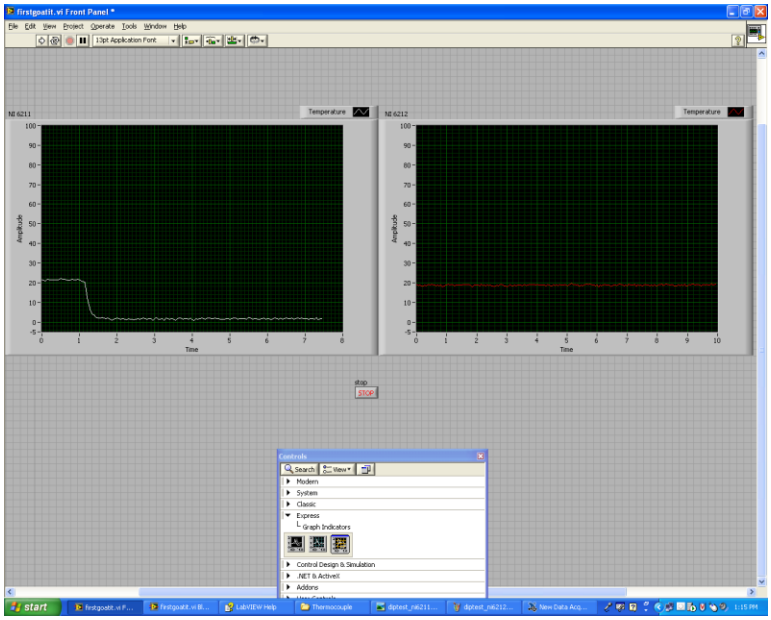


Figure 27 LabVIEW Front Panel

5.1.3 Procedure

Once the test was setup, the procedure was simple.

1. Run LabVIEW file
2. Observe that the thermocouples are recording room temperature
3. Plunge one of the thermocouples into the icebath
4. Stop the LabVIEW file when the graph shows the cooling curve recorded by the thermocouple

5.1.4 Results

Recall that the response of a thermocouple is a decaying exponential curve where the time constant, τ refers to the time when 63.2% of the final value has been reached. A value at which 99.7% of the final value, 5τ, has been reached is easily observed in the LabVIEW results. Figure 28 and Figure 29 show samples of the cooling curve result for each DAQ. The time of the cooling was interpreted as the time where the downward curve begins to the time when the value has reached a final steady state minimum.

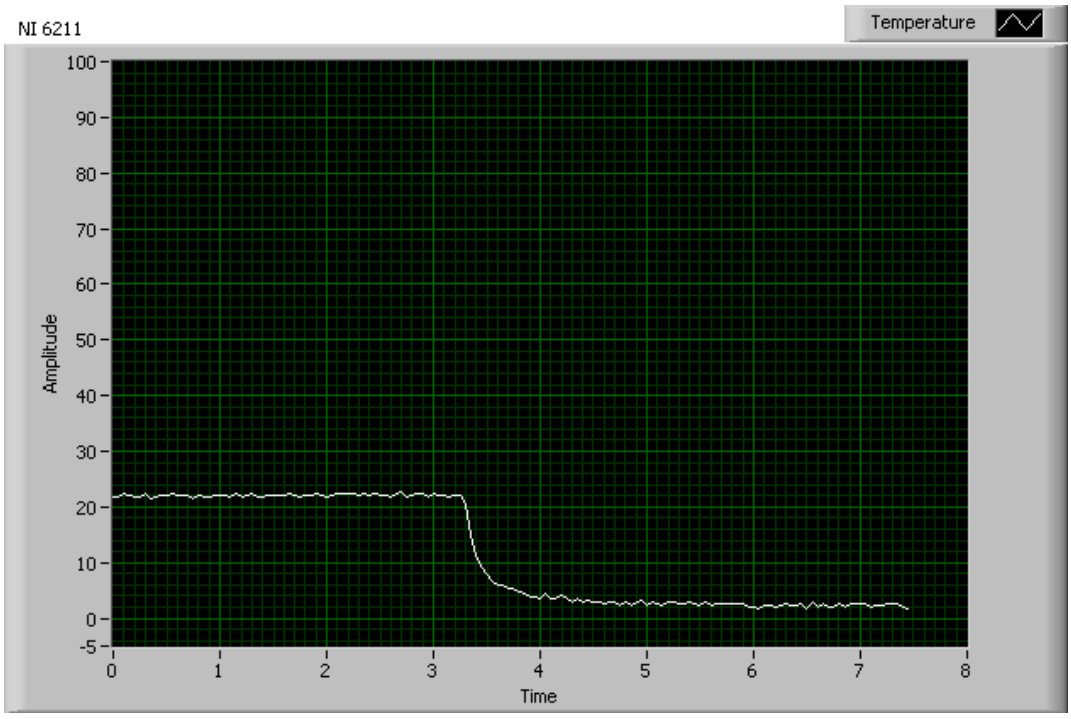


Figure 28 NI 6211 Cooling Curve

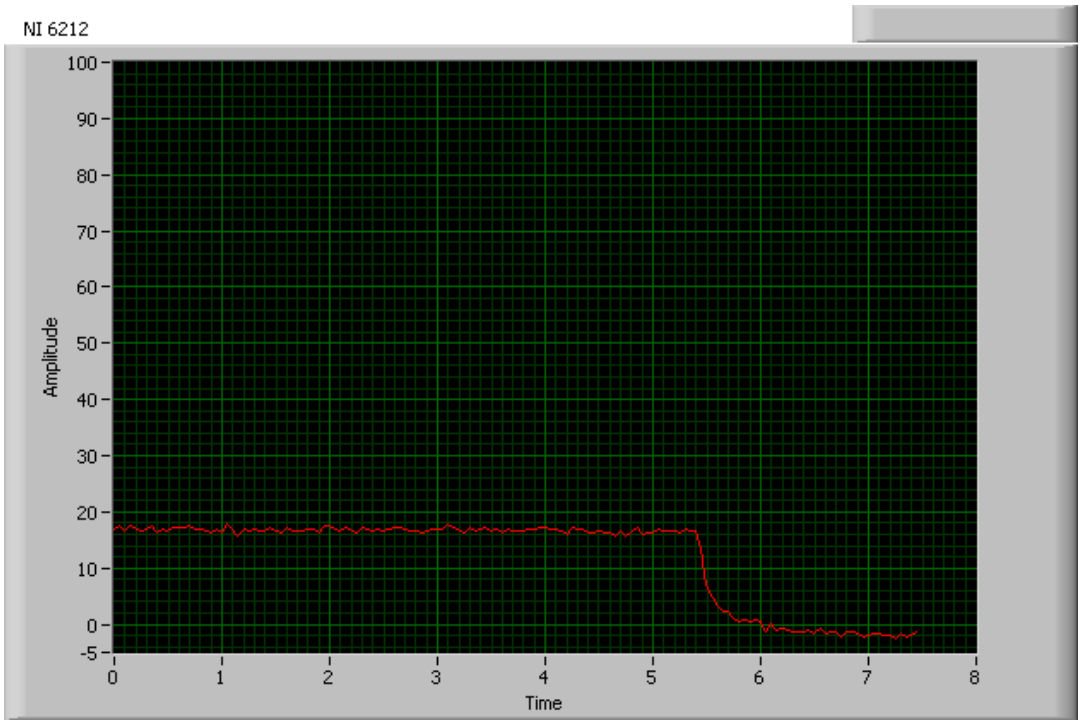


Figure 29 NI 6212 Cooling Curve

Table 3 Plunge Test: Full Response Times

Reading	NI 6211 (s)	NI 6212 (s)
1	1.3	1
2	0.85	1.2
3	0.9	0.8
4	0.9	1.1
Average	**0.9875**	**1.025**

The test data in Table 3 shows that both DAQs show a full time response (5τ) of roughly 1 second. This was estimated graphically, and is most likely conservative.

Table 4 shows the calculation for a freezing water bath, both natural convection and transient conduction are shown. The biot number is estimated to provide a heat transfer coefficient similar to those found in 5.3 during flow tests with ice water. If the biot number is increased

slightly, a coefficient similar to the natural convection case can be derived from the data, with a full time response of 0.367s.

Table 4 Transient Conduction vs. Natural Convection Time Constant Calculation

Water @ 0.01C Constants			
k W/(m*Δ°C) =	0.561		
Pr =	13.5		
v (m^2/s) =	1.7870E-03		
Radius Factor for Pair=	1.20000		
Pair Length (m)=	5.00E-04		
Material	Nickel		
Spec. Heat Cap. (J/kg*K)	446		
Material Density (kg/m^3)	8906		
k (W/m*K)	90.5		
Tinf (°C)	20		
Ts (°C)	100		
Natural Convection			
Wire Gauge	24		
Wire Diameter (m)	5.11E-05		
Raleigh Number	1.51E-06		
Nusselt Number	0.4090801	**Transient Conduction**	
h (W/(m^2*Δ°C)	4.59E+02		
Surface Area (m^2)	9.63E-08	Lc	8.52E-06
Mass (kg)	1.32E-08	Bi	0.00003
		h	318.79
τ (s)=	*0.1327*	b	9.42E+00
5τ (s) =	*0.6633*	*5τ (s) =*	*0.489*

5.1.5 Conclusions

Looking at the data, both graphical and numerical, it is shown that the time response for transient conduction is approximately between one half to a full second to reach a new temperature value. While the data doesn't match theory, one must keep in mind that the graphical data was interpreted conservatively and that the transient heat conduction model is also approximate and used an estimated heat transfer coefficient. The analysis done in the previous section only accounts for transient conduction into the thermocouple; this does not include conduction into the interface between the water and thermocouple. Water has a much higher heat capacity than water; this would slow the conduction in the interface and could account for the discrepancy between measured and theoretical data here. It should also be noted that for a thermocouple being plunged into an environment the time constant does not necessarily followed the first-order behavior assumed here [4]. Nonetheless, both sets of data and models show, consistently, the order of magnitude for the time response in this case.

This test, while insightful, highlighted two problems in narrowing down a time response for a thermocouple. First, the current LabVIEW setup does not let the user know the exact moment when the thermocouple is plunged into the ice bath. There is no way to know whether the cooling curve actually starts at the exact moment the thermocouple is plunged or a fraction of a second later. Second, the time over which the cooling curve begins is estimated graphically. Since thermocouple measurements, like any electronic measurement method, fluctuated slightly; the nature of the waveform makes determining the end time of the 5τ curve approximately.

Moving forward from a thermocouple standpoint, the time response in tests using flowing water will be undertaken. It was also found that improvements that need to be made on the LabVIEW DAQ front as well. The LabVIEW used for these initial tests only outputs data to the graph for a finite time period, resetting the graph at every time period or loop. For future tests, it will be not only useful, but essential to make a LabVIEW file that could output each loop into a file. This will allow data from time zero until stop time to be recorded. This will be especially necessary for the final thermocouple rake and its intended application.

5.2 Additional Plunge Test Work

After reviewing the data for the simple plunge test, it was apparent that the heat transfer coefficient for plunging the thermocouple into an environment was much different than when encountering a transient in a flow. Thus, additional runs were done where the TC was dipped into boiling water and allowed to cool by natural convection. Also, LabVIEW file was created that successfully writes to a comma separated values file (.csv) which is easily exported into Microsoft Excel for data visualization and analysis.

5.2.1 Objectives, Setup and Procedure

The objectives, setup, and procedure for this experiment are roughly the same as the initial plunge test work. The key difference is that here the thermocouple will be plunged into a boiling environment and then be allowed to cool via natural convection

5.2.2 Results

The heat transfer coefficient is well defined for the case of natural convection. For this set of tests, the time response sheet used for flow transient response was modified for natural convection. Table 5 below shows the data used to calculate the time constant for our thermocouples experiencing natural convection cooling in room temperature air. Two cooling curves are shown in Figure 30 and Figure 31. Some electromagnetic interference was encountered during the data collection for Figure 31. The data, however, is presentable with two portions of the curve removed; a running average trend line is added to the curve to fill the gaps for presentation purposes.

Table 5 Natural Convection Time Constant Calculation

Air @ 20C Constants	
k W/(m*Δ°C) =	0.02699
Pr =	0.7241
v (m^2/s) =	1.7500E-05
Radius Factor for Pair=	1.20000
Pair Length (m)=	5.00E-04
Material	Nickel
Spec. Heat Cap. (J/kg*K)	446
Material Density (kg/m^3)	8906
Tinf (°C)	20
Ts (°C)	100
Wire Gauge	24
Wire Diameter (m)	5.11E-05
Raleigh Number	8.44E-04
Nusselt Number	0.4884763
h (W/(m^2*Δ°C)	2.64E+01
Surface Area (m^2)	9.63E-08
Mass (kg)	1.32E-08
τ (s)=	*2.3093*
5τ (s) =	*11.5466*

Table 5 above was created using the methodology described in Section 3.6.2 to calculate the time response of a thermocouple exposed to natural convection heat transfer.

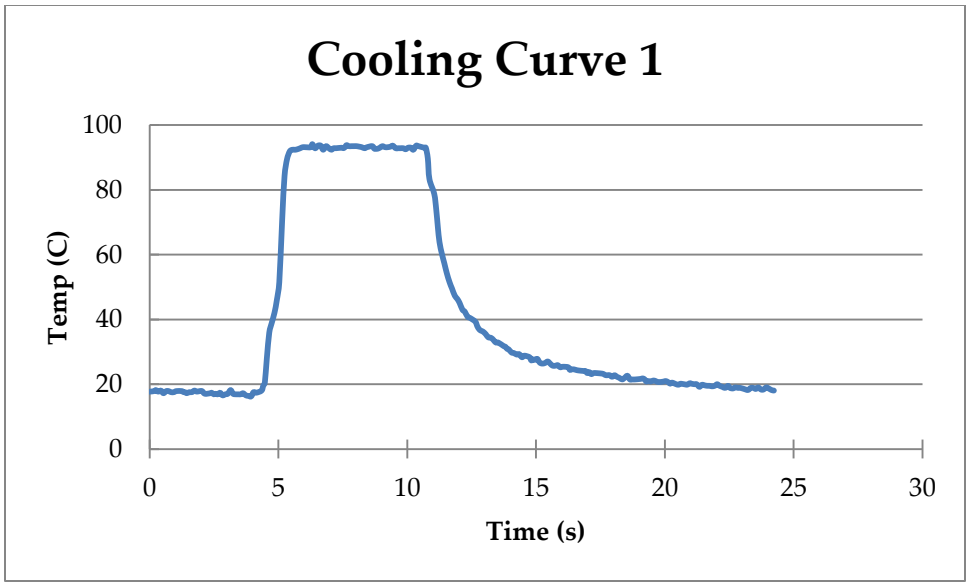


Figure 30 Cooling Curve 1

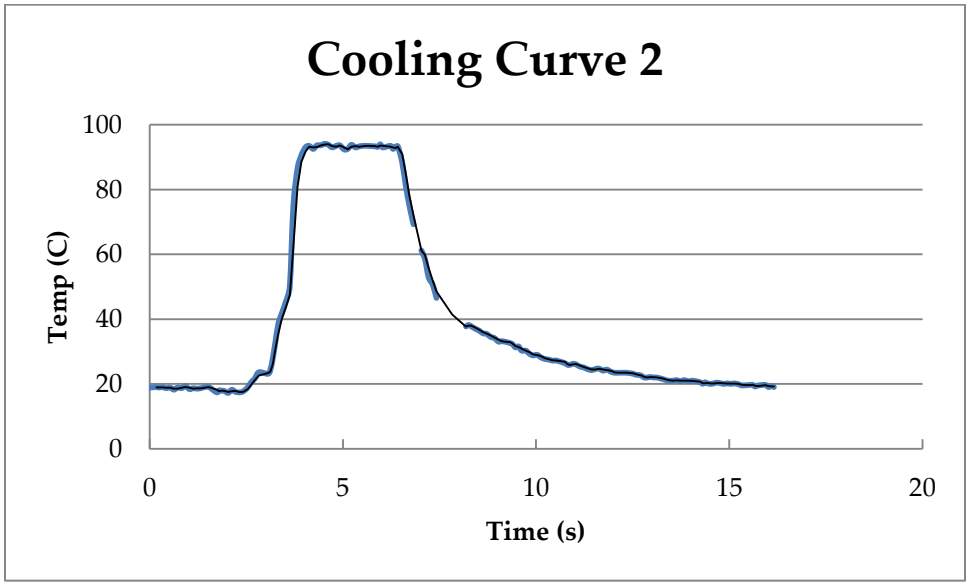


Figure 31 Cooling Curve 2

Table 6 Time Constant Data Comparison

Time	Curve 1	Curve 2	Theory
$5\,\tau$	9.515	11.331	11.547
τ	1.903	2.2662	2.309

5.2.3 Conclusions

The main conclusions drawn are that the time constants shown in Table 6 correspond with the time constants given in the theory. This is an experimental validation of the equation for time response given in 3.6 Thermocouple Time Response, Eq. (9).

5.3 First Flow Test

While the initial plunge tests provided an excellent initial experience with thermocouples; it still did not accurately model the environment they would be put into. Thus, the next course of action was to make an attempt at quantifying the time response for welded and twisted pair thermocouples in a flow consisting of water. A generalization of this test is: create a flow channel with a screened chamber near the inlet; dump ice into that chamber; and attempt to quantify the time response for the thermocouples to register the cooling of the flow.

5.3.1 Objectives

5. Create an open flow channel system to be used in the following objective
6. Evaluate the time response of Type K Thermocouples in a Flow

5.3.2 Setup

The following materials were used in this test:

- 1x NI USB-6212 Multifunction DAQ
- 1x Omega HH11B Thermometer
- 2x Type K thermocouples 24 AWG made from Omega TT-K-24 spool
    - 1x welded, 1x twisted pair
- 1x computer
- 1x 8 oz cup of ice
- 1x acrylic flow chamber
    - Dimensions: 2′ length, 3″ height, 2′ ¼″ width
    - Open flow channel with 2″ dam at the end
    - Inlet port connects via tubing to sink
- 1x sink

For this round of tests an open flow channel was created. Pictures of the channel are shown in Figure 32 and Figure 33. The channel was constructed out of 1/8″ thick acrylic plastic.

The channel measures 2′ long, 3′ tall, and 2′ ¼″ wide. The inlet has a mounted fitting to allow connection to a sink which will provide the flow. At 4 inches past the inlet, there is a vertical screen erected which makes an enclosure for ice to be dropped in. At 7 inches from the inlet (3 from the edge of the ice chamber) the thermocouples are mounted and allowed to be fully immersed at the top of the flow. The flow channel terminates in a 2 inch tall dam. Water is forced into the inlet using a standard sink faucet as the driving force and is allowed to freely flow over the dam back into the sink.

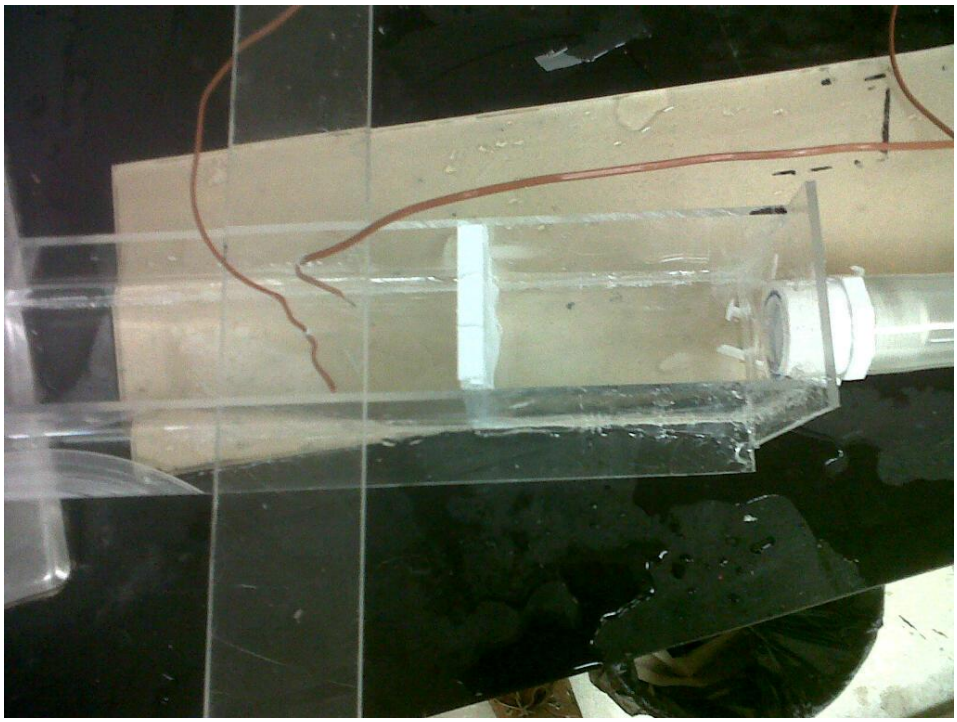


Figure 32 View of Inlet with Ice Chamber and Thermocouples in View



Figure 33 View from the End of the Flow Channel

With the flow channel constructed, the thermocouples were put in place and connected to the DAQ system.

5.3.3 Procedure

1. Run LabVIEW file
2. Use the Omega thermometer to measure room temp to use as the CJC
3. Turn on the sink and wait for the flow in the channel to reach a steady state
4. Recording the time down to a tenth of a second; dump the cup of ice into the ice chamber
5. Wait until the ice has completely melted and the flow has reached the supplied temperature from the faucet.

5.3.4 Results

The test data came out largely as expected; the data shows the thermocouple temperature dropping and then raising again as the ice in the chamber melts away. For this experiment it was assumed that any cooling transferred from the ice chamber to any point downstream was done so primarily by advection. It is thus assumed that once the ice is dumped, cooling at the thermocouples begins after such time that water flowing through the chamber travels the 3 inches downstream to the thermocouples. In order to calculate this 'offset' the flow velocity must be known. A flow meter is attached to the input port, allowing a particular flow rate to be recreated easily. For each run a flow rate of 1.16 gpm was recorded. A simple method is used to evaluate the velocity at the surface: a camera records a small piece of styrafoam being carried by the flow with a ruler in view.

In analyzing the data, three data points are shown in each graph. These are shown below with their respective number marker:

1. Insertion of ice into the chamber
2. Calculated time (based on flow velocity) for water from the chamber to reach the thermocouples after ice has been inserted
3. Point where 63.2% of the temperature drop was recorded

The time constant will be measured as the time between points 2 and 3.

This lab consisted of 2 runs; the first is shown in full detail below in Figure 34 and Figure 35. The sampling rate for both runs was arbitrarily set at 50 Hz. This value is adjusted later to avoid aliasing with 60 Hz noise.

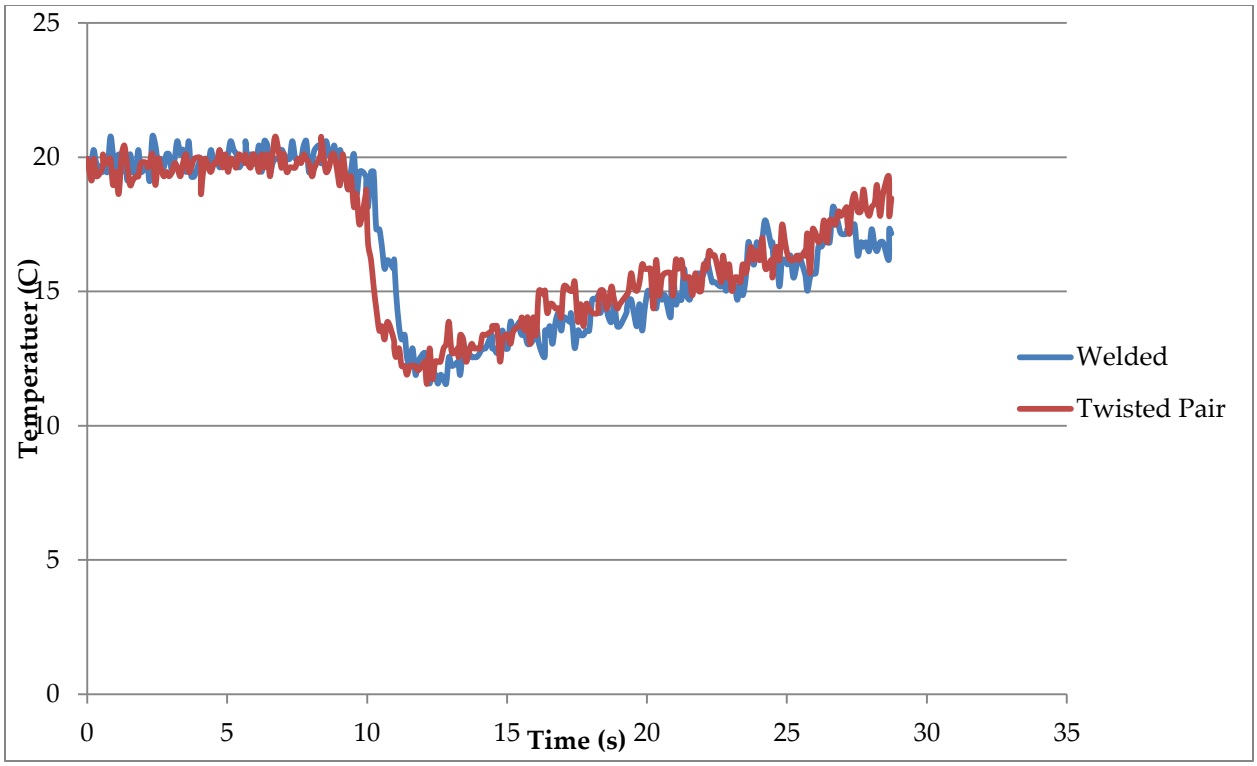


Figure 34 Full Data from Run 1

After reviewing the graph and the data; it was determined that a temperature drop from 20°C down to 12°C. This would make the temperature after the time constant has elapsed 63.2% of 20°C (14.94°C). This point occurs at 10.1 seconds and is shown below in Figure 35 which highlights the points of interest in the first data set.

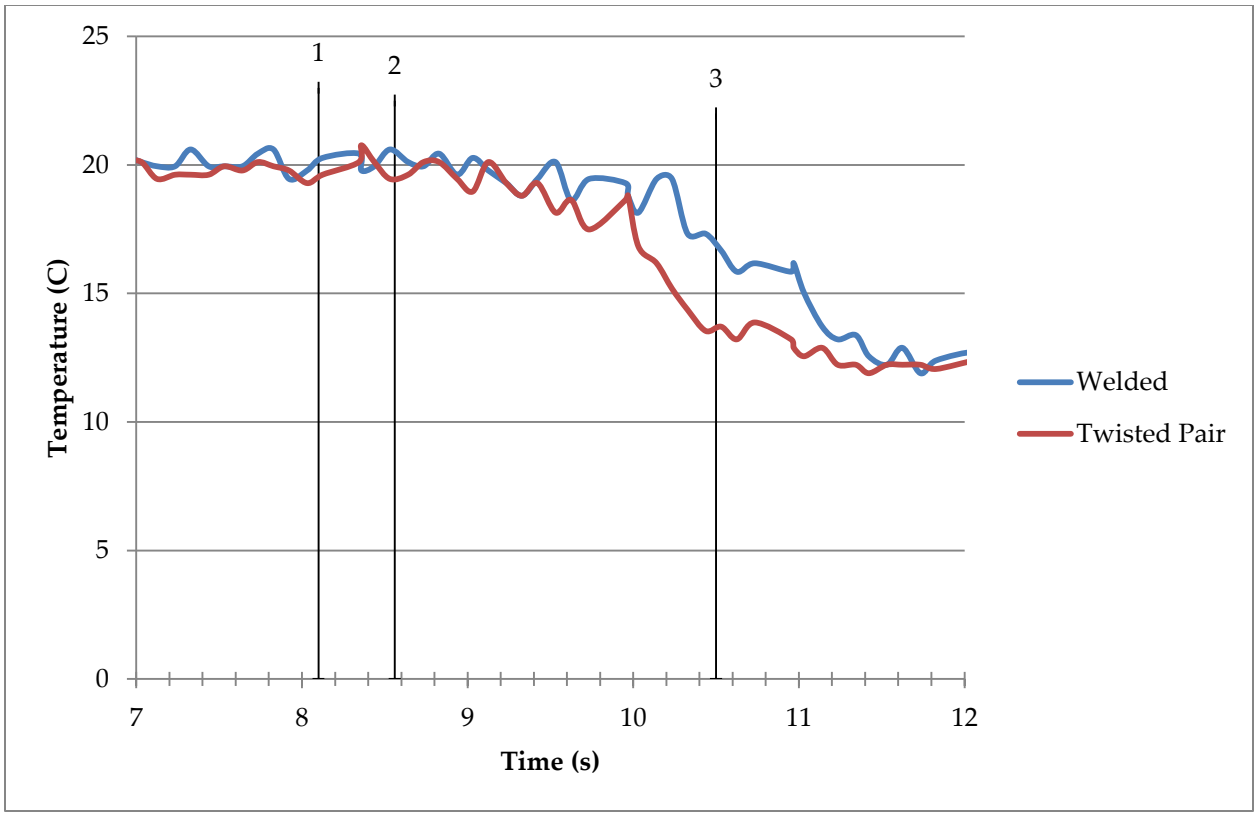


Figure 35 Data of Interest from Run 1

Table 7 Times of Interest from Run 1

Marker	Time (s)
1	8.1
2	8.56
3	10.5

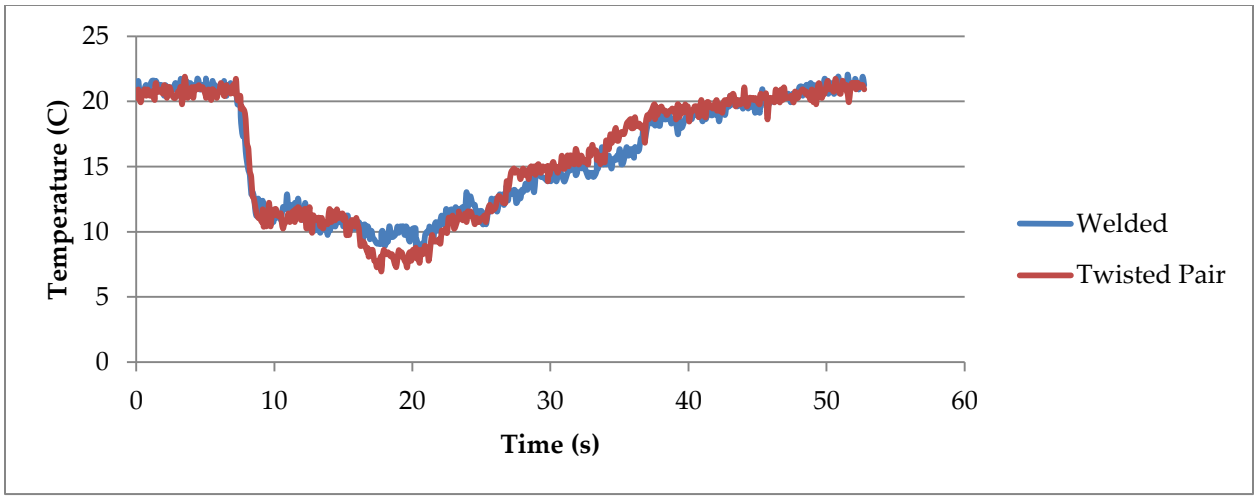


Figure 36 Full Data from Run 2

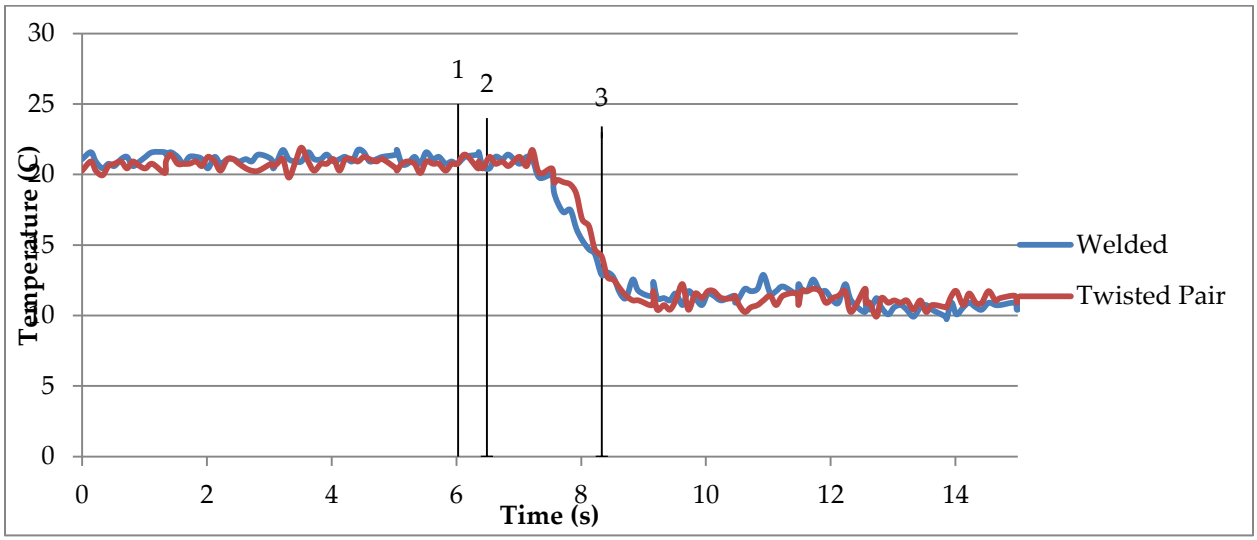


Figure 37 Data of Interest from Run 2

Table 8 Times of Interest from Run 2

Marker	Time (s)
1	6.03
2	6.49
3	8.33

Reviewing the data, the time constants for Runs 1 and 2 are, respectively, 1.99s and 1.84s. The time constants are found, as mentioned above, as being the difference between the time where 63.2% of the temperature change has occurred (marker 3) and the time when cold water reaches the thermocouples (marker 2).

Table 9 Forced Convection Time Constant Calculation

Water	
Local Constants	
Material	Nickel
Spec. Heat Cap. (J/kg*K)	446
Material Density (kg/m^3)	8906
Velocity (m/s)	0.1524
Wire Gauge	24
Wire Diameter (m)	5.11E-04
Reynolds Number	0.0001
Nusselt Number	0.3110591
h (W/(m^2*Δ°C)	3.03E+02
Surface Area (m^2)	9.84E-07
Mass (kg)	1.34E-06
τ =	*2.0073*
5τ =	*10.0366*

5.3.5 Conclusions

The test was largely successful. An open flow channel, which can be used for further thermocouple tests, was created and used to provide basic time response data for thermocouples in a flow. As expected, the thermocouple time response is much slower in a

flow compared to the response of a plunge test. The time constants recorded for the flow were much larger as those found for the basic plunge test and agreed with the forced convection model. Two major issues still need to be addressed, signal noise and the temperature change in the flow

The data is still "noisy". The uneven, non-cyclical fluctuations are obviously noticeable in both thermocouple signals. This could be caused by a number of things individually or collectively most likely improper sampling rate and electromagnetic interference (EMI).

While the channel setup with an ice dump did provide a cooling curve as predicted, the flow did not settle on a steady state minimum. As the run progresses with the ice dumped in, the ice melts and the temperature begins to rise again in the channel, as shown by the data. As a result, it is unknown whether the thermocouples actually reached the end of their time response or not. The idea behind this setup was that once the ice was dumped into the flow, it would impart roughly the same temperature change on the tap water flow at every time step, essentially providing a new steady state minimum that would last longer than the thermocouples response time. This was not the case as the ice melted quicker than expected. While data that lined up well with the theoretical values was obtained, a longer steady state final value needs to be maintained in order to fully show that the flow reached a minimum.

This initial round of flow tests provided some basic time response data for thermocouples in a flow. It also highlighted two issues in the current flow testing methodology. One of which, noise issues, must be dealt with moving forward. It also showed that numerical solution for thermocouple time response is appropriate and highlights that a slower time response should be expected for the twin jet mixing environment.

5.4 Calibration

Measurement devices in general need to be calibrated against known values in order to ensure their accuracy. As such, a calibration was done on the thermocouple rake. Calibration data for every thermocouple on the rake was obtained and entered into LabVIEW.

5.4.1 Objectives

1. Obtain calibration of a single TC over varying temperatures
2. Obtain calibration data for all thermocouples on the TC Rake

5.4.2 Setup

The following materials were used in this test:

- 1x NI USB-6212 Multifunction DAQ
- 1x Mercury thermometer FISHER brand 14-985B
- 1x Type K thermocouples 24 AWG made from Omega TT-K-24 spool, welded ends
- 1x Thermocouple Rake with multiple thermocouples
- Electric hot plate
- Beaker
- Ice

5.4.3 Procedure

Once the test was setup, the procedure was pretty simple.

1. Run the single TC through a range of temperatures
    a. Done by slowly heating water in a beaker on an electric hot plate
2. Plot the calibration curve for the single TC
3. Run every TC on the rake at boiling and freezing points
4. Obtain calibration data for every TC on the rake

5.4.4 Results

The results for the single TC are shown below in Table 10. Plotting the calibration curve, which is the actual temperature measured by the mercury thermometer versus the thermocouple's measurement. The main uncertainty in the measurement is the reading of the mercury thermometer which is +/- 1 °C

Table 10 Calibration Values for a Single Type K Thermocouple

Temp °C	TC °C
0	-2.08
11	7.6
17	12.7
18.5	14.62
20.5	16.74
22	17.58
100	94.27

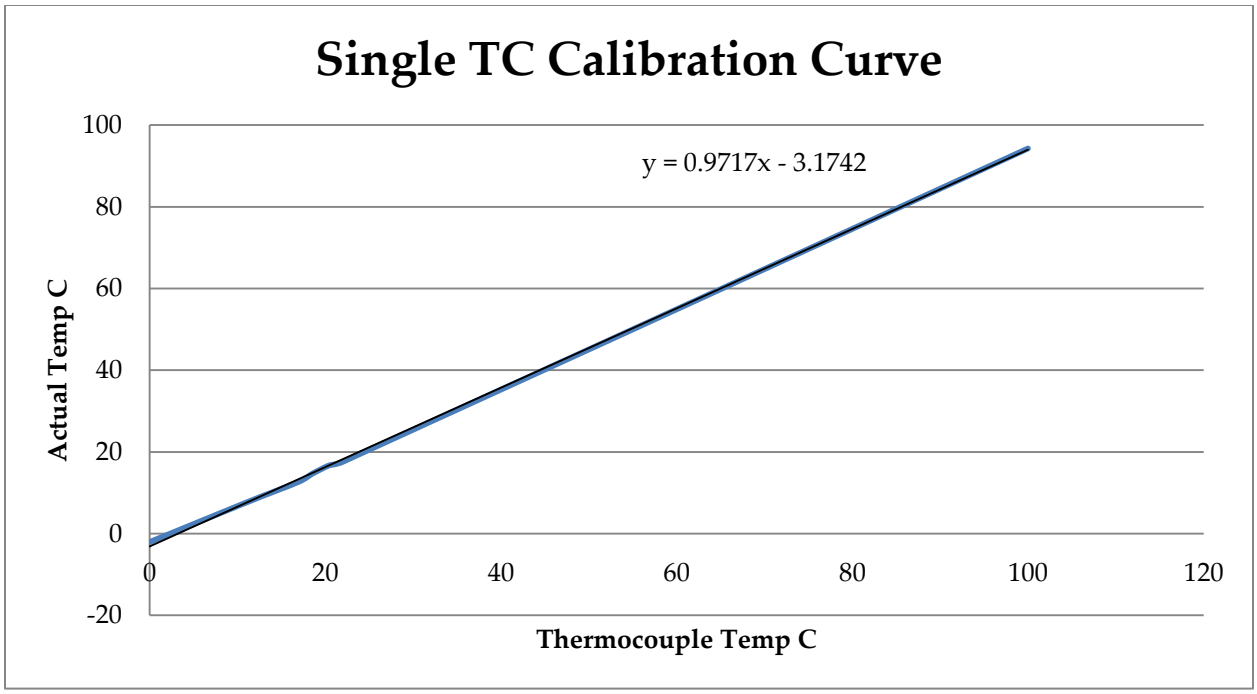


Figure 38 Single TC Calibration Curve

Figure 38 Single TC Calibration Curve shows the calibration curve for the single TC with a trend line and its equation imposed over the data. The line is mostly linear at first glance, but most of the calibration data was taken between 10 and 22 degrees Celsius, allowing the outliers of 0 and 100 to dominate the curve. To verify a linear line fit, a close up in the 10 to 22 Celsius range is shown with the trend line in Figure 39.

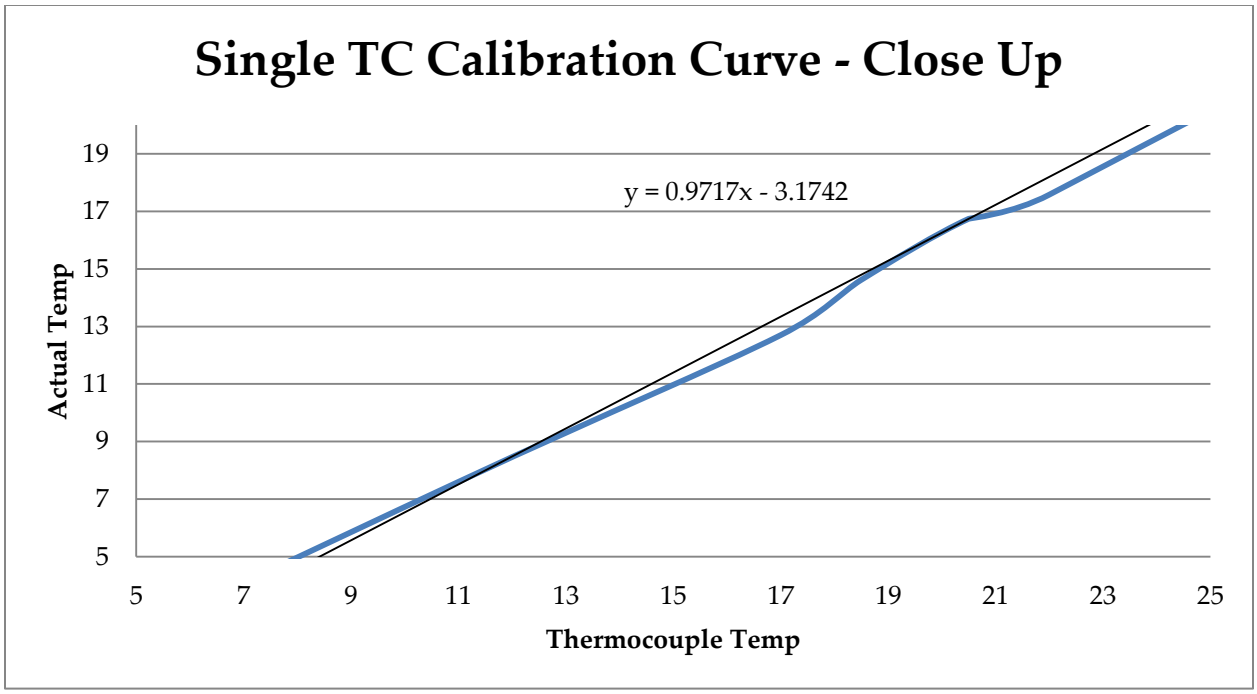


Figure 39 Close Up of Single TC Calibration Curve

Since a linear fit line provides an adequate approximation for a calibration curve, the thermocouple rake will be calibrated using only two calibration values at freezing and boiling. The data is shown below in Table 11. Each data point is the average of roughly 100 measurements taken while the TC was immersed in either an ice bath or boiling water.

Table 11 Rake Calibration Values

Rake Calibration Values		
TC	0 C	100 C
1	-1.50	93.54
2	-1.27	93.56
3	-1.97	93.51
4	-1.43	93.38
5	-1.73	93.18
6	-2.04	92.80
7	-1.26	93.19
8	-1.27	93.38
9	-1.85	93.06
10	-1.51	93.06

Interestingly enough, the statistical data for the rake calibration values shows that there is a very small deviation from the average un-calibrated value as shown in Table 11.

Table 12 Statistical Data for Rake Calibration

Statistical Data		
	0 C	100 C
Average Error	-1.58	6.73
Deviation	0.28	0.23

5.4.5 Conclusions

The calibration curve of a single type K thermocouple was shown to be approximately linear. This information was used in the decision to calibrate the TC rake using only two end points for the calibration curve. The data from the rake shows that the thermocouples, being of the same type and spool, do have similar calibration characteristics, as shown by the small standard

deviation in the full rake data. This test successfully provided calibration data that can be entered into LabVIEW to provide a better tolerance on the accuracy of the rake's measurements.

5.5 Interference and Signal Filtering

Thermocouples, being essentially long wires, sometimes act as a device that many of us use every day: an antenna. This behavior, coupled with the fact that the voltages produced by thermocouple emfs are on the order of mV, makes electromagnetic interference (EMI) a consideration in any thermocouple system. Throughout this project, EMI manifested itself as an issue, largely as 60 Hz interference caused by various electric systems.

5.5.1 Examples of Electromagnetic Interference

As mentioned previously, EMI could be observed throughout this project. Some examples are shown below:

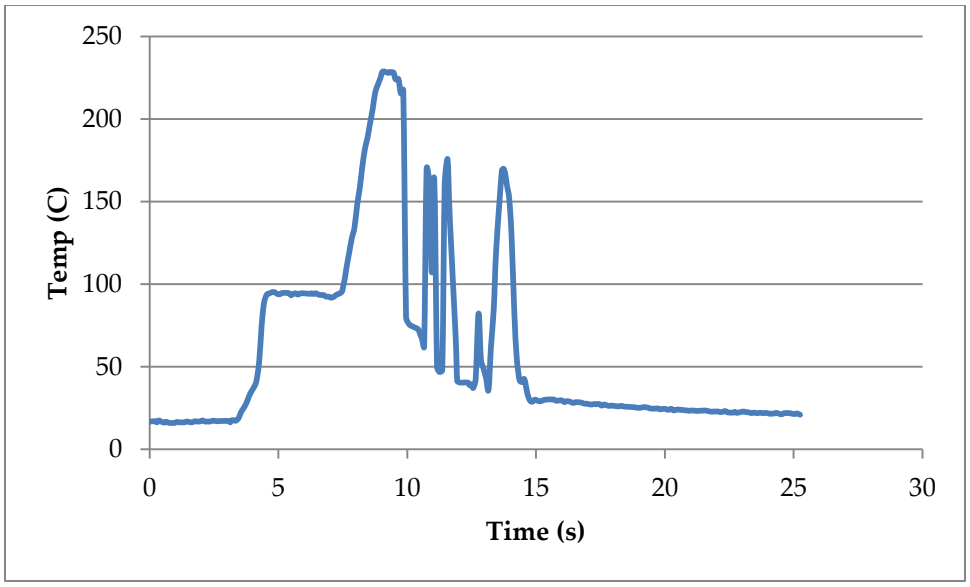


Figure 40 EMI Example 1

Figure 40 was data taken as part of the time response test done in section 5.2. Looking at the data plot, while the thermocouple was cooling in air, it experienced an EMI. This EMI actually induced additional voltage that was interpreted by the DAQ as temperatures ranging 150-200 degrees Celsius

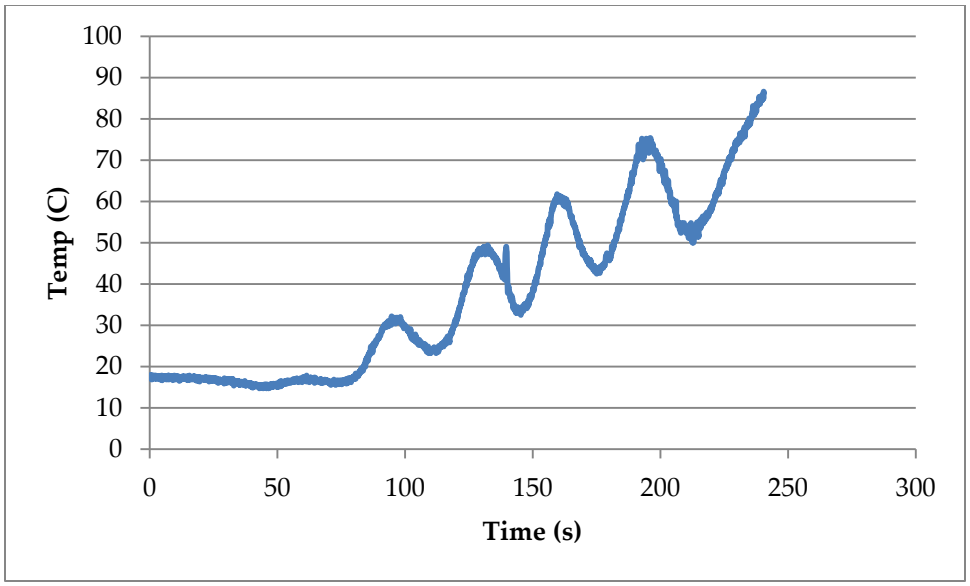


Figure 41 EMI Example 2

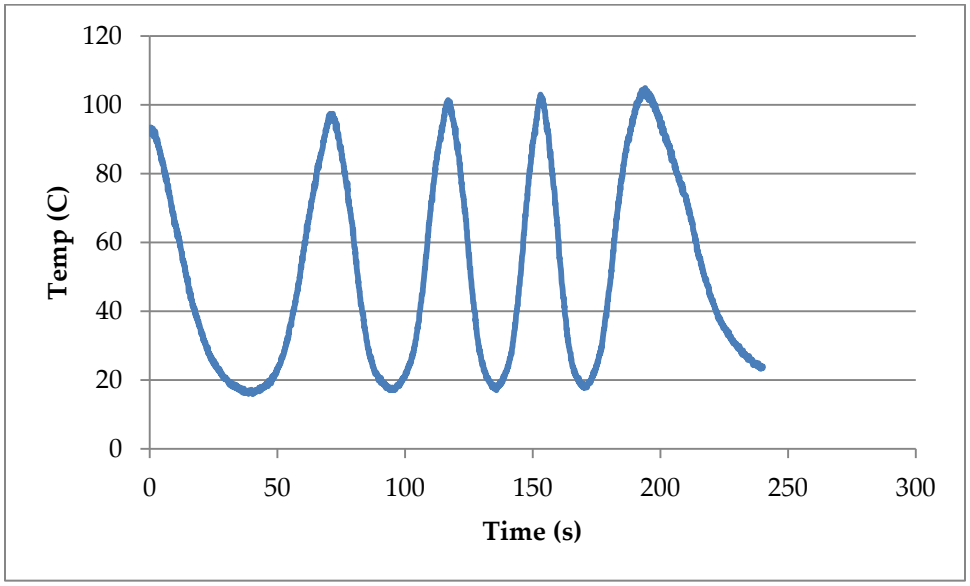


Figure 42 EMI Example 3

Figure 41 and Figure 42 were taken while a thermocouple was measuring steady room temperature air. Taking a look at Figure 41 EMI Example 2; the first 75 seconds go just fine, with the thermocouple registering a reading between 17-19 degrees Celsius. One thing to note is how thick the band is on the graph, showing low amplitude interference on the signal causing the data to look "jittery". Eventually, however, the EMI beings to dominate the thermocouple signal, manifesting as a 60 Hz sinusoidal curve that continues to grow in amplitude. Figure 42 shows a thermocouple measurement that is essentially just a 60 Hz noise.

5.5.2 Causes of Electromagnetic Interference in the Lab

In the lab space being used various causes for electromagnetic interference have been identified. One of the most obvious causes is a 220 V power line located along the ceiling in a corner of the space. This source of EMI produces the strongest type of noise in the thermocouples and is responsible for the patterns shown in Figure 41 and Figure 42. This source is present during tests in the testing environment. Providing proper distance, roughly 8-10 feet from the wall where the circuit is located and ensuring no equipment is drawing power off the circuit, is adequate enough to eliminate the noise from the 220 V power line source.

A second source, discovered by undergraduate assistant Christopher Baxter, is found within the laptop being used for DAQ. It was found that EMI is created when the laptop battery is charging while simultaneously running the laptop. Thermocouple data with the noise from the laptop power supply is shown in Figure 43 EMI caused by Laptop Charging Circuit.

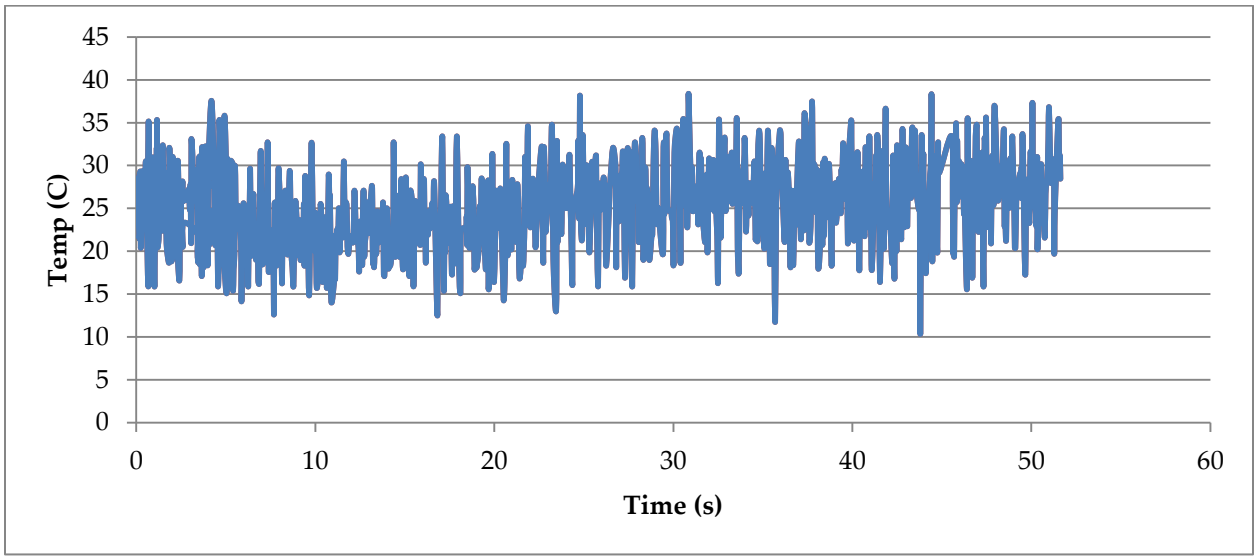


Figure 43 EMI caused by Laptop Charging Circuit

This EMI causes the data to fluctuate. Fortunately, it also is easily solved. Simply ensuring the laptop is fully charged and removing the charging chord while taking measurements ensures no problems from this EMI.

A final source of EMI, only present during time response and calibration tests, is the electric hot plate used in those tests. It can be removed by simply turning off the hot plate when a measurement needs to be made.

5.5.3 Filtering

Despite identifying large sources of EMI, small fluctuations in the data from other 60 Hz sources still persist. In order to provide, clean, analyzable data signal filtering must be used.

Signal filtering can be done actively by hardware; some higher end model DAQ's for thermocouples have this feature. The NI-6112, however, does not. This leaves filtering as a data post-processing activity. MATLAB's digital signal toolbox has a filter design tool, which aids in the design and application of filters for data sets.

While thermocouples have higher response times (full response times on the order of 5 – 10 seconds based on flow velocity), it is still useful to use a high sampling rate, in order to sample at a rate that is faster than the ambient noise. This provides extra data points, which aid in the filtering process.

A low pass filter was designed using the MATLAB Filter Design & Analysis Tool. It is shown in Figure 44 Low Pass Filter. The filter was designed to cut off any frequency less than 200 Hz and attenuate the magnitude of everything over that frequency.

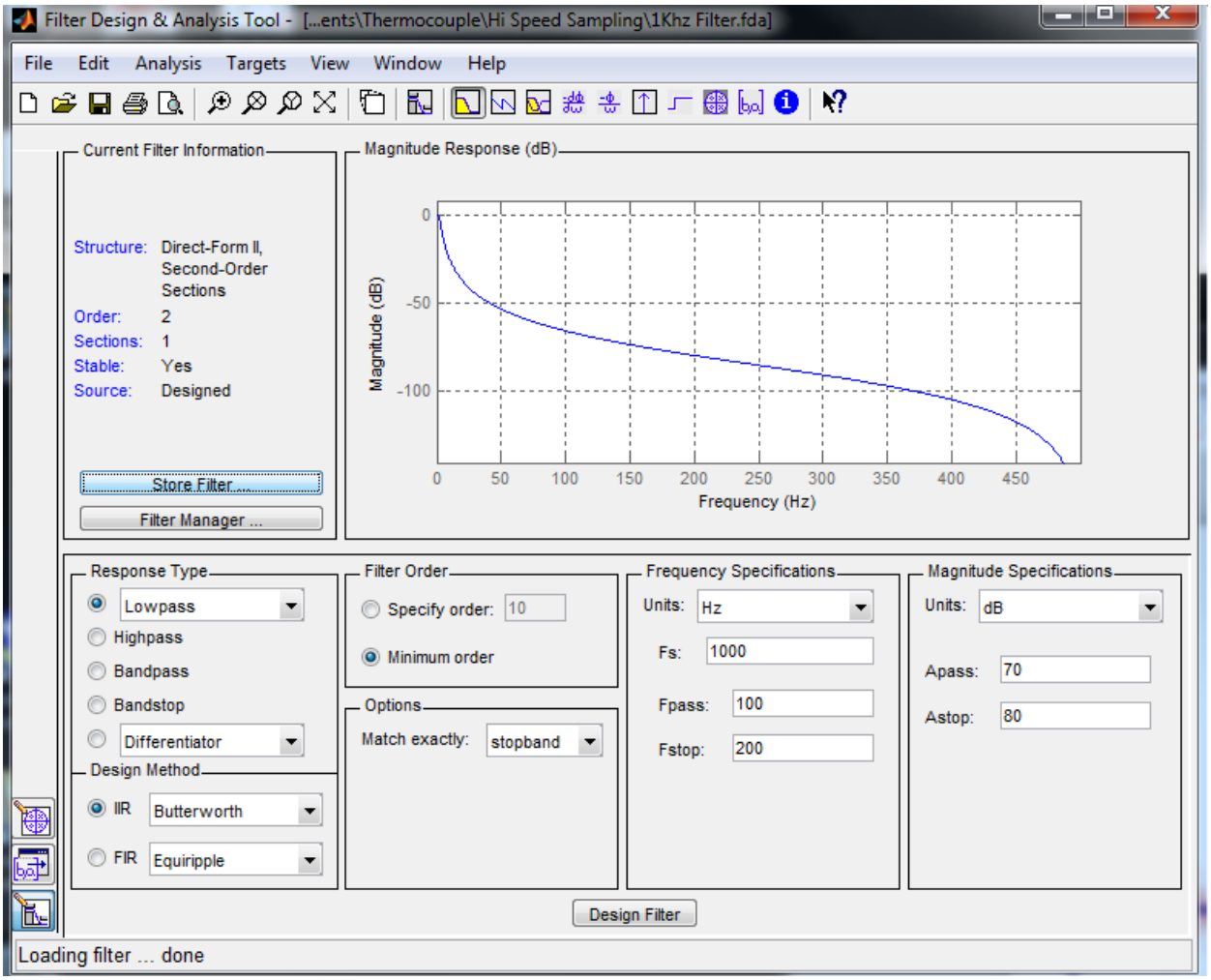


Figure 44 Low Pass Filter

Data was recorded from TC 6 on the rake while the rake was just sitting in room temperature air. The low pass filter mentioned previously was then applied to the data. Figure 45 Filtered (blue) vs Unfiltered Data shows the unfiltered data (red dashed line) versus the filtered data (solid blue). The attenuation effect of the filter is pronounced, significantly reducing the drift in the thermocouple signal. The filter, through its mathematical interpolation, does add a line coming up from 0. While not desired completely, it can easily be avoided by running data logging a few seconds prior to the period where measurements need to be recorded.

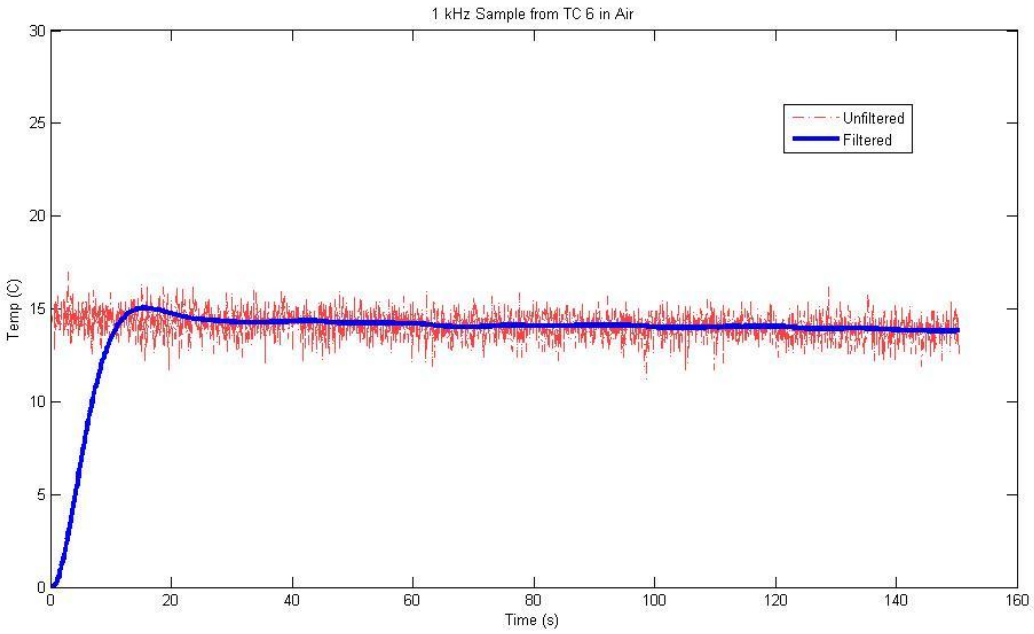


Figure 45 Filtered (blue) vs Unfiltered Data (red)

5.6 In-Tank Tests

A run of the test section at the University of Tennessee was undertaken to collect thermal mixing data for a hot/cold tank run. A thermocouple rake consisting of 10 thermocouples was placed over the middle of the jet inlet and data was taken at various locations.

5.6.1 Objectives

This test was the first time the test section was to be operated with a hot and cold tank. The objectives for this test were to generate filtered data sets for thermal mixing and identify any issues toward the final goal of taking quantifiable measurements for the Twin Jet project.

5.6.2 Procedure and Setup

The test twin jet flow test section was prepped with one tank containing tap water around room temperature (20°C) and another tank holding hot water (88°C). These are designated as the hot and cold tanks respectively. The rake is positioned with its centerline over the middle of the jet head. Figure 46 shows the general positioning with respect to jet and thermocouple locations. In Figure 46, it can be seen that thermocouples 5 and 6 are directly over the centerlines for the cold and hot jets, respectively. The rake was then moved vertically to various positions above the jet.

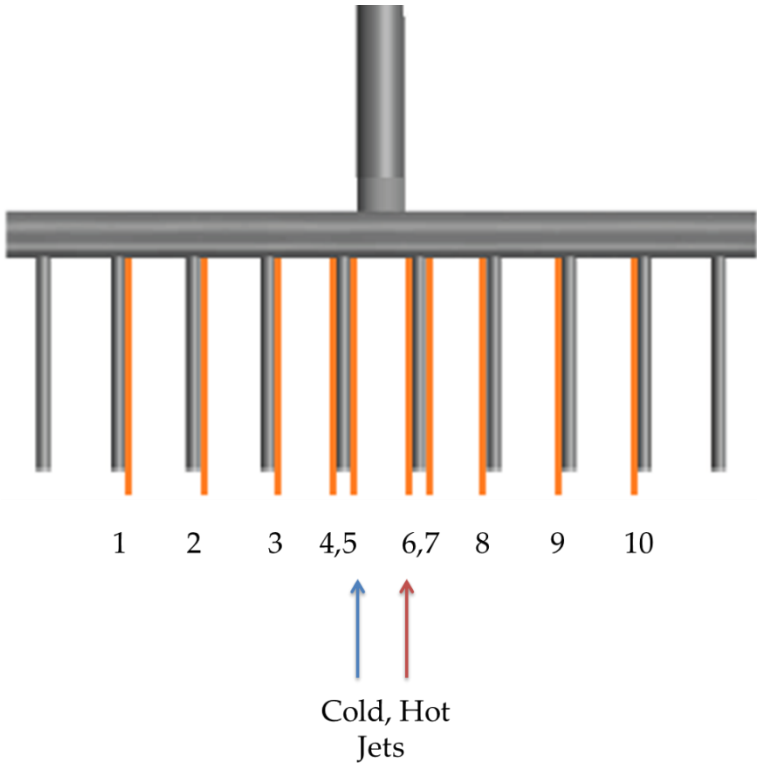


Figure 46 General Rake Positioning, with Thermocouples and Jets Labeled

5.6.3 Results

Results are shown in Figures Figure 47 to Figure 49

In the plots vertical distance in the titles correspond to height over jet inlets, Series 1-10 corresponds with TC 1-10, left to right, with the hot jet being on the right side of the rake (toward TC 6-10). The jets are typically started a few seconds after data acquisition begins.

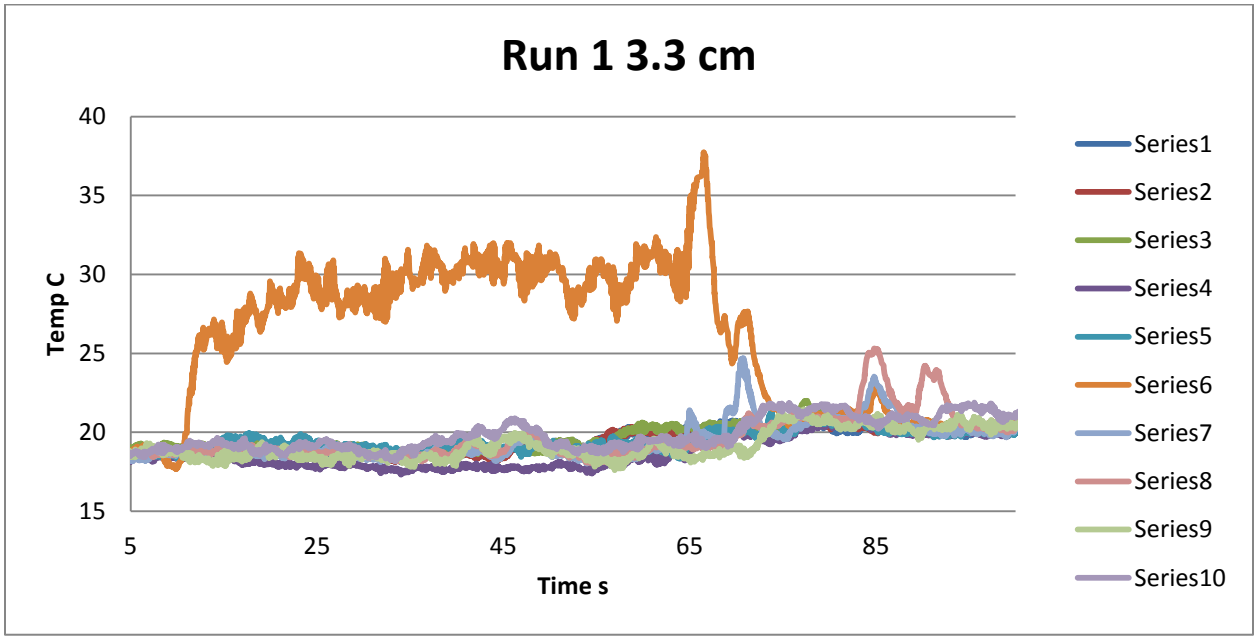


Figure 47 Run 1

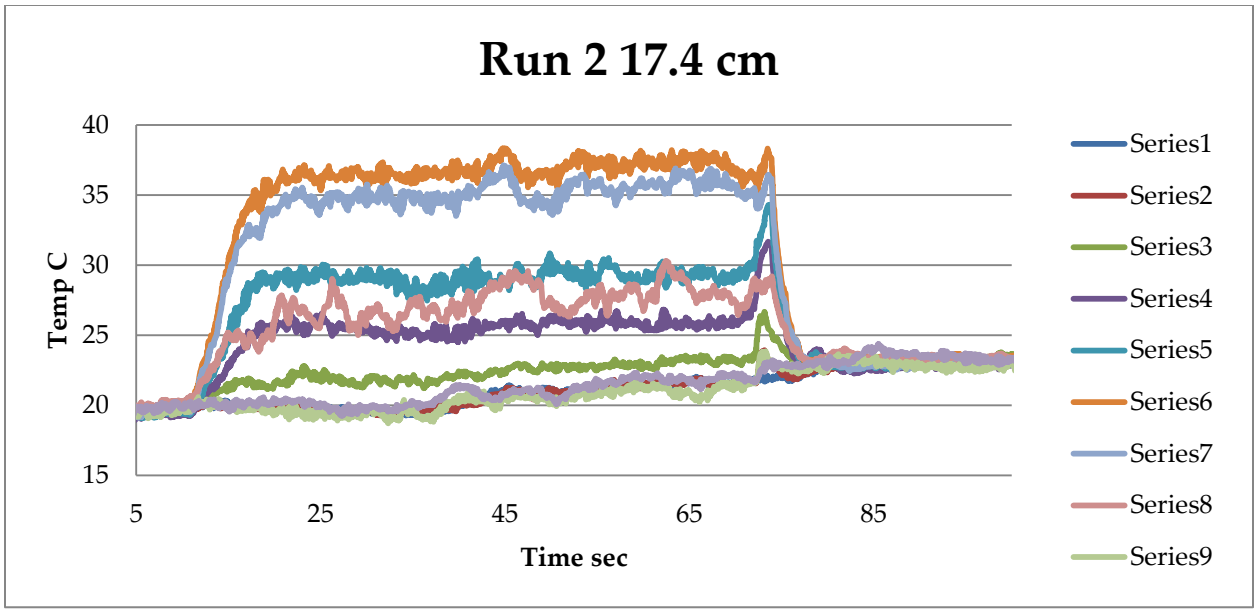


Figure 48 Run 2

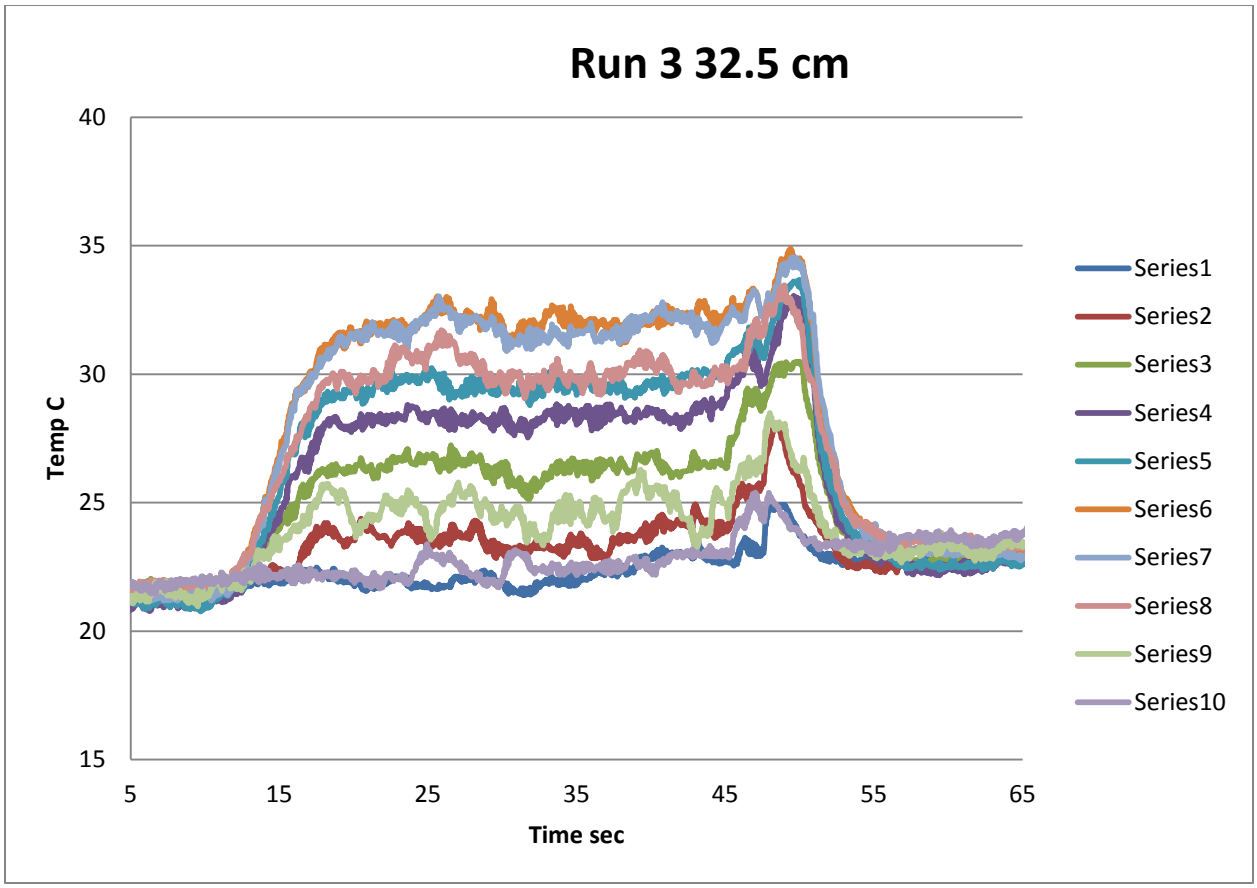


Figure 49 Run 3

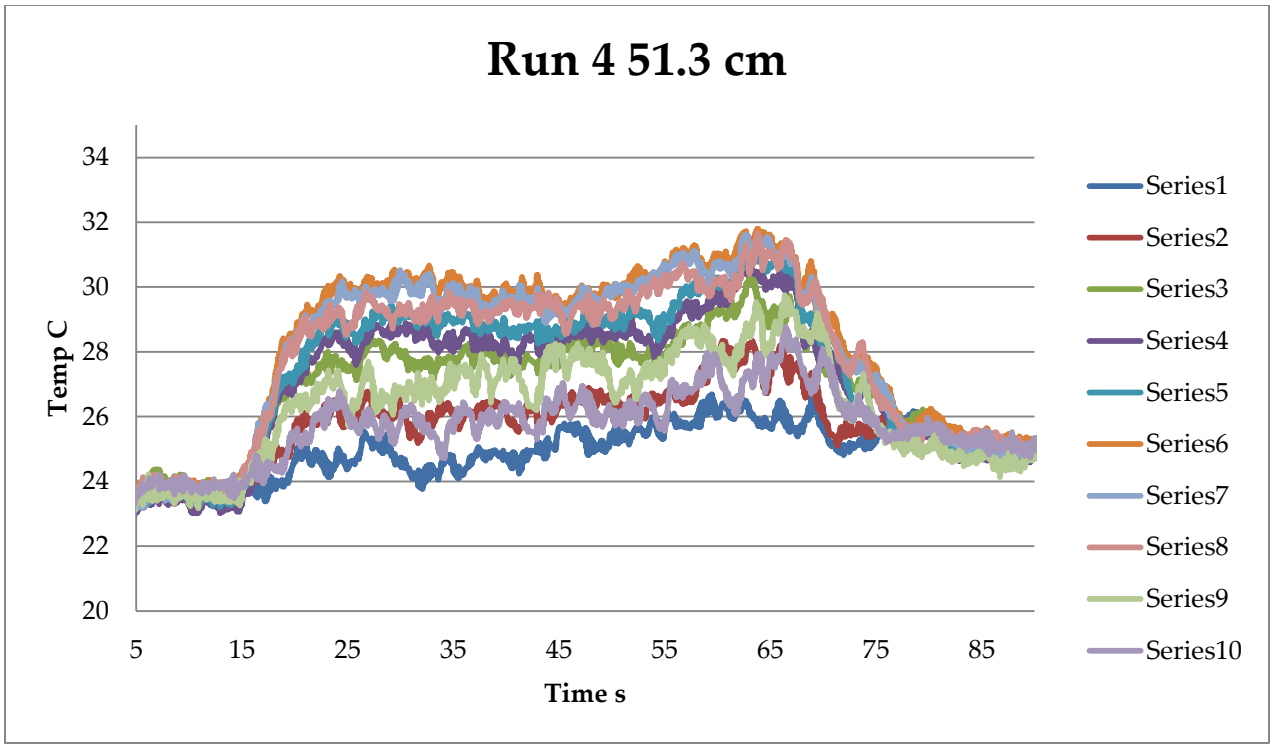


Figure 50 Run 4

5.6.4 Conclusions

Looking at the data, specifically from Run 1, it can be shown that there is a height low enough that hot jet and any areas it mixes into, are only being measured by a single thermocouple. For Run 1 it was TC 6. Looking at the rest of the runs, it is obvious that at higher vertical distances such as those for Runs 3 and 4, the thermocouples do not span the entire length of the jet. For final data runs, data at the top of the jet will require multiple runs near the top of the tank, shifting the rake's centerline off the center of the jet head.

The following measurements were proposed, 8 vertical measurement taken at: 5, 10, 15, 25, 35, 45, 55, and 65 cm vertical distance over the jet heads.

Chapter 6. Experimental Implementation of Thermocouple Rake

This chapter summarizes the experimental implantation of the thermocouple rake in the twin jet testing environment. This includes the mounting and positioning, data acquisition, and a data post processing activities involved in the experimental implementation.

6.1 Mounting and Positioning

In order to take measurements that could be comparable to a CFD code outcome, the position of the rake has to be accurately described within the test environment. Figure 51 shows the rake mounted in the test section and is annotated with items of interest. The support beams are the iron braces that run on either side of the tank, the mounting system sits on these beams. The mounting rods are two metal rods that are perpendicular to the beams and span the distance between them. The mounting block is the block that the thermocouple rake is attached to and hangs from.

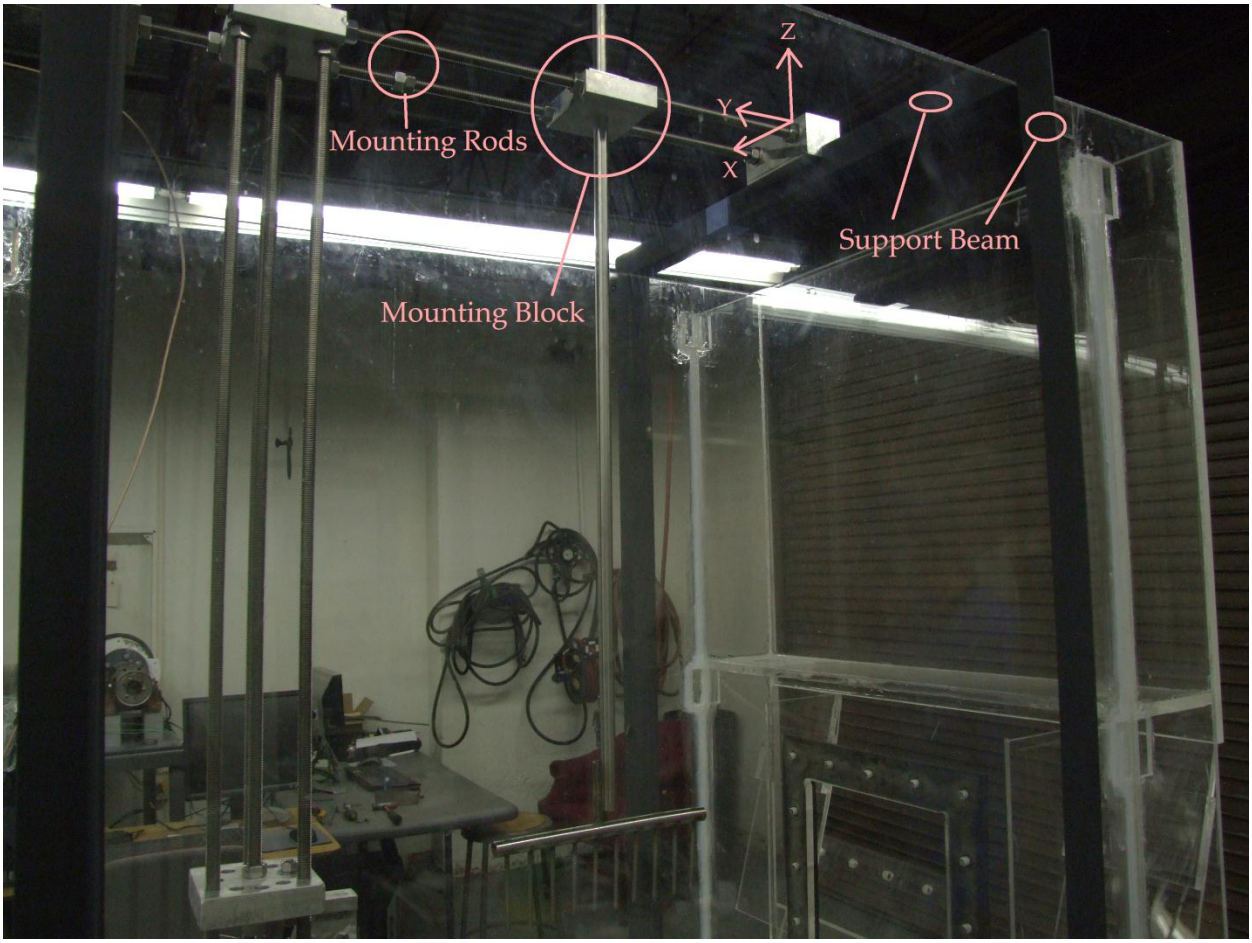


Figure 51 Rake Mounting and Positioning Annotated

The coordinate system arbitrarily adopted for this experiment is shown in Figure 51 and again with a closer view in Figure 52. In the system '*Z*' direction runs parallel with the rake mast and is noted as vertical distance. The '*X*' direction runs along the support beams and is parallel to the jet inlets. The '*Y*' direction runs parallel with the mounting rods and the rake head and is also perpendicular to the jet inlets.

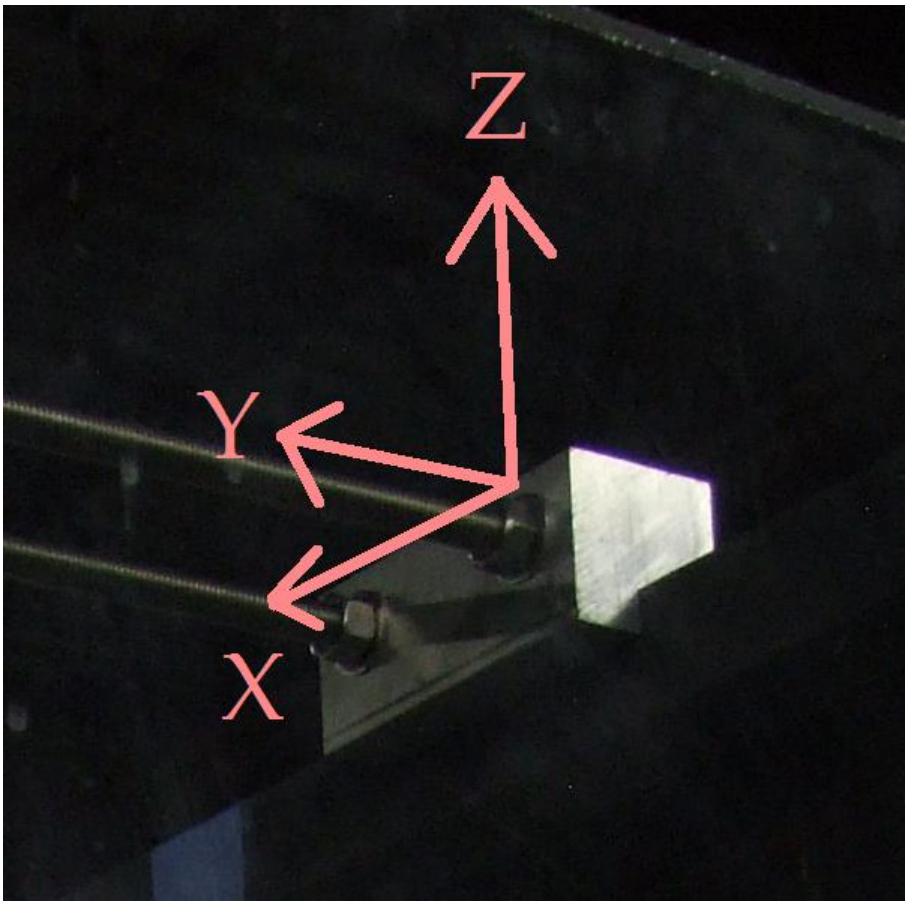


Figure 52 Coordinate System Close Up

Measuring the position in the vertical (*Z*) direction was done by positioning the rake so that the thermocouples were just barely in contact with the jet inlets below. This position was marked with a notch carved into the rake as shown in Figure 53. Distance measured from the top of the support block directly corresponds to vertical distance over the jet inlet. Using Figure 53 as an example, the rake would be 2 cm above the jet inlet.

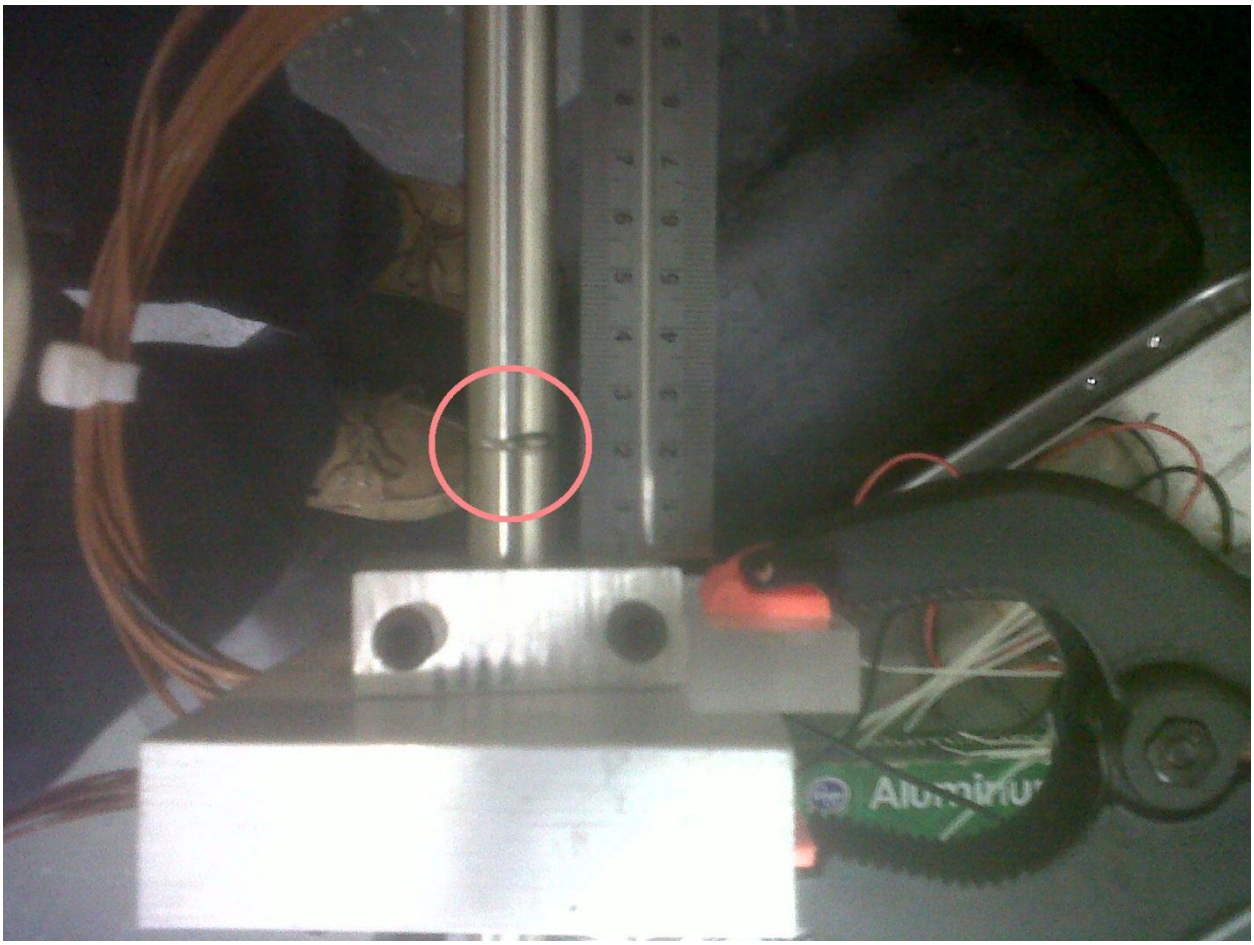


Figure 53 Vertical 'Z' Direction Positioning

Measurement in the '*X*' direction was done by attaching adhesive measuring tapes to the sides of the support beams as shown in Figure 54. The two marks thick black marks shown correspond to positioning the rake over one end and the middle of the jet inlets.

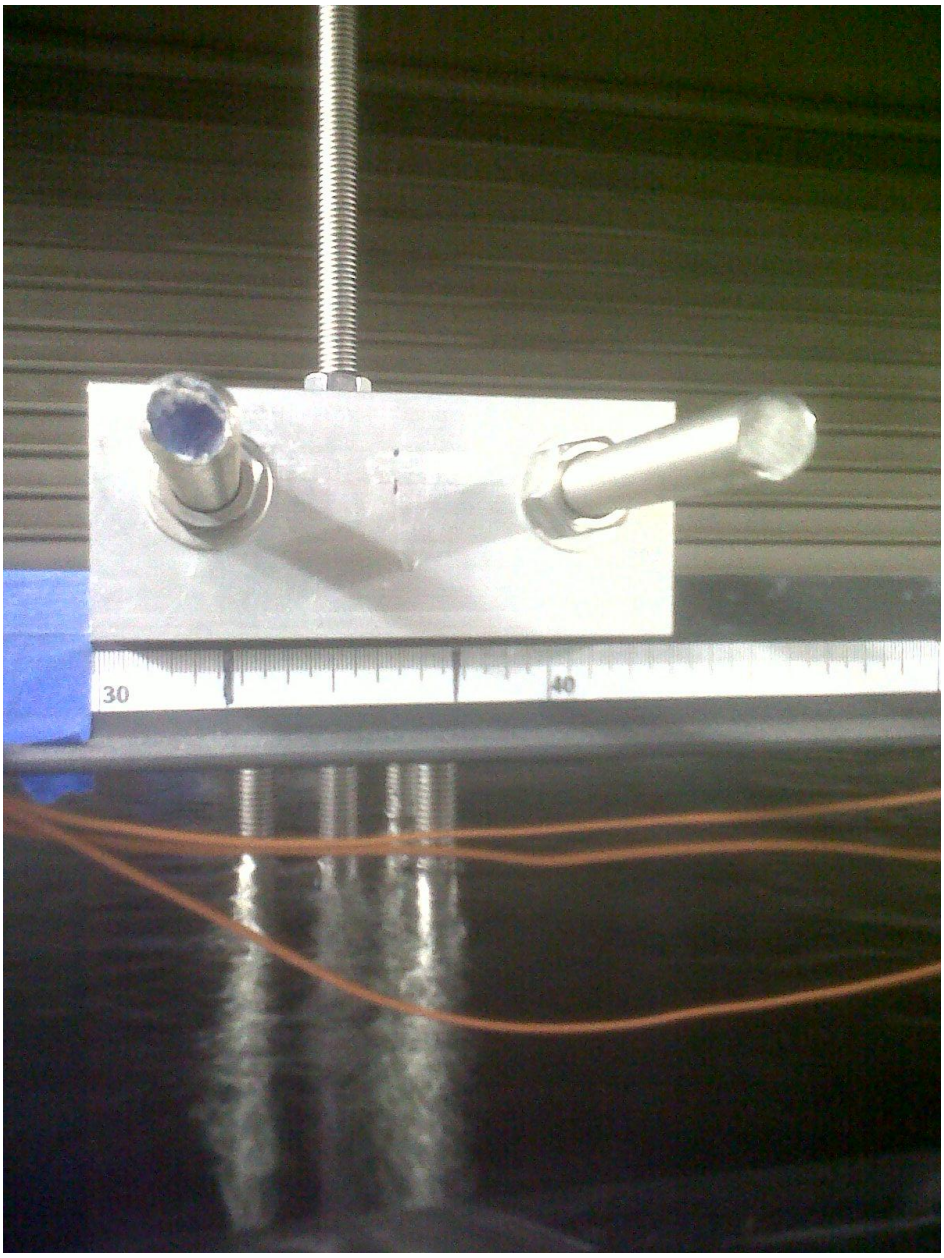


Figure 54 'X' Direction Positioning

Positioning in the '*Y*' Direction is done manually, typically allowing the centerline of the thermocouple rake (a line extending down the mast) to be aligned over the center gap between the two jets.

6.2 Data Acquisition

Data Acquisition for this project is handled through the National Instruments USB-6112 model and LabVIEW Software. The LabVIEW file takes in data for the 12 thermocouples and writes output to an excel file along with a time stamp. The 'front panel' of the LabVIEW file created

for this activity is shown Figure 55. The front panel lets the operator set the file path for excel output, view a waveform graph from the thermocouples to ensure that there is no large source of interference, and view the temperature profile across the rake via the 12 thermometer graphics spaced out below the waveform graph.

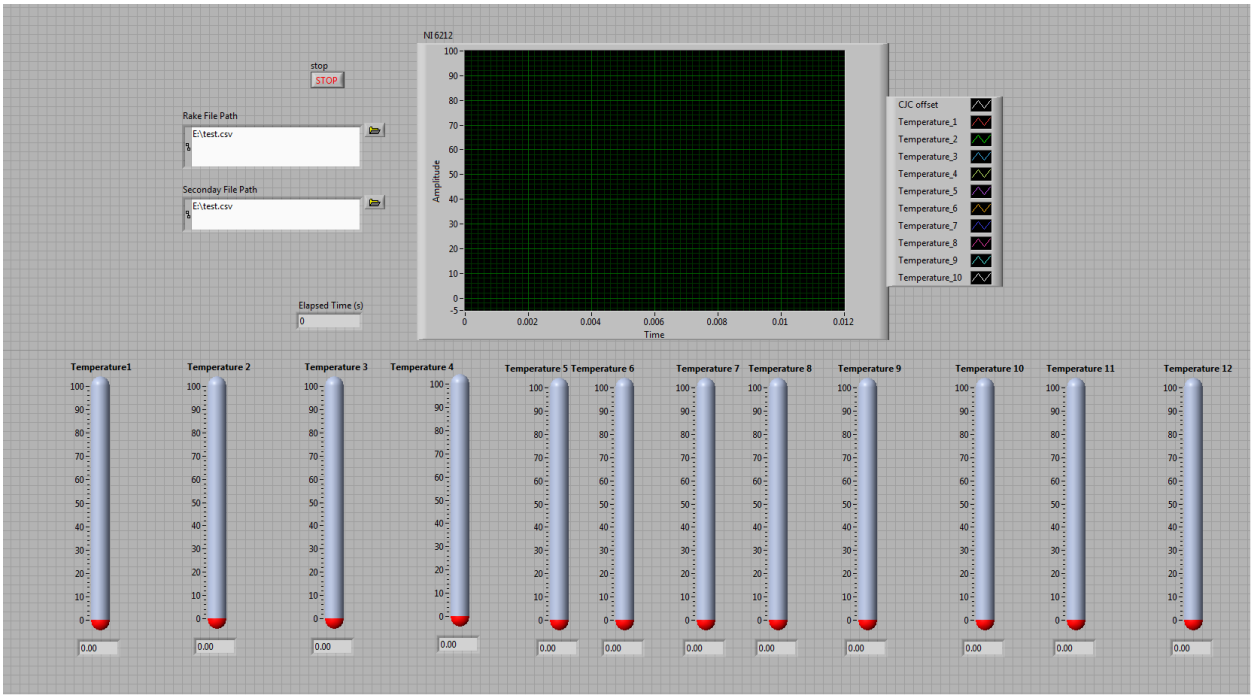


Figure 55 LabVIEW Operator View

6.3 Post Processing

Despite ensuring that large sources of interference are not present during a test run (such as the laptop's charging circuit), there still remains noise that needs to be scrubbed out from the collected data. As in Section 5.5.3, MATLAB software is used to filter data collected from the thermocouples. The filter used for post-processing is shown along with the MATLAB Filter Design & Analysis GUI in Figure 56.

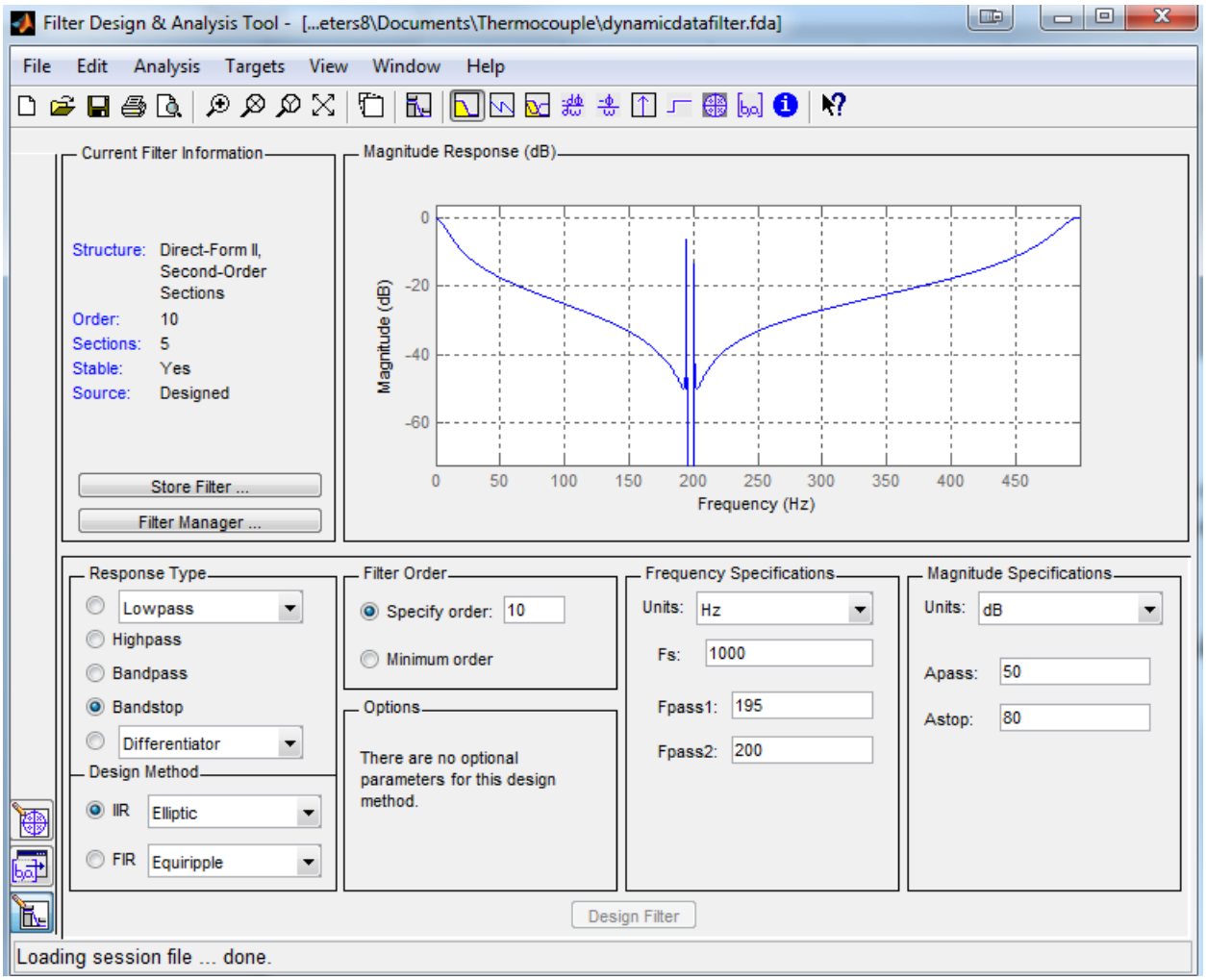


Figure 56 Filter used for Final Data Collection

The effects of this filter on in tank data from a single thermocouple are shown below in Figure 57.

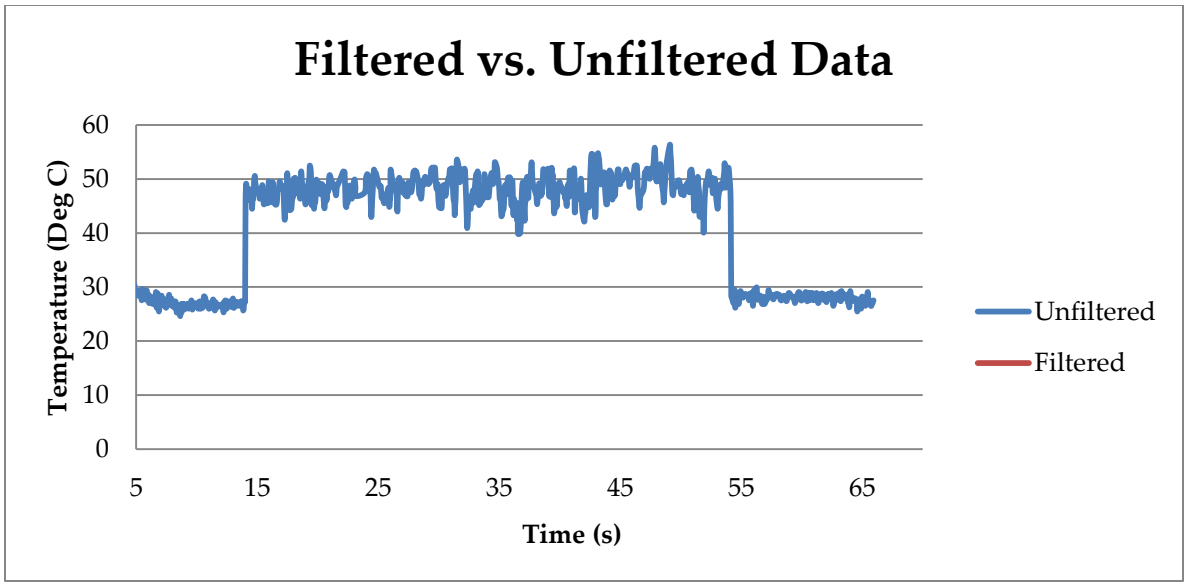


Figure 57 Filtered vs. Unfiltered Data

Chapter 7. Twin Jet Thermal Mixing Experimental Data and Discussion

This chapter presents data collected for the twin jet project and discussion of the results.

7.1 Centerline Data Acquisition Information

The collected data that is presented in this section was acquired with the rake aligned perpendicular to the jet inlets and centered in the X-Y plane of the jet inlets. This positioning is shown in Figure 58; the rake is shown from the top down with the support block removed in order to see the jet inlets below the rake.

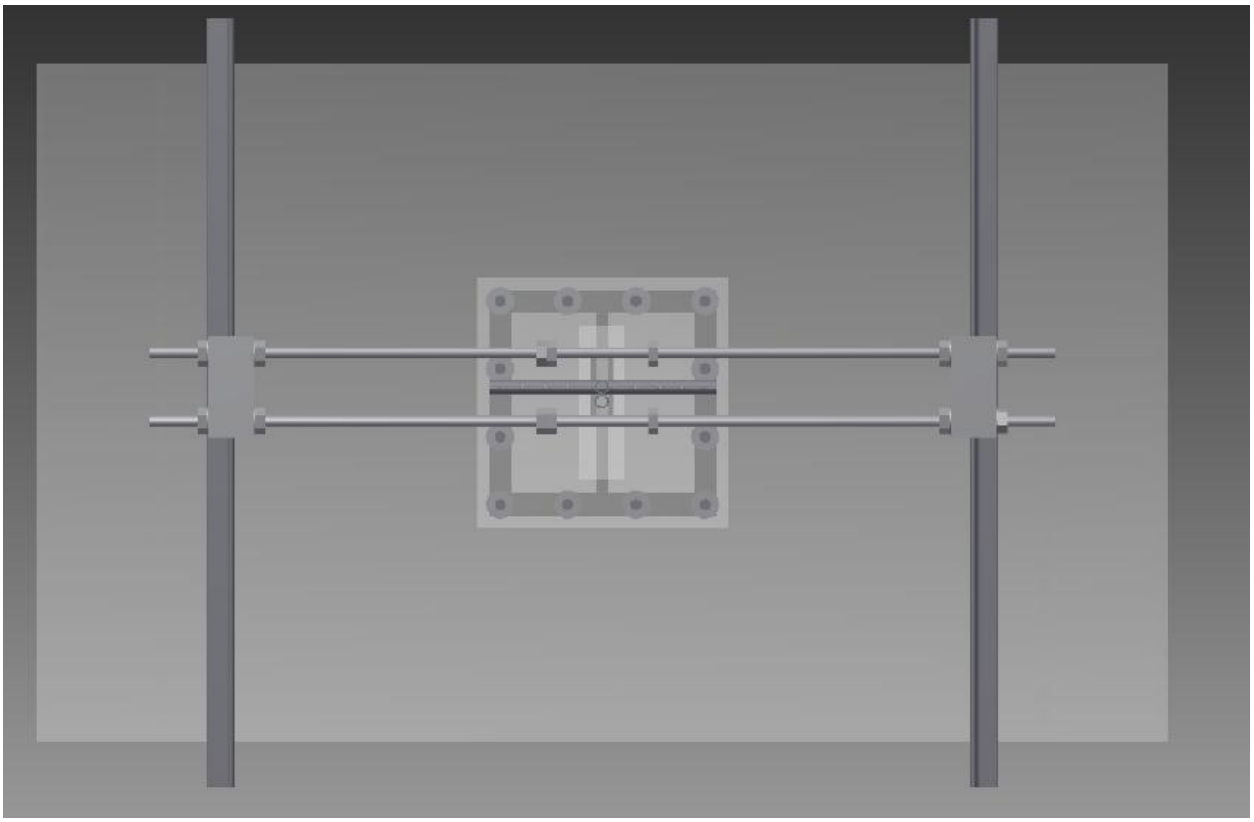


Figure 58 Centerline Measurement Positioning Diagram

The approximate location of each numbered thermocouple with respect to the hot and cold jets are shown in Figure 59. Since the thermocouples are lashed on the outside of the rake, it is of interest to know the relative distance between each thermocouple. The distances between each thermocouple are marked in Figure 60.

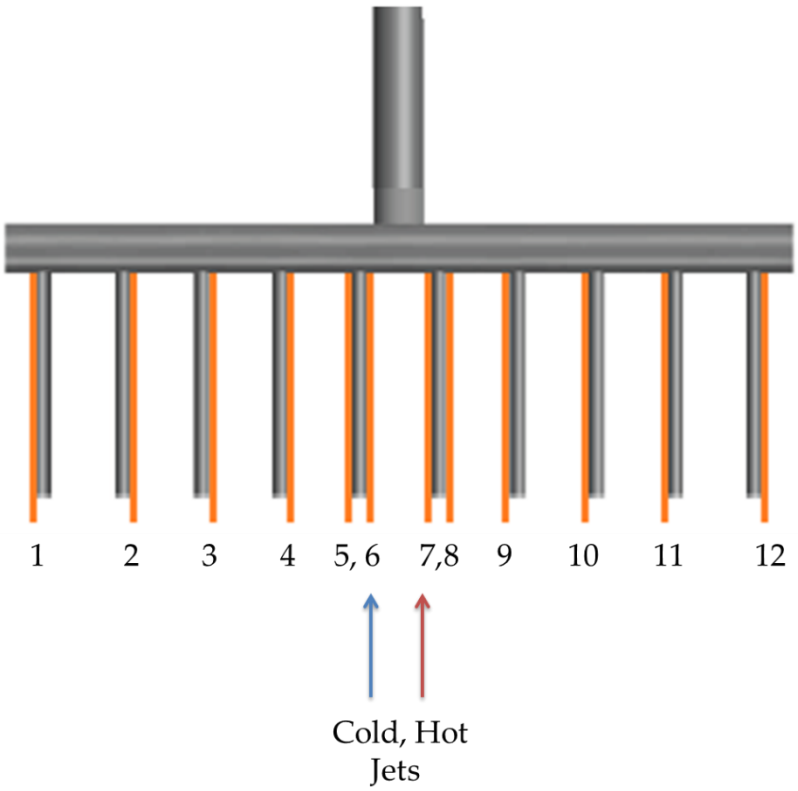


Figure 59 Thermocouple Identifications for Centerline Data Acquisition

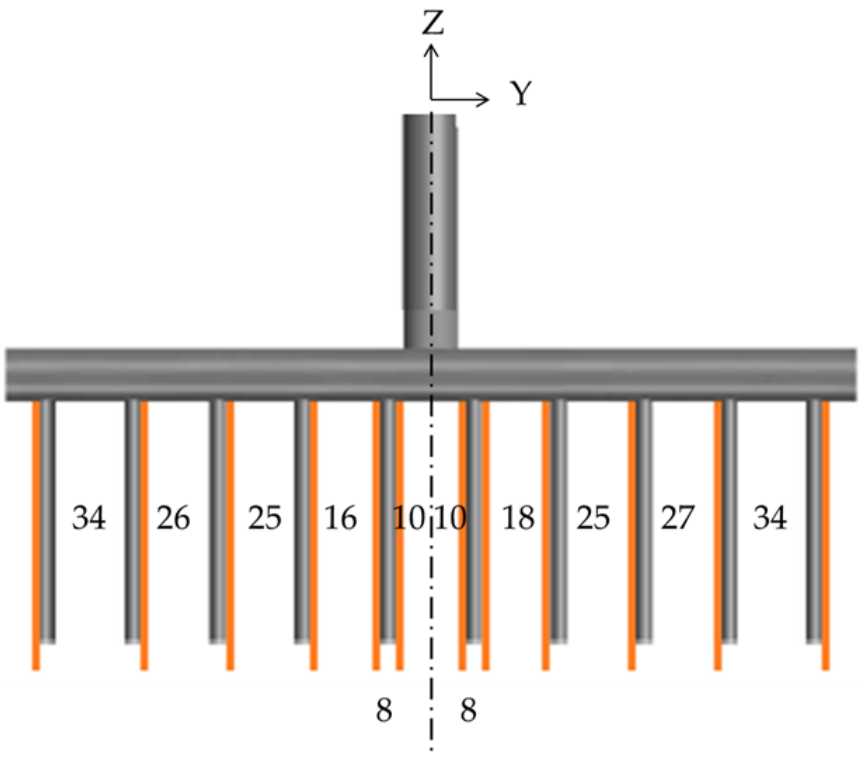


Figure 60 Distances between Thermocouples, Distances in mm

During the run data was recorded at various heights above the jet inlets; these include 5, 10, 15, 25, 35, 45, 55 and 65 cm. Due to a software problem, the data presented in the next section from 5 and 10 cm does not include thermocouple 1.

The tanks were initially set with cold water ~25 °C (77 °F) and hot water ~89 °C (160°F). The hot water tank is always refilled from the same water supply, the cold tank is refilled through backfilling from the test section. This causes the temperature in the cold tank to increase slightly after multiple tests; however the ambient in tank temperature is recorded for each run in data that comes before the pumps are turned on and is equal to the temperature in the cold stream. The flow rate for these tests was 12 gal/min, or 45.42 L/min. This corresponds to a flow rate of 1.513 m/s or 4.965 ft/s given the area of the jet inlet and a flow Reynolds number of 5.00E+04 (hot jet) and 1.64E+04 (cold jet). The temperature data recorded for the thermocouple rake during each run is shown in Figure 62 through Figure 69 in the next section.

7.2 Centerline Data Presentation and Discussion

Vertical graphs that plots the 12 TCs versus time are shown later in Figure 62 through Figure 69. Initially presented in Figure 61 are the temperature profiles across the rake at various vertical distances. The horizontal axis shown in Figure 61 corresponds with distance along the rake head with negative values being toward the cold jet (TC's 1-6), 0 being the centerline, and positive values being toward the hot jet (TC's 7-12).

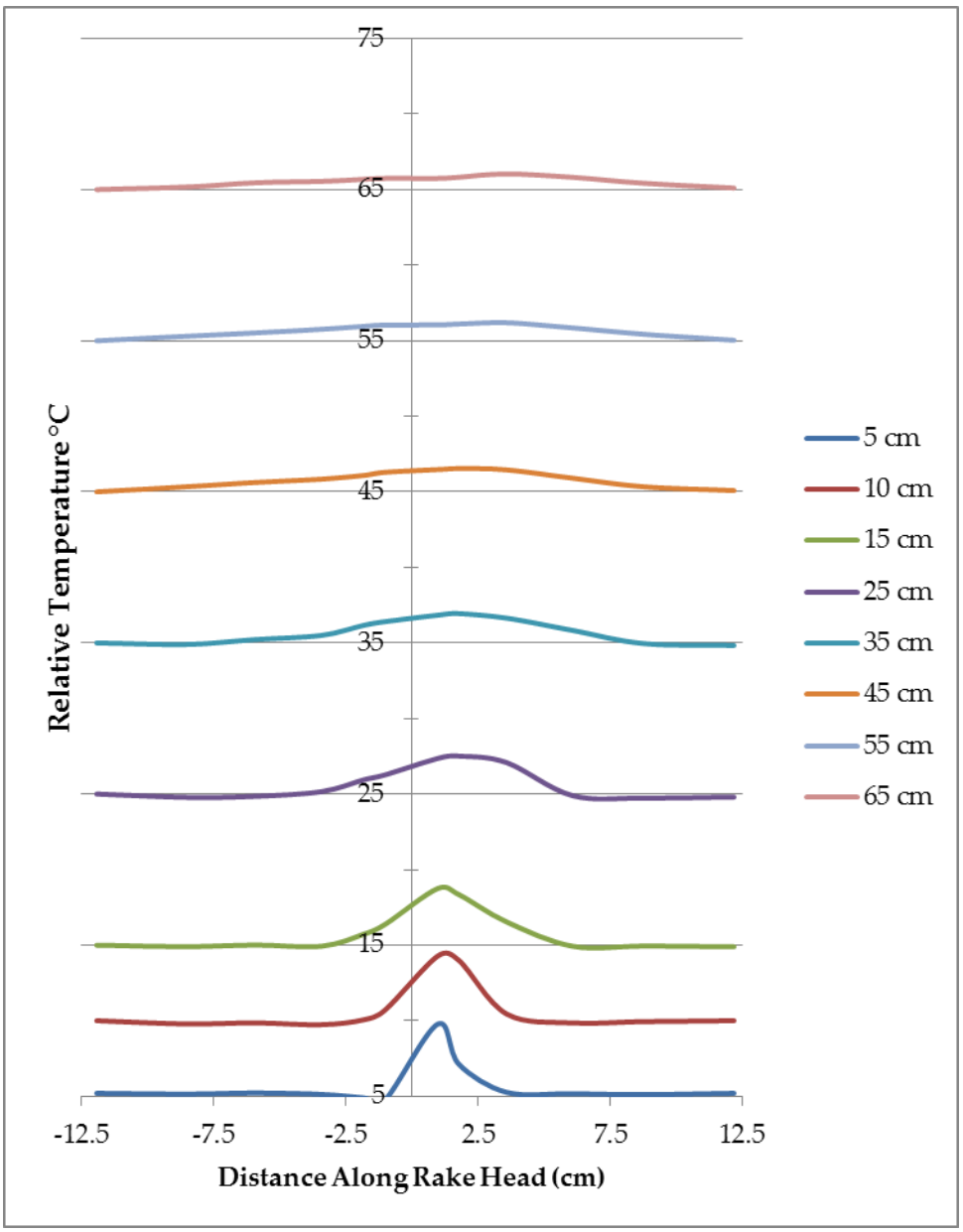


Figure 61 Temperature Profiles at Various Vertical Locations on Jet Centerline

The profiles were created by averaging steady-state values for each thermocouple, and then normalizing them against the left edge (which is the ambient tank temperature and the cold jet temperature). The profiles show a relative increase from ambient temperature the left ends (set at a number corresponding to the height in order to give spacing to the profiles). Figure 61 is presented to give the reader a better understanding of the results that are further presented here.

Looking over all of the data sets shown in Figure 62 through Figure 69, there are few points of interest that relate to all of the sets. Each data set starts out measuring the ambient water temperature shown by the period that runs between 5-15 seconds. The pumps are then turned on and an observable rise is shown from some of the thermocouples.

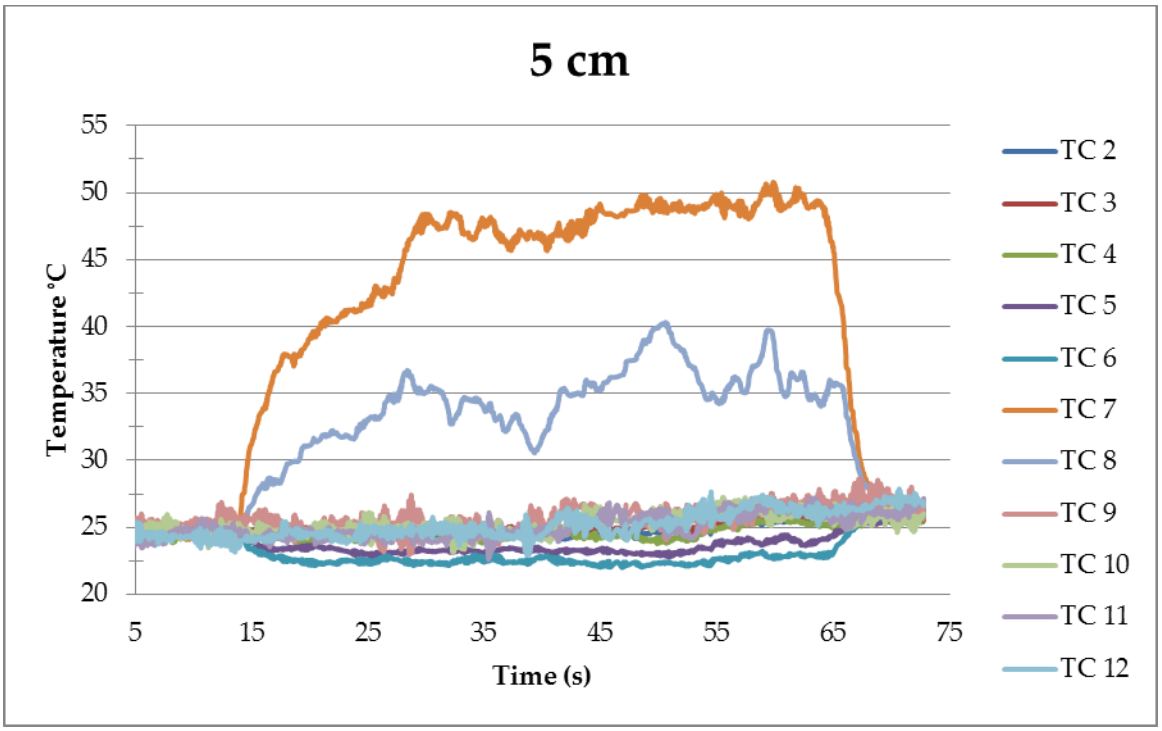


Figure 62 Centerline Data at 5 cm

Figure 62 was the closest measurement made to the jet head. At this height it is observable that TC 7 lies mostly in the hot flow as it registers the highest temperature along the rake. TC 8 shows some mixing between the edge of the hot jet and ambient tank water. TC 8 has large plus or minus 5 degree fluctuations that may be attributed to large fluctuations seen at the edge

of the jet during dye tests.. Given the velocity of the flow, an eddy would flow past the thermocouple much faster than the time range (0.5-1s) for transient conduction response; causing any temperature change associated with it to not fully register with the thermocouple. For this run, the cold tank was slightly colder than the ambient tank temperature (usually the two are the same). This resulted in a decrease in temperature for TC's 6 and 5.

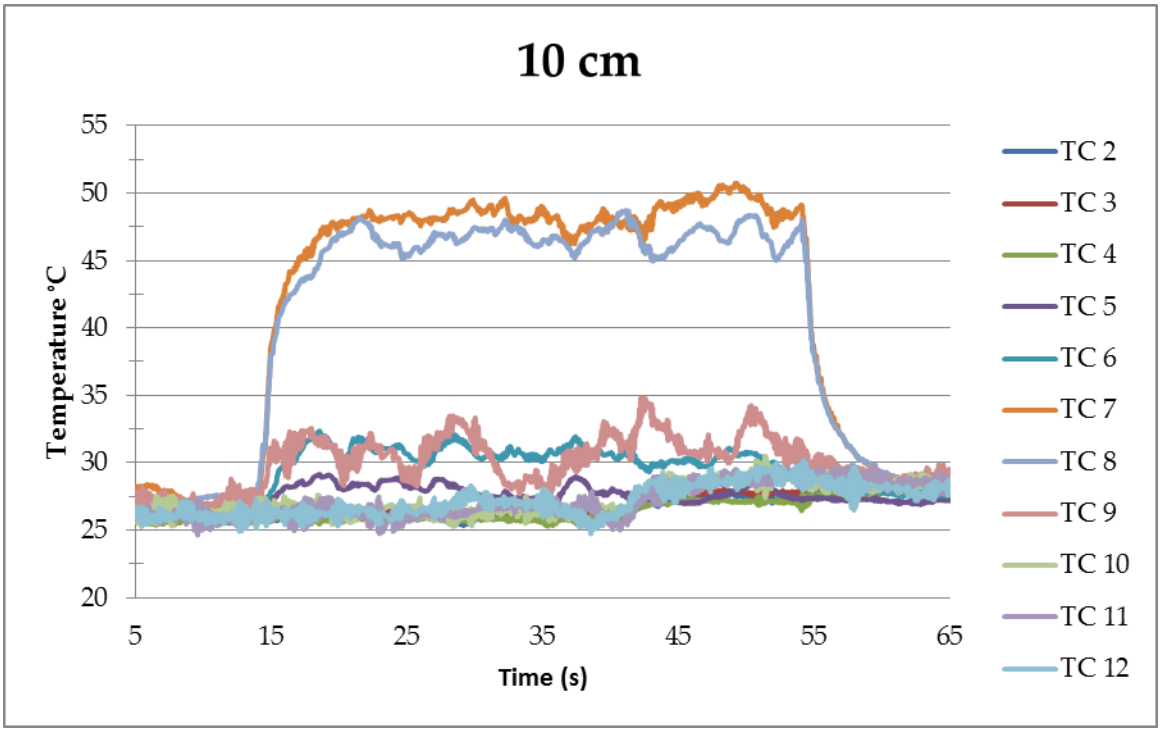


Figure 63 Centerline Data at 10 cm

As the thermocouple rake moves higher, the width of the hot jet widens and TCs 7 and 8 begin measuring similar temperatures. Also TC 9 beings exhibiting behavior similar to TC 8 at the 5cm mark. TC 6 shows an elevated temperature, meaning the mixing region is growing in width.

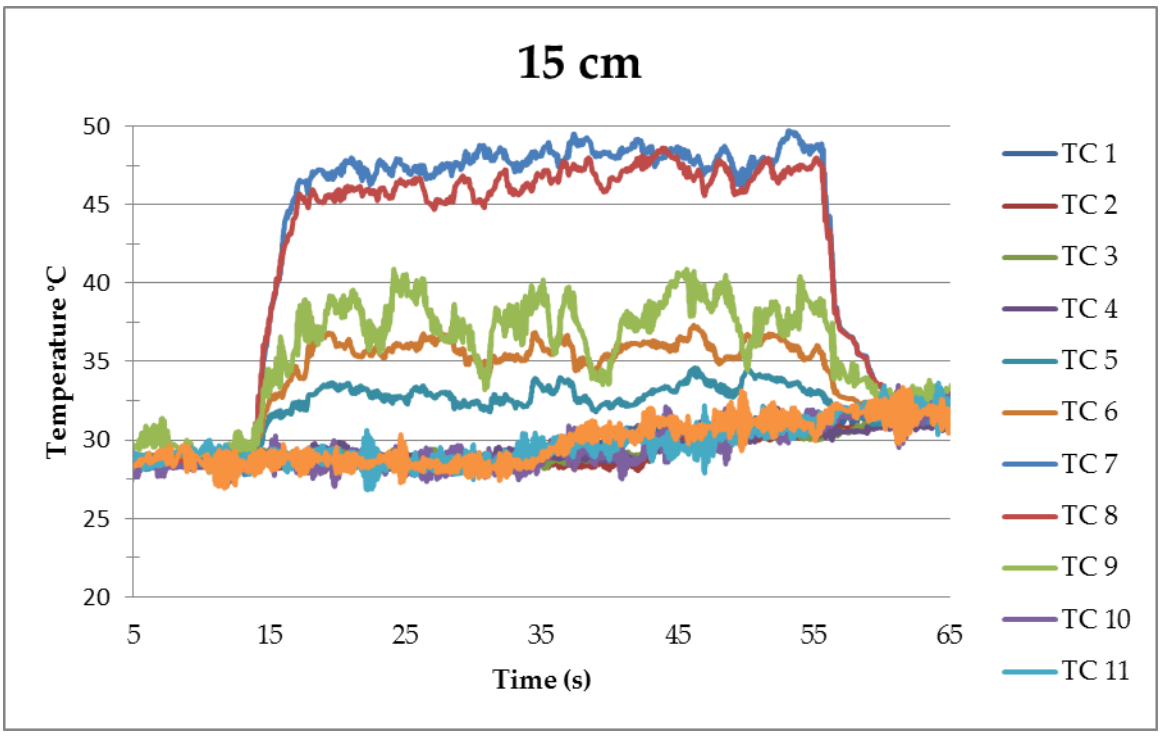


Figure 64 Centerline Data at 15 cm

At the 15cm mark, TC's 5 and 6 continue encountering increased mixing with the hot stream, resulting in higher temperatures being recorded. Thermocouple 9 seems to still be being buffeted by a mixture of hot jet and ambient water.

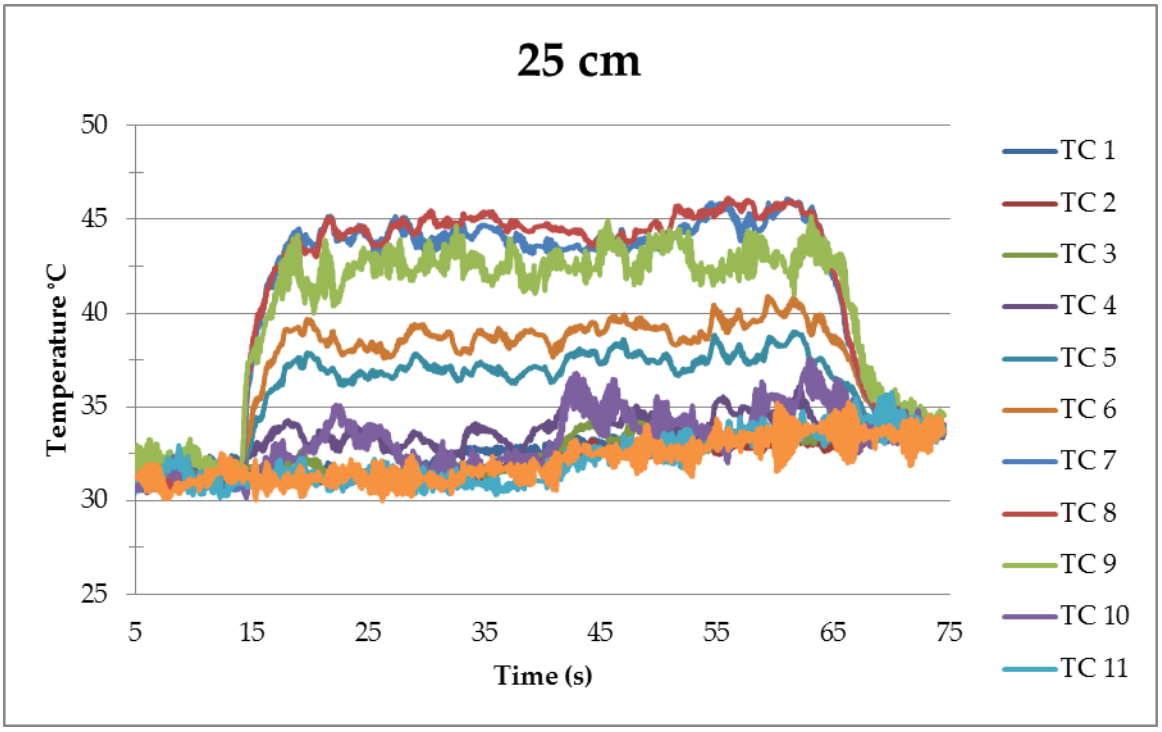


Figure 65 Centerline Data at 25 cm

At 25 cm above the jet inlets, the jets and their mixing region are continuing to widen. TC 9 still has fluctuations, but is reading a temperature more closely relating to TCs 7 and 8. Also TC's 7 and 8 are showing a lower temperature than in previous runs as a result of increased mixing with the cold jet.

The trends being shown at 35 cm in Figure 66 below continue as measurements are taken toward the 65 cm location. The mixing region grows, causing the thermocouples toward the middle of the rake to head toward a converging value. The portions of the jet mixing that are still dominated by mostly one jet are pushed toward the outside thermocouples. This accounts for TC 9 registering increasingly higher values.

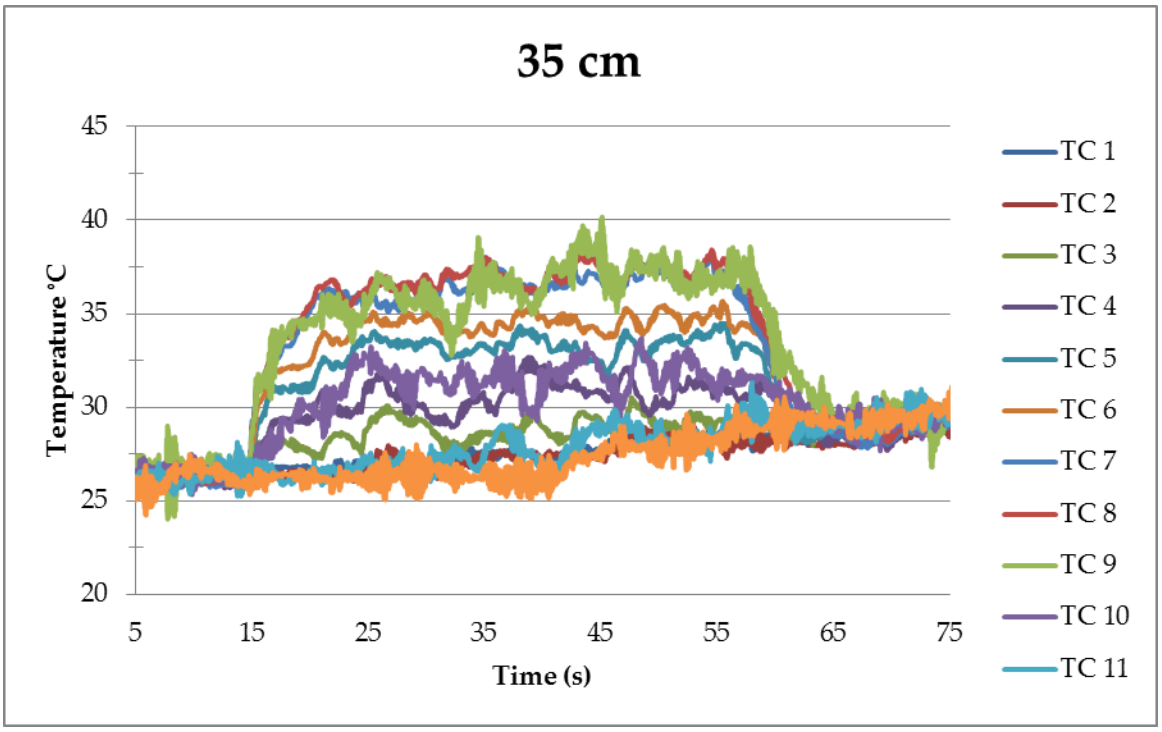


Figure 66 Centerline Data at 35 cm

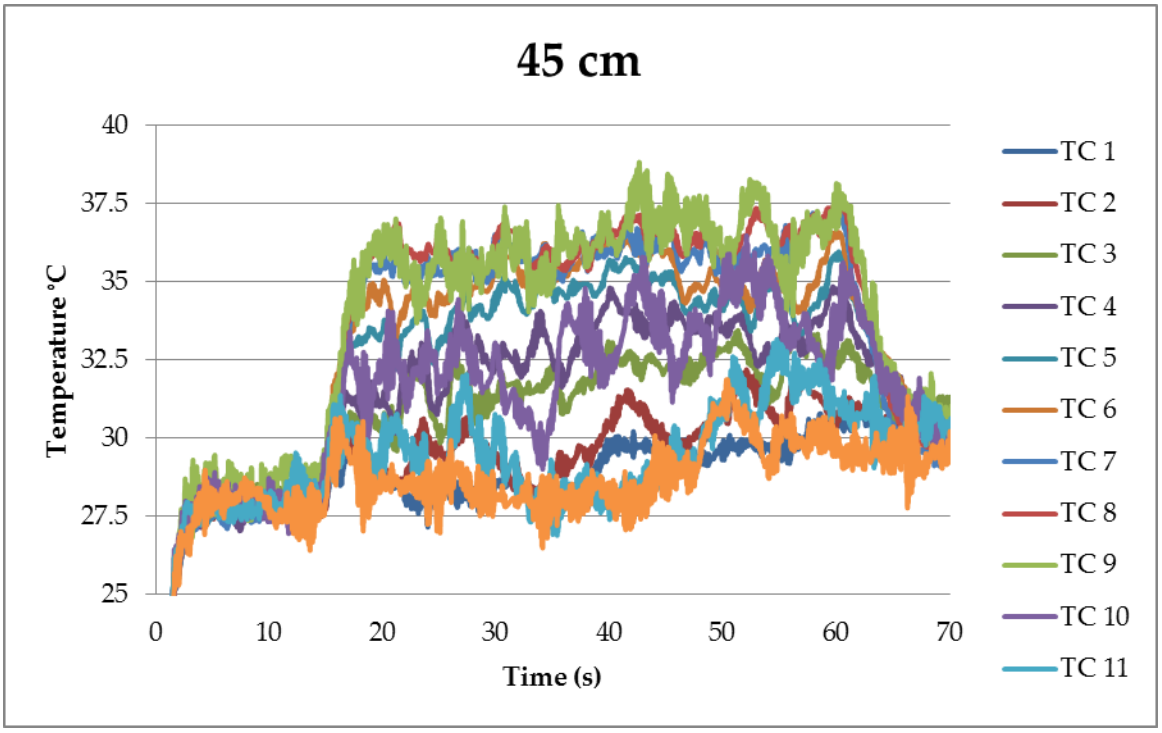


Figure 67 Centerline Data at 45 cm

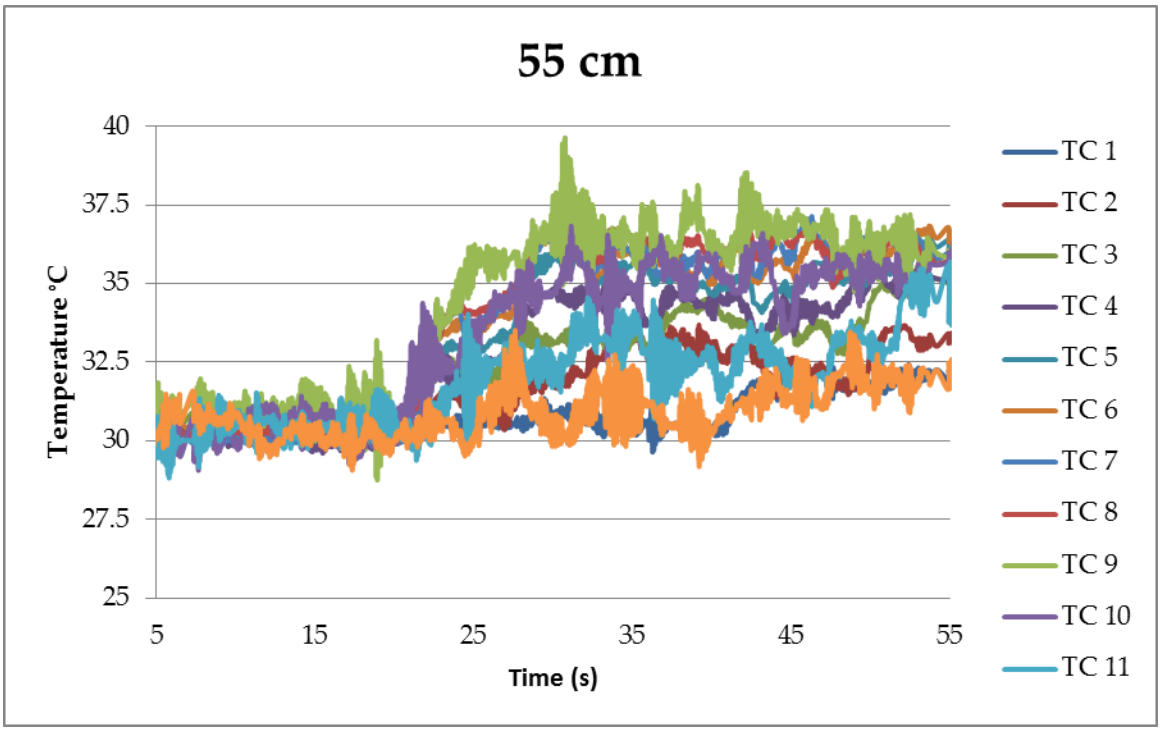


Figure 68 Centerline Data at 55 cm

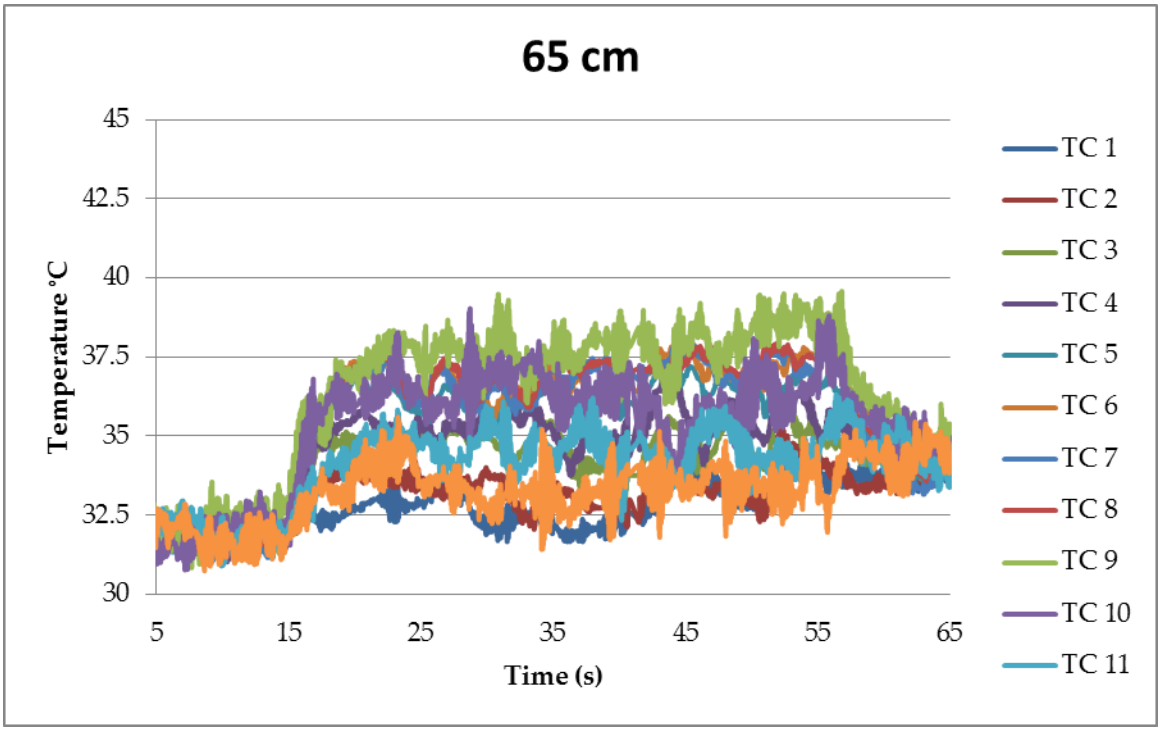


Figure 69 Centerline Data at 65

7.3 Data Acquisition Conclusions

After reviewing the data, it can be concluded that the rake recorded temperature profiles that would be expected for this type of flow interaction. The rake showed that the thermocouples in the flow at low heights above the jet inlets are exposed to a flow region that is dominated by one jet or the other. Measurements taken by the rake at increasing vertical heights show that the mixing region widens with the jets, causing the regions that are dominated by one jet to be located increasingly toward the edge of the thermocouple rake. These trends continue causing the thermocouples to being converging toward a narrower temperature profile.

Despite filtering, the thermocouples still show a degree of fluctuation. This is most likely partially caused by noise that was not filtered out; however flow eddies whose temperature changes at the thermocouple are not fully recorded due to the slow time response may also cause some of the measured fluctuations.

A supplemental file to this thesis (File 1, NEUP_TwinJet_Thermal_Data.zip) contains the data set presented here and additional thermal mixing data that was collected as part of this research. Data sets are either in .xslx or .csv (comma separated values format) that can be loaded into excel. The first column of data is time and each successive coloumn of data corresponds to thermocouples 1-12. All of this information is mentioned in the 'location notes' text files in each directory of the attachment.

Chapter 8. Conclusions and Future Work

This thesis presented the theory behind thermocouples including the thermocouple electric effects governing their operation. In addition to the thermoelectric theory, information regarding the time response and separate effects tests of thermocouples was presented. A temperature rake for use in the twin jet mixing water environment was designed, tested, and implemented. The rakes final implementation was documented along with the data procured in a parallel twin jet turbulent mixing region.

Moving forward, additional temperature measurements made at different locations within the plume need to be taken to provide additional data for modeling the jet mixing. Improvements to be made for the water thermocouple rake can be made in the areas of noise reduction and thermocouple time response. Additionally, a thermocouple rake for measurements in mercury will be constructed for this research. To that end, a few conclusions can be drawn from this body of work to aid in the construction of a mercury rake. It should be noted that mercury is a thermoelectric fluid; thus any thermocouples need to be electrically isolated from a mercury environment. Thermocouples in mercury have much faster response times than water; however any material used to electrically isolate the thermocouples causes additional thermal resistance and should be accounted for in time response calculations. Finally, any tubing that is welding needs to be properly selected and purged to avoid sugaring and deformation of the interior diameter.

It is the intent of the author that this thesis serves as a record and guide to the students who will continue to work on this project in the future. Information useful to twin jet research moving forward is contained in sections discussing theory, rake construction, small effects tests, and experimental implementation.

List of References

1. **National Aeronautics and Space Administration.** Navier-Stokes Equations. [Online] http://www.grc.nasa.gov/WWW/k-12/airplane/nseqs.html.

2. **Kerlin, Thomas W. and Shepard, Robert L.** *Industrial Temperature Measurement.* s.l. : Instrument Society of America, 1982.

3. **Duckworth, Henry E.** *Electricity and Magnetism.* New York : Rinehart and Winston, 1960.

4. **American Society for Testing and Materials (ASTM).** *Manual on the Use of Thermocouples in Temperature Measurement.* Fourth. Baltimore, MD. : s.n., 1993.

5. **Pollock, Daniel D.** *Thermoelectricity: Theory, Thermometry, Tool.* Ann Arbor, Mi : ASTM, 1985.

6. **University of Coloroda Mechanical Engineering Department.** First Order System: Transient Response of a Thermocouple to a Step Temperature Change. [Online] 09 06, 2006. [Cited: 30 2011, September.] http://www.colorado.edu/MCEN/Measlab/background1storder.pdf.

7. **Todreas, Neil E. and Kazimi, Mujid S.** *Nuclear Sysms I Thermal Hydraulic Fundamentals.* s.l. : Hemisphere Publising Corporation, 1990.

8. **Cengel, Yunus A.** *Heat and Mass Transfer, A Practical Approach.* New York : McGraw-Hill, 2007.

9. **Lentech Water Treatment Solutions.** Stainless Steel 316L. [Online] [Cited: 9 8, 2011.] http://www.lenntech.com/stainless-steel-316l.htm.

10. **Barton, Dave.** *Welding Design & Fabrication.* [Online] July 19, 2006. [Cited: September 19, 2011.] http://weldingdesign.com/processes/news/wdf_22581/.

Vitae

Spero Michael Peters was born in Memphis, Tennessee in July of 1986. He graduated from Germantown High School in May 2005. He attended the University of Mississippi, graduating with a Bachelors of Science in Mechanical Engineering in May 2010. In December of 2011 he earned a Master's of Science in Nuclear Engineering from the University of Tennessee Knoxville. During his undergraduate career, Spero interned for Memphis Light Gas and Water, a public three service utility in Memphis, TN and worked as an undergraduate research assistant at the University of Mississippi's National Center for Physical Acoustics. As a graduate student at the University of Tennessee he worked as a research assistant under the NANT Fellowship.